SLAC-PUB--2868

DE82 009526

SLAC-PUB-2868
January 1982
(T/E)

HADRONIC AND NUCLEAR INTERACTIONS IN QCD*

Stanley J. Brodsky
Stanford Linear Accelerator Center
Stanford University, Stanford, California 94305

written with collaboration from

Tao Huang
Stanford Linear Accelerator Center
Stanford University, Stanford, California 94305
and
Institute of High Energy Physics
Beijing, People's Republic of China

and

G. Peter Lepage
Laboratory of Nuclear Studies
Cornell University, Ithaca, New York 14853

This report is based on lectures presented at:

The Ninth Summer Institute on Particle Physics
Stanford Linear Accelerator Center
July 27 to August 7, 1981

The Banff Summer Institute in Particles and Fields
Banff, Alberta, Canada
August 16 to 28, 1981

and

The KfK Summer School on Quarks and Nuclear Forces
Bad Liebenzell, Germany
September 27 to October 3, 1981

*Work supported by the Department of Energy, contract DE-AC03-76SF00515.

I. INTRODUCTION

An historic and central goal of physics has been the determination of the fundamental theory of the nuclear force. Incredibly, it appears that the search may well be over: Quantum Chromodynamics [1] (QCD), the $SU(3)_{color}$ non-Abelian gauge theory of quarks and gluons appears to be the theory of the strong and nuclear interactions in the same sense that quantum electrodynamics accounts for electrodynamic interactions. QCD solves many crucial problems: the meson and baryon spectra, quark statistics, the structure of the weak and electromagnetic currents of hadrons, the scale-invariance of interactions at short distance, and most-likely, color (i.e., quark and gluon) confinement at large distances. Many different and diverse tests [2] have confirmed the basic features of QCD although the fact that the tests of quark and gluon interactions must be done within the confines of hadrons, as well as various technical difficulties, have prevented truly quantitative confirmation of the theory. The structure of the theory satisfies all prerequisites of elegance and beauty.

Despite the evidence that QCD — or something close to it — gives a correct description of the structure of hadrons and their interactions, it seems paradoxical that the theory has thus far had very little impact in nuclear physics. One reason for this is that the application of QCD to distances larger than 1 fm involves coherent, non-perturbative dynamics which is beyond present calculational techniques. For example, in QCD the nuclear force can evidently be ascribed to quark interchange and gluon exchange processes. These, however, are as complicated to analyze from a fundamental point of view as is the analogous covalent bond in molecular physics. Since a detailed description of quark-quark interactions and the structure of hadronic wavefunctions is not yet well-understood in QCD, it is evident that a quantitative first-principle description of the nuclear force will require a great deal of theoretical effort.

Another reason for the limited impact of QCD in nuclear physics has been the conventional assumption that nuclear interactions can for the most part be analyzed in terms of an effective meson-nucleon field theory or potential model in isolation from the details of short distance quark and gluon structure of hadrons. However, in these lectures, I will argue that this view is untenable: in fact, there is no "correspondence principle" which yields traditional nuclear physics as a rigorous large-distance or non-relativistic limit of QCD dynamics. On the other hand, the distinctions between standard nuclear physics dynamics and QCD at nuclear dimensions are extremely interesting and illuminating for both particle and nuclear physics. For example:

(1) Meson and nucleon degrees of freedom are insufficient to describe nuclei in QCD: mixed color configurations appear as Fock components of ground state nuclei and as excited multiquark nuclear states. In fact, the hidden color wavefunction

components contribute to basic properties of nuclei including magnetic and quadrupole moments, charge distributions, etc.

(2) The usual impulse approximation formula for elastic form factors of nuclei,

$$F_A(Q^2) \cong F_N(Q^2)\ F_A^{Body}(Q^2),$$

which is conventionally used to separate nucleon size effects from nuclear dynamics is incorrect in QCD because of off-shell and recoil effects. An alternative, QCD-based formula is discussed in Section VIII. We also shall show (see Sec. IV) that even so-called static properties such as the nuclear magnetic moment which are derived in the limit $Q^2 \to 0$ receive non-trivial recoil contributions.

(3) Since quarks are the ultimate carriers of the electromagnetic current in QCD, the identification of specific nucleon anti-nucleon pair production terms in the analysis of the electromagnetic structure of nuclei cannot be justified.

(4) Conventional effective meson-nucleon field theories with nucleons coupled to isovector ρ-mesons violate unitarity in tree graph (Born) approximation. Since such theories are not renormalizable they have no predictive content in higher orders. A renormalizable theory requires tri-linear and quartic vector meson couplings and a spontaneous symmetry breaking mechanism to provide meson masses.

The real conflict between quark and nuclear physics is at a very basic level: because of Lorentz invariance a conserved charge must be carried by a local (point-like) current; there is no consistent relativistic theory where fundamental constituent nucleon fields have an extended charge structure.

The plan of these lectures is as follows. In Section II we review the basic structure and features of QCD. Light-cone perturbation theory is then introduced in Section III. This method can be regarded as an elegant relativistic generalization of ordinary Schroedinger many body theory and it has many applications to nuclear physics problems. Sections III through VII are intended as a general introduction to QCD analysis and phenomenology with special emphasis on exclusive and inclusive large momentum transfer reactions, and the structure of hadronic wavefunctions.

The most dramatic and definitive area of application of QCD to nuclear physics is the short distance structure of the nuclear force and large momentum transfer nuclear reactions. We will discuss these applications in detail in Section VIII. The importance of these predictions is not only the asymptotic large momentum behavior, but also the analytic constraints placed on nuclear amplitudes. For example, we give predictions for the power-law form of effective meson-nucleon couplings as dictated by the underlying renormalizable gauge theory. In Section IX we conclude with a list of experiments which could illuminate QCD dynamics within nuclei. The eventual goal is the complete synthesis of nuclear, hadronic and quark/gluon dynamics. Indeed, if QCD is correct, it must account for all the features and interactions of nuclei as well as mesons and baryons.

II. BASIC FEATURES OF QCD

In quantum chromodynamics the fundamental degrees of freedom of hadrons and their interactions are the quanta of quark and gluon fields which obey an exact internal SU(3) (color) symmetry. The spin-1/2 quarks are in the fundamental (triplet) representation of $SU(3)_c$, the spin-1 gluons are in the adjoint (octet) representation, and hadrons are identified with singlet states; e.g., mesons $|M\rangle \sim \sum_{i=1}^{3} |q_i\bar{q}_i\rangle$ and baryons $|B\rangle \sim \sum \epsilon_{ijk}|q_iq_jq_k\rangle$. In addition, gluonium (color-singlet bound states of 2 and 3 gluons) should exist. As we discuss in Section VI, new types of "hidden color" nuclear states are also predicted in QCD. The different types of quarks, u,d,s,c,b,...are distinguishable by their flavor label and mass.

It is well known that the general structure of QCD meshes remarkably with the facts of the hadronic world, especially quark-based spectroscopy (including the charm and beauty quark systems); current algebra; the dimensional-counting parton-model structure of large momentum transfers reactions (up to computable logarithmic corrections to scale-invariance). Experiments at large momentum transfer, both exclusive and inclusive, are consistent with the QCD postulate that the electromagnetic and weak currents of hadrons are carried by point-like spin-1/2 quarks which interact via a Dirac coupling to spin-1 gluons. The most important phenomenological evidence for QCD comes from inelastic lepton scattering, e^+e^- annihilation processes, and those high momentum transfer exclusive and inclusive reactions where the structure of perturbative quark and gluon subprocesses can be studied in relative isolation from the bound state dynamics of the hadrons. From the theoretical standpoint, the elegant structure of QCD makes it appear almost compelling as a fundamental theory of hadronic and nuclear phenomena, even though many crucial questions concerning quark and gluon confinement, and the effects of non-perturbative phenomena remain unanswered.[3]

A critical feature of QCD is asymptotic freedom, [4] i.e., the logarithmic decrease of the effective quark and gluon coupling constant $\alpha_s(Q^2)$ with momentum transfer which implies that the strong interactions become weak, and even calculable in perturbative theory at short distance. The fact that the annihilation ratio

$$R_{e^+e^-}(s) = \frac{\sigma(e^+e^- \to \text{hadrons})}{\sigma(e^+e^- \to \mu^+\mu^-)} \qquad (1.1)$$

is empirically [5] close to the zeroth order QCD prediction, $R^0 = 3\sum_q e_q^2$ for energies above the heavy quark thresholds, is a crucial check of asymptotic freedom and the color, charge, and spin assignments of the quark quanta in QCD. Critical features of QCD are also confirmed by the observed logarithmic breaking of scale-invariance in deep inelastic lepton-scattering [2] and the measurements of two-jet and three-jet structure of e^+e^- annihilation final states. [5] The recent observations of jet structure [6] in two-photon reactions (consistent with $\gamma\gamma \to q\bar{q}$ subprocesses), and measurements [7] of the photon structure function also provide fundamental checks of predictions which are essentially unique to QCD. However, despite these successes, there is no direct experimental evidence for (near) scale-invariant quark-quark, quark-gluon, or gluon-gluon scattering amplitudes as predicted by QCD; the cross section for large transverse momentum hadron production in hadron-hadron collisions appears to reflect much more complicated dynamical mechanisms. On the other hand, as we discuss in Section IV, the fact that the proton form factor $G_M(Q^2)$ scales as $(Q^2)^{-2}$ reflects the fact that the minimum Fock state in the nucleon contains 3 quarks, and that the internal quark-quark interactions which control the nucleon wavefunction at short distances are consistent with scale invariance. [8,9] Thus far experiments are not sufficiently sensitive to distinguish a logarithmically decreasing $\alpha_s(Q^2)$ from a constant; i.e., fixed point behavior. The sensitivity of the nucleon form factors to the form of $\alpha_s(Q^2)$ is discussed in Section VI.

Although there have been remarkable technical achievements in perturbative QCD calculations in the past few years, [1,2,10] there has also been the realization that precise and detailed comparisons with experiment require consideration of effects and phenomena not readily computable with present methods. There are, in fact, only a very few large momentum transfer processes which can be studied rigorously to all orders in perturbation theory such as $R_{e^+e^-}(s)$, [1] the meson form factors $F_M(Q^2)$ [11] (and $F_{\gamma \to M}(Q^2)$), the two photon processes [12] $\gamma\gamma \to M\bar{M}$ at large momentum transfer, the photon structure function, [13] and the Q^2-evolution of the hadron structure functions. Although, in principle, these processes can be calculated to arbitrary orders in perturbation theory, in practice, there are serious complications involving the dependence of predictions made to finite order on the choice of renormalization scheme and the scale parameterization chosen for

the argument of α_s. [2,13] We shall discuss a new method [14] for avoiding these ambiguities in Section II. Aside from this, there is always the question of the radius of convergence of the perturbation expansion. Even for processes which can be calculated to arbitrary orders in α_s, there are (presently) uncalculable power-law suppressed (higher twist) contributions [15] which must be included in detailed fits to experiment, especially at the edge of phase space. [16]

In the case of jet production, QCD-based predictions based on the elementary features of $e^+e^- \to q\bar{q}$ and $q\bar{q}g$, $\gamma\gamma \to q\bar{q}$, etc. must also take into account higher twist contributions, model-dependent non-perturbative effects intrinsic to hadron formation and decay, [5] and possibly dynamical effects due to quark confinement. [3] In the case of some exclusive processes such as the baryon form factor there are non-leading QCD contributions which are asymptotically suppressed by Sudakhov form factors. [9,10] The precise evaluation requires an all orders resumption of perturbation theory. QCD predictions for elastic hadron-hadron scattering are complicated by the presence of Landshoff [17] pinch singularity contributions which are only partially suppressed by Sudakhov form factors. [10] Despite these complications, we can still derive general properties for exclusive reactions such as hadron-helicity conservation [18] and the leading power-law behavior. [19]

An even more interesting (and perplexing) situation occurs for all inclusive high momentum transfer inclusive reactions involving hadronic initial states such as Drell-Yan massive lepton pair production, direct photon production, and large p_T hadron production. As shown in Ref. 20, initial state interactions violate the usual QCD factorization theorem order by order in perturbation theory and affect the normalization and transverse momentum dependence of the inclusive cross sections. In addition, final state interactions also affect the associated multiplicity and transverse momentum dependence of the outgoing jets in deep inelastic lepton scattering reactions. A detailed report on these effects is given in Ref. 20.

Perhaps the most serious complication to QCD phenomenology is the presence of higher twist subprocesses, since power-law suppressed contributions can often mimic (and thus confuse the identification) of the logarithmic modifications predicted for the leading twist contributions. [16] Examples of this for deep inelastic structure functions and fragmentation distributions are discussed in [21] and [22] and Section V. In the case of three-jet production in e^+e^- annihilation, higher twist terms give contributions [23] $dN/dk_T^2 \sim (k_T^2)^{-2}$ for the hadron transverse momentum distribution in quark and gluon jets. These hard components can complicate the separation of the $e^+e^- \to q\bar{q}g$ and $e^+e^- \to q\bar{q}$ subprocesses. In the case of hadron production at large transverse momentum, "direct-coupled" higher twist subprocesses such as $gq \to \pi q$ actually dominate [24] the leading twist $qq \to qq \to q\pi q$ subprocesses at large $x_T = 2p_T/\sqrt{s}$. Evidence for direct-coupled $\pi q \to \gamma^* q$ subprocesses in $\pi p \to \mu^+\mu^- X$ reactions is discussed in Section V and Ref. 22.

Present QCD phenomenology is also incomplete in the sense that although much attention is paid to the Q^2 evolution of hadron structure functions there is no real understanding of the basic x-dependent form of the quark and gluon distribution in hadrons, or how to relate them to other hadronic phenomena. The relation of the $x \sim 1$ behavior of structure functions to the exclusive fixed W^2, high Q^2 domain is only roughly understood. [25] The $x \sim 0$ behavior of structure functions and the connection to the photoabsorption cross section at fixed Q^2, high ν, and nuclear shadowing phenomena is also not well understood. [26]

The main purpose of these lectures is to begin to extend QCD phenomenology by taking into account the physics of hadronic wavefunctions. [27] Our eventual goal is to obtain a parameterization of the wavefunctions which will bridge the gap between the non-perturbative and perturbative aspects of QCD. The lack of knowledge of hadronic matrix elements is the main difficulty in computing and normalizing dynamical higher twist contributions for many processes.

In Section III we emphasize the utility of a Fock state representation of the meson and baryon wavefunctions as a means not only to parameterize the effects of bound state dynamics in QCD phenomena, but also to interrelate exclusive, inclusive, and higher twist processes. It is particularly convenient to choose a momentum space Fock state basis [19,27]

$$\psi_n(x_i, k_{\perp i}; \lambda_i) \quad ; \quad \sum_{i=1}^{n} x_i = 1 \ , \quad \sum_{i=1}^{n} k_{\perp i} = 0 \quad ,$$

defined at equal "time" $\tau = t + z$ on the light cone. Here $x_i = (k^0 + k^3)_i/(p^0 + p^3)$, $k_{\perp i}$, and λ_i specify the longitudinal and transverse momenta and spin projection S_z of each (on-mass-shell) quark and gluon in the n-particle Fock state ($n \geq 2$ for mesons and $n \geq 3$ for baryons). We also choose the light-cone gauge $A^+ = A^0 + A^3 = 0$ so that only physical polarizations of the gluons occur. The color singlet wavefunctions are regulated so that they are finite in both the infrared and ultraviolet regimes. [28]

There are a number of reasons why this representation of hadrons in terms of the quark and gluon degrees of freedom is useful:

(1) In light-cone perturbation theory, the perturbative vacuum is also an eigenstate of the total QCD Hamiltonian on the light-cone; perturbative calculations are enormously simplified by the absence of vacuum to pair production amplitudes.

(2) All form factors, charge radii, magnetic moments, etc. have exact expressions in terms of the ψ_n.

(3) The structure functions $G_q(x,Q)$ and $G_g(x,Q)$ (and more general multiparticle distributions) which control large momentum transfer (leading and higher twist) inclusive reactions, and the distribution amplitudes $\phi(x,Q)$ which control large momentum transfer exclusive reactions (and directly coupled inclusive reactions) are each specific, basic measures of the ψ_n. Examples of these calculations are schematically illustrated in Figs. 1 through 3.

(4) Other physical quantities such as decay amplitudes provide rigorous sum rule or local constraints on the form of the valence components of meson and baryon wavefunctions. [2]

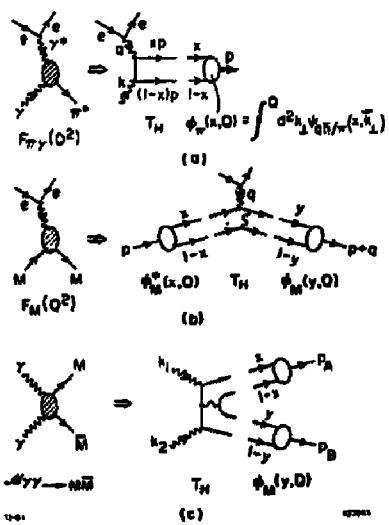

Fig. 1 Calculable large momentum transfer meson processes in QCD, and their connection to the meson Fock state wavefunction $\psi_{q\bar{q}}$ and distributions amplitude $\phi(x,Q)$. Only a representative diagram for the hard scattering amplitude T_H is shown. (a) The $\gamma \to \pi^0$ transition form factor (measurable in single tagged ee → ee π^0 experiments), (b) the meson form factor, (c) the $\gamma\gamma \to M\bar{M}$ scattering amplitude. Details are discussed in Sec. IV.

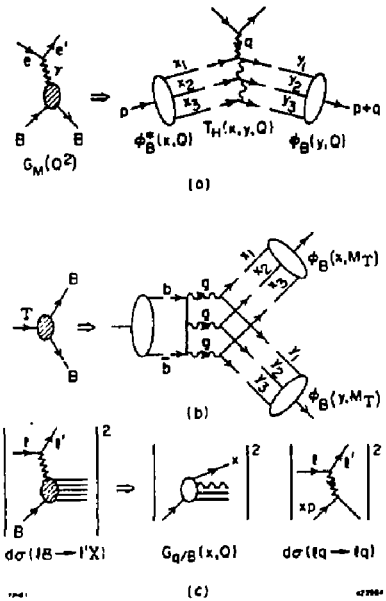

Fig. 2 Baryon processes at large momentum transfer in QCD and the connection to the baryon Fock state wavefunction. (a) Baryon form factors, (b) heavy quarkonium decay $T \to p\bar{p}$, (c) deep inelastic lepton-baryon scattering. Only representative contributions are shown. The inclusive cross section and structure function $G_{q/B}(x,Q)$ is computed from the square of the baryon wavefunction summed over all contributing Fock states.

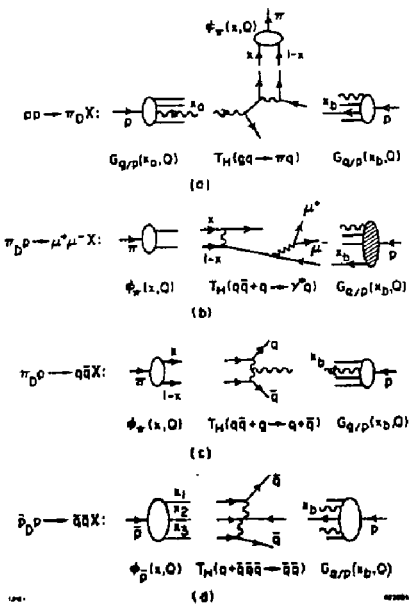

Fig. 3 Examples of QCD-computable higher twist "direct-coupled" subprocesses for inclusive reactions. The subscript D indicates that the hadronic wavefunction is involved directly in the high momentum transfer subprocesses. (a) Direct production of high p_T mesons in hadron-hadron cross section. The predicted cross section is proportional to the meson form factor $F_M(p_T^2)$ times the leading twist cross section. (b) Higher twist contribution to meson-induced massive lepton pair production. The predicted cross section is equivalent to a contribution $F_L(x,Q^2) \sim C/Q^2$ to the longitudinal structure function of the meson. (c) Direct meson production of quark jets in meson-baryon collisions. All of the meson energy is used to produce jets at large transverse momentum. The cross section is proportional to $F_M(p_T^2)$ times the leading twist $qq \to qq$ cross section. (d) Direct production of anti-quark jets in $B\bar{B}$ collisions. The cross section is proportional to $G_M^B(p_T^2)$ times the leading twist $qq \to qq$ cross section. In each case the direct process dominates over the leading twist contribution in a large x kinematic region.

In the remainder of this section we will give a brief introduction to QCD and asymptotic freedom. We then discuss a new method to avoid scheme and scale ambiguities in perturbative QCD predictions. In Section III we give a detailed discussion of light-cone perturbation theory and the Fock state expansion of hadronic wavefunctions. The QCD equation of motion is also discussed. In Section IV we discuss measures of the hadronic and nuclear wavefunctions (form factors, magnetic moments, etc.), and the QCD analysis of high momentum transfer exclusive processes. We also show how meson distribution amplitudes can be measured in $\gamma\gamma \to M\bar{M}$ reactions. The connection of the Fock state basis to leading and higher twist contributions to deep inelastic scattering is given in Section V. In Section VI we discuss how many different QCD processes are interrelated (as in Figs. 1 through 3) through the hadronic Fock states. We also discuss a novel type of QCD subprocess — direct coupled hadron-induced reactions. [29] A new prediction for the proton form factor is also given. In Section VI we also introduce a simple phenomenology of hadron wavefunctions and discuss present constraints on the form and normalization of the valence meson and nucleon Fock states. An important conclusion is that the valence Fock state as defined at equal time or the light cone appears to have a significantly smaller radius than that of the physical hadron; [27] higher Fock states thus play an essential role in low momentum transfer phenomenology. Applications to quark jet diffraction excitation [30] and the hidden heavy quark Fock state structure of hadrons are also discussed. [31] The effects of initial and final state interactions on QCD inclusive reactions are discussed in Ref. 20.

A. The QCD Lagrangian

An essential feature of QCD is that $SU(3)_c$ is an exact local symmetry: rotations in color space can be made independently at any space-time point. The mathematical realization of this is the Yang-Mills non-Abelian gauge field theory. The QCD Lagrangian density is [1]

$$\mathscr{L}_{QCD} = \bar{\psi}(i\not{D} - m)\,\psi - \frac{1}{4}\,Tr\,F_{\mu\nu}^2 \tag{2.1}$$

$$iD^\mu = i\,\partial^\mu\,I + g A^\mu \tag{2.2}$$

$$F^{\mu\nu} = \partial^\mu A^\nu - \partial^\nu A^\mu + g[A^\mu, A^\nu] \tag{2.3}$$

Here

$$\psi(x) = \begin{pmatrix} q_R(x) \\ q_Y(x) \\ q_B(x) \end{pmatrix}$$

is the color triplet of quark fields, and $A^\mu(x) = \sum_{a=1,8} \lambda_a A_a^\mu(x)$ is the color octet gluon field summed over the 3×3 traceless matrices λ_a satisfying $[\lambda_a, \lambda_b] = i f_{abc} \lambda_c$ and $Tr[\lambda^a \lambda^b] = 2\delta^{ab}$. $\mathscr{L}_{QCD}$ is obviously a color singlet. Local gauge invariance and color symmetry follows from the invariance of $\mathscr{L}_{QCD}$ under the general gauge transformation

$$\psi(x) \to U(x)\,\psi(x) \tag{2.4}$$

$$A^\mu(x) \to U(x)\,A^\mu(x)\,U^{-1}(x) + \frac{i}{g}\,U(x)\left(\partial^\mu U^{-1}(x)\right) \tag{2.5}$$

where the unitary matrix $U(x) = \exp i \sum_a \lambda_a \theta_a(x)$ is an arbitrary function of space and time. Note that the field strength $F^{\mu\nu}(x) \to U(x)\,F^{\mu\nu}\,U^{-1}(x)$ is not invariant

since it is in the adjoint representation of $SU(3)_c$. The local gauge invariance of the Yang-Mills is an essential ingredient in proving the renormalizability and consistency of the theory. [1]

In general, a sum over quark flavors $i = u,d,s,c,b...$ is understood in $\mathscr{L}_{QCD}$. (In fact, the mass matrix m_{ij} is not diagonal when the weak and electromagnetic interactions are taken into account. [32]) The fundamental origin of the quark flavors and their masses remains an outstanding problem in hadron physics.

In a sense QCD can be regarded as the non-Abelian generalization of QED:

$$\mathscr{L}_{QED} = \bar{\psi}(x)(i\not{D} - m)\,\psi - \frac{1}{4}F_{\mu\nu}^2 \qquad (2.6)$$

where $iD^\mu = i\partial^\mu + eA^\mu$, $F^{\mu\nu} = \partial^\mu A^\nu - \partial^\nu A^\mu$. From the point of view of formal perturbation theory there are close similarities in the Feynman rules and treatment of ultraviolet renormalization and infrared divergences. The Feynman rules for QCD are given in Table I. In the case of covariant gauges one must formally include "ghost" scalar particles in loops, or else unitarity of amplitudes involving the non-Abelian-couplings will be lost. In the case of axial gauges ($\eta^\mu A_\mu = 0$ where η^μ is a fixed 4-vector) there are no ghosts, but renormalization is somewhat more complicated. The color trace algebra for any Feynman diagram can be done almost automatically using the graphical rules given by CVITANOVIC. [33] The main algorithm is that as far as color is concerned, the gluon propagator ~ in SU(N) is equivalent to two quark lines $\rightrightarrows$ minus 1/N times the identity (to remove the U(N) singlet). The complete rules are given in Ref. 33.

Although QCD and QED perturbation theory have many similarities, there are non-perturbative aspects of the non-Abelian theory which have no analog in electro-

Table I Feynman rules for quantum chromodynamics*

Fermion Propagator		$\frac{i}{\not{p}-m+i\varepsilon}\,\delta_{\alpha\beta}$
Gluon Propagator		$-i\left[g_{\mu\nu}-(1-a)\frac{p_\mu p_\nu}{p^2+i\varepsilon}\right]\frac{\delta_{ab}}{p^2+i\varepsilon}$
Ghost Propagator		$\frac{i\,\delta_{ab}}{p^2+i\varepsilon}$
Fermion Vertex		$ig\,\gamma_\mu\,\lambda^a_{\alpha\beta}$
Triple Vertex		$g f_{abc}\left[g_{\mu\nu}(k-q)_\sigma + g_{\nu\sigma}(q-r)_\mu + g_{\sigma\mu}(r-k)_\nu\right]$
Quartic Vertex		$-ig^2\left[f_{abe}f_{cde}(g_{\mu\sigma}g_{\nu\rho}-g_{\mu\rho}g_{\nu\sigma}) + f_{ace}f_{bde}(g_{\mu\nu}g_{\sigma\rho}-g_{\mu\rho}g_{\nu\sigma}) + f_{ade}f_{cbe}(g_{\mu\sigma}g_{\nu\rho}-g_{\mu\nu}g_{\sigma\rho})\right]$
Ghost Vertex		$g\,f_{abc}\,r_\mu$

*From A. J. Buras, Ref. 1.

dynamics, e.g., classical ("instanton") solutions to the pure gauge theory. These solutions can have profound consequences for the QCD vacuum state. [34] Furthermore, the absence of asymptotic color states implies that, at best, the perturbation rules are only valid in a far-off-shell short-distance regime.

Fortunately for many processes of experimental interest it is possible to prove factorization theories which separate the long-distance dynamics associated with the hadron wavefunction and color confinement from quark and gluon subprocesses which only involve short distance propagation of color. [35] If this factorization can be proved to all orders in perturbation theory, it is reasonable to assume that the corresponding perturbative predictions are legitimate predictions of the complete theory. In the case of predictions dependent o hadronic fragmentation from quark or gluon jets one has to make an extra assumption that the essential effects of color confinement are restricted to large distances. [3]

B. QCD Perturbation Theory

As in QED, one can sum the effects of vacuum polarization into a "running" coupling constant ($\alpha_s = g^2/4\pi$)

$$\alpha_s(Q^2) = \frac{\alpha_s(Q_0^2)}{1 - \alpha_s(Q^2)\left[\pi(Q^2) - \pi(Q_0^2)\right]} \tag{2.7}$$

where $\pi(Q^2)$ can be computed (in some gauges) from the single-particle-irreducible contributions to the gluon propagator. Given the gluon propagator at any scale Q_0^2, one can use Eq. (2.7) to determine the effective interaction at the scale Q^2. To lowest order in perturbation theory the quark and gluon loop insertions give $\left[Q^2, Q_0^2 \gg m_i^2,\ i = 1, 2 \ldots n_f\right]$

$$\pi(Q^2) - \pi(Q_0^2) = \frac{1}{4\pi} \log \frac{Q^2}{Q_0^2}\left[\frac{2}{3} n_f - 11\right] + \mathcal{O}(\alpha_s) \tag{2.8}$$

i.e., for $n_f < 33/2$, $\alpha_s(Q^2)$ decreases with Q^2, exactly opposite to QED. More generally, one can calculate the Q^2 dependence of α_s in higher orders

$$\frac{\partial}{\partial \log Q^2} \alpha_s(Q^2) \equiv \beta\left[\alpha_s(Q^2)\right] = \frac{-\beta_0}{4\pi} \alpha_s^2(Q^2) - \frac{\beta_1}{(4\pi)^2} \alpha_s^3(Q^2) \tag{2.9}$$

$$+ \ldots$$

where [1] $\beta_0 = 11 - 2/3\, n_f$, $\beta_1 = 102 - 38/3\, n_f$. The solution for $\alpha_s(Q^2)$ at large Q^2 to two loop accuracy then has the form

$$\alpha_s(Q^2) = \frac{4\pi}{\beta_0 \log \frac{Q^2}{\Lambda^2} + \frac{\beta_1}{\beta_0} \log \log \frac{Q^2}{\Lambda^2}} \tag{2.10}$$

where Λ is introduced as a constant of integration. The fact that $\alpha_s(Q^2)$ decreases at large momentum transfer [asymptotic freedom] is an extra-ordinary feature of QCD which in principle allows a systematic computation of short distance processes. A graph of $\alpha_s(Q^2)$ showing the effect of the β_1/β_0 term is shown in Fig.4. It should be emphasized that perturbation theory does not determine the form of α_s at small Q^2 where its magnitude becomes large. As noted by PARISI and PETRONZIO, [36] consistent calculations of perturbative loops demand that $\alpha_s(Q^2)$ remains finite at all values of the loop integration. Thus far there is no <u>direct</u> experimental evidence that $\alpha_s(Q^2)$ decreases logarithmically.

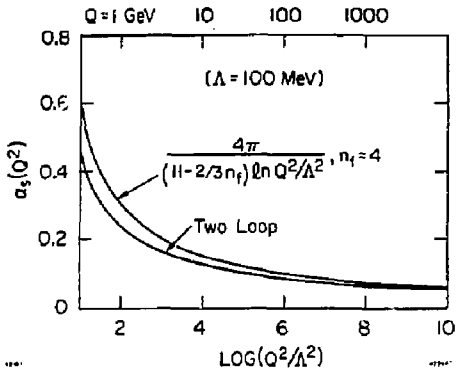

Fig. 4 The QCD coupling constant $\alpha_s(Q^2)$ for $n_f = 4$ to one- and two-loop accuracy. Empirical specifications of Λ in a given scheme should use the two-loop formula (Eq. (2.10).

If we choose Q_0^2 to be the ultimate ultraviolet cutoff scale of QCD then $\alpha_s(Q_0^2) = \alpha_s^0$ is the "bare charge" of the theory. We can then identify $\alpha_s(Q^2)$ as the effective coupling constant which takes into account all vacuum polarization contributions of invariant mass $\mathcal{M}^2$: $Q^2 < \mathcal{M}^2 < Q_0^2$. Similarly, we can define the running quark mass $m(Q^2)$ which takes into account all self-energy insertions in the range $Q^2 < \mathcal{M}^2 < Q_0^2$.

Let us now define a cutoff Lagrangian $\mathscr{L}^{\kappa}_{QED}$ density for QCD by excluding all intermediate states with $\mathcal{M}^2 > \kappa^2$. The fact that the theory is renormalizable implies that

$$\mathscr{L}^{\kappa}_{QCD} = \bar{\psi}\left(i\partial\!\!\!/ + g(\kappa)A\!\!\!/ - m(\kappa)\right)\psi - \frac{1}{4}\,\mathrm{Tr}\,F^2 \qquad (2.11)$$

$$+ \mathcal{O}\frac{1}{\kappa^2}\, m(\kappa)\ \bar{\psi}\,\sigma_{\mu\nu}F^{\mu\nu}\,\psi + \ldots$$

i.e., all effects of very high mass states $\mathcal{M}^2 > \kappa^2$ are completely contained in the effective coupling constant $g(\kappa)$, the quark running mass $m(\kappa)$, and "higher twist" power-law suppressed $1/\kappa^2$, $1/\kappa^4$, etc. terms. If κ^2 is taken at the ultimate cutoff scale Q_0^2 then $\mathscr{L}^{\kappa}_{QCD}$ is the bare Lagrangian. If κ^2 is chosen sufficiently large then the higher twist terms are negligible in (2.11).

The classic perturbative calculation in QCD is that of the annihilation cross section $\sigma_{e^+e^-\to\text{hadrons}}$ which can be computed from the hadronic absorptive part of the forward $e^+e^- \to e^+e^-$ amplitude to order α^2. Since there are no external color charges there can be no gluon-mass infrared divergences or quark mass singularities. Thus the only relevant scale is $Q^2 = s = E^2_{c.m.}$, and we can compute perturbatively from $\mathscr{L}^{\kappa}_{QCD}$ with $\kappa^2 = Q^2$. The result to order $\alpha_s^2(Q^2)$ is

$$R_{e^+e^-}(Q^2) = 3\sum_q e_q^2\left[1 + \frac{\alpha_s^{\overline{MS}}(Q^2)}{\pi} + \frac{\alpha_s^2(Q^2)}{\pi^2}\,(B + A\,n_f) + \ldots\right] \qquad (2.12)$$

where the $A\,n_f$ term arises from virtual quark loops. An essential and unique prediction of asymptotic freedom is that $\lim_{Q^2\to\infty} R(Q^2) = 3\sum e_q^2 = R^0$, the free quark prediction. The specific values of B and A in Eq. (2.12) depend on the method of implementing the ultraviolet cutoff. In the $\overline{MS}$ scheme (a particular dimensional regularization scheme) one finds [37] $B \cong 1.98$, $A \cong -0.115$. However, in analogy to QED, it is clear that the $A\,n_f$ term should be identified with the fermion loop vacuum polarization contribution to the running coupling constant in the $\alpha_s(\kappa)/\pi$

term; the particular numerical value for A is rather arbitrary since we could have chosen any scale $\kappa^2 = f^2Q^2$ for the perturbation expansion. In QCD, α_s is essentially a function of $\beta_0 = 11 - 2/3\ n_f$. Thus we write $B + A\ n_f = -3/2\ \beta_0 A + C$, where $C = (33/2)A + B \cong 0.0825$ must be scheme independent (since to the order of interest the cutoff schemes can only differ by the definition of the scale constant Λ^2). We thus have the QCD prediction: [14]

$$R_{e^+e^-}(Q^2) = 3\sum_q e_q^2\left[1 + \frac{\alpha_s^{\overline{MS}}(f^2Q^2)}{\pi} + 0.0825\,\frac{\alpha_s^2}{\pi^2} + \ldots\right] \tag{2.13}$$

where $f = f_{\overline{MS}} = e^{3A} \cong 0.71$ in the $\overline{MS}$ scheme. Let us imagine that eventually measurements of $\sigma_{e^+e^-\to(Q^2)\ \text{hadrons}}$ will be sufficiently accurate that we can choose $R(Q^2)$ to define a "canonical" measurement of the QCD running coupling constant:

$$\alpha_s^R(Q^2) \equiv \pi\left[\frac{R(Q^2) - R^0}{R^0}\right]\left[1 - 0.0825\left(\frac{R - R^0}{R^0}\right)\right] = \alpha_s^{\overline{MS}}(f^2Q^2) \quad . \tag{2.14}$$

Our goal is then to show that all observables in QCD which have a perturbative expansion in α_s can (in principle) be expressed in terms of $\alpha_s^R(Q^2)$ without any scheme or scale ambiguity. We will define the scale parameter $\Lambda = \Lambda^R$ using Eq. (2.10) for α_s^R.

We thus propose the following prescription for making scheme and scale independent perturbative QCD predictions: [14] For any observable $\rho(Q^2)$ which has a perturbative expansion in $\alpha_s(Q^2)$ one can compute in a given renormalization scheme

$$\rho(Q^2) = \frac{\alpha_s(Q^2)}{\pi} + (A_\rho\ n_f + B_\rho)\,\frac{\alpha_s^2(Q^2)}{\pi^2} + \ldots \tag{2.15}$$

As in the case of $R(Q^2)$, we identify $(-3/2)\beta_0 A_\rho$ as the vacuum polarization correction to the running coupling constant in the α_s/π term. Thus

$$\rho(Q^2) = \frac{\alpha_s^R(\hat{Q}_\rho^2)}{\pi} + C_\rho\left(\frac{\alpha_s}{\pi}\right)^2 + \ldots \tag{2.16}$$

where

$$\hat{Q}_\rho^2 = e^{3A_\rho - 3A_R}\,Q^2 \tag{2.17}$$

and

$$C_\rho = \frac{33}{2}A_\rho + B_\rho \tag{2.18}$$

are scheme-independent. The leading order prediction for $\rho(Q^2)$ can thus be written unambiguously in terms of α_s^R. If $C_\rho\,\alpha_s/\pi$ is reasonably small, then we can expect that Eq. (2.16) gives a meaningful perturbative QCD prediction. An important task will be to carry out the above procedure to higher orders in α_s.

As an example of the above method, let us consider the decay rate for pseudoscalar quarkonium states which is computed in terms of $Q\bar{Q} \to gg$ plus higher order subprocesses. In the $\overline{MS}$ scheme: [29] (C is a known color factor)

$$\frac{\Gamma(\eta_c \to \text{hadrons})}{\Gamma(\eta_c \to \gamma\gamma)} = C\left[\alpha_s^{\overline{MS}}\left(M_{\eta_c}^2\right)\right]^2\left\{1 + \frac{\alpha_s^{\overline{MS}}}{\pi}\left(17.13 - \frac{8}{9}n_f\right) + \ldots\right\} \tag{2.19}$$

$$= C\left[\alpha_s^R\left((.37M_{\eta_c})^2\right)\right]^2\left\{1 + 2.46\frac{\alpha_s^R}{\pi} + \ldots\right\}$$

i.e.: the effective scale in the vacuum polarization contributions is $\sim 0.37\, M_{\eta_c}$ relative to the scale in $e^+e^- \to$ hadrons. If $\alpha_s \cong 0.2$, then the correction term in Eq. (2.19) gives only a 7% correction to the determination of α_s. In the case of the hadronic decays of $J^{CP} = 1^{--}$ heavy quarkonium states, the correction to the $Q\bar{Q} \to 3g$ decay amplitude appears to be very large so that the leading order expressions may not be meaningful. One finds [40]

$$\frac{\Gamma(\Upsilon \to \text{hadrons})}{(\Upsilon \to \mu^+\mu^-)} = \frac{10(\pi^2 - 9)}{81\,\pi}\frac{\alpha_s^2}{e_b^2\,\alpha^2}\left[\alpha_s^R\left((.22M_\Upsilon)^2\right)\right]^3\left\{1 - 13.94\frac{\alpha_s^R}{\pi} + \ldots\right\} \tag{2.20}$$

For $\alpha_s \cong 0.2$, the correction term gives a correction of order 30% to the determination of α_s. Note that even in QED, the radiative corrections to orthopositronium decay are very large:

$$\Gamma_{3\gamma} = \Gamma^0_{3\gamma}\left\{1 - 12.61\,(3)\frac{\alpha}{\pi} + \ldots\right\} \tag{2.21}$$

so this appears to be an intrinsic problem to this type of decay process. Additionally, the QCD prediction for quarkonium decay is complicated by some uncertainties from relativistic and higher Fock state components in the quarkonium wavefunction.

One of the most important predictions from QCD is the logarithmic variation of structure function moments, $M_n(Q^2) = \int_0^1 dx\, x^n F_3(x,Q)$. Using the above renormalization procedure we find [14]

$$\frac{d}{d\log Q^2}\log M_n(Q^2) = \frac{-\gamma_n}{8\pi}\alpha_s^R\left(f_n^2\, Q^2\right)\left[1 - \frac{\alpha_s^R}{\pi}C_n + \ldots\right]$$

where the γ_n are known anomalous dimensions (see Sec. IV). The coefficient C_n varies from ~ -0.27 to 1.1 for non-singlets moments $n = 2$ to 10, thus giving reasonably small corrections to the lowest order predictions. The monotonic decrease of f_n with n reflects the fact that the momentum scale for gluon emission becomes increasingly restricted at large n ($\langle 1 - x\rangle \sim O(1/n)$) due to phase-space effects. [41] Further applications and discussions will be given in Ref. 14. We also note that in processes with several large momentum transfer scales, the effective argument for α_s^R in the leading order predictions can be very complicated. For example in the case of large p_T jet production due to $qq \to qq$ scattering, the subprocess scattering amplitude involves α_s evaluated at the subprocess invariants $\hat{t}$ and $\hat{u}$, whereas the evolution of each hadronic structure function is sensitive to its respective x-dependent phase-space boundary as well as the quark momentum transfer.

III. HADRONIC WAVEFUNCTIONS IN QCD [27]

Even though quark and gluon perturbative subprocesses are simple in QCD, the complete description of a physical hadronic process requires the consideration of many different coherent and incoherent amplitudes, as well as the effects of non-

perturbative phenomena associated with the hadronic wavefunctions and color confinement. Despite this complexity, it is still possible to obtain predictions for many exclusive and inclusive reactions at large momentum transfer provided we make the ansatz that the effect of non-perturbative dynamics is negligible in the short-distance and far-off-shell domain. (This assumption appears reasonable since a linear confining potential $V \sim r$ is neglibible compared to perturbative $1/r$ contributions.) For many large momentum transfer processes, such as deep inelastic lepton-hadron scattering reactions and meson form factors, one can then rigorously isolate the long-distance confinement dynamics from the short-distance quark and gluon dynamics — at least to leading order in $1/Q^2$. [35] The essential QCD dynamics can thus be computed from (irreducible) quark and gluon subprocesses amplitudes as a perturbative expansion in an asymptotically small coupling constant $\alpha_s(Q^2)$.

An essential part of the QCD predictions is the hadronic wavefunctions which determine the probability amplitudes and distributions of the quark and gluons which enter the short distance subprocesses. The hadronic wavefunctions provide the link between the long distance non-perturbative and short-distance perturbative physics. Eventually, one can hope to compute the wavefunctions from the theory, e.g., from lattice or bag models, or directly from the QCD equations of motions, as we shall outline below. Knowledge of hadronic wavefunction will also provide explicit connections between exclusive and inclusive processes, and will allow the normalization and specification of the power law (higher twist) corrections to the leading impulse approximation results. As we shall discuss in Sec. VI, there are a number of novel QCD phenomena associated with hadronic wavefunctions, including the effects of intrinsic gluons, intrinsic heavy quark Fock components, diffraction dissociation phenomena, and "direct" hadron processes where the valence Fock state of a hadron enters coherently into a short-distance quark-gluon subprocess.

The most convenient representation of a wavefunction in a relativistic field theory is to use a momentum space Fock state basis defined at equal time" $\tau = t + z$ on the light cone (see Fig.5a): [42]

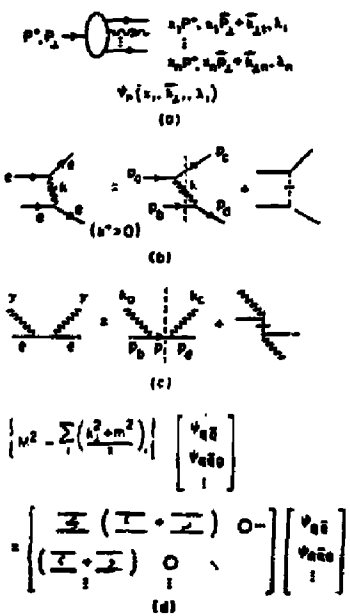

Fig. 5 (a) the n-particle Fock state amplitude defined at equal τ. The state is off the p^- light-cone energy shell (see Eq. (3.12)). (b,c) Examples of light-cone time-ordered perturbation theory calculations. The frame is chosen so that $k^+ > 0$. (d) QCD equation of motion for the meson wavefunction.

$$\left|\psi_n(\vec{k}_{\perp i}, x_i; \lambda_i)\right\rangle \tag{3.1}$$

Momentum conservation requires

$$\sum_{i=1}^{n} \vec{k}_{\perp i} = 0, \qquad \sum_{i=1}^{n} x_i = 1, \qquad 0 < x_i < 1 \quad . \tag{3.2}$$

The $\vec{k}_{\perp i}$ are the transverse momentum of the (on-mass-shell) constituents relative to the bound state 3-momentum $\vec{P} = P^3$. The x_i are the light-cone momentum fractions $\left(k^{\pm} = k^0 \pm k^3,\ A \cdot B = 1/2(A^+B^- + A^-B^+) - \vec{A}_\perp \cdot \vec{B}_\perp\right)$

$$x_i = \frac{k_i^+}{P^+} = \frac{(k^0 + k^3)_i}{P^0 + P^3} \tag{3.3}$$

(In a frame where $P^3 \to \infty$, the x_i are the longitudinal momentum fractions.) The mass shell condition is $k^2 = m^2$, or $k^- = (k_\perp^2 + m^2)/k^+$. As we shall see, the equal-τ formalism is equivalent to the usual Schroedinger equal-time theory in the non-relativistic limit.

A unique and remarkable advantage of quantizing a relativistic theory at equal τ is the fact that the perturbative vacuum state $|0\rangle$ is also an eigenstate of the full Hamiltonian. Matrix elements where particles are created out of the vacuum are excluded because of the fact that all particles must have $k_i^+ > 0$. Furthermore, the charge operator and the current $J^+ = J^0 + J^3$ are diagonal in the Fock state basis. It is particularly advantageous to choose the light-cone gauge $A^+ = A^0 + A^3 = 0$ since unphysical degrees of freedom do not appear. A comparison between time-ordered and τ-ordered perturbation theory is given in Table II.

Thus at a given "time" we can define the (color singlet) basis

$$|0\rangle \tag{3.4}$$

$$|q\bar{q}\rangle = a^+_{k^+,\vec{k}_\perp}\, b^+_{k^{+\prime},\vec{k}^{\prime}_\perp}\, |0\rangle$$

$$\vdots$$

The pion state, for example, can be expanded as

$$|\pi\rangle = |q\bar{q}\rangle\, \psi_{q\bar{q}} + |q\bar{q}g\rangle\, \psi_{q\bar{q}g} + \ldots \tag{3.5}$$

where $\psi_n = \langle n|\pi\rangle$ is the amplitude for finding the Fock state $|n\rangle$ in $|\pi\rangle$ at time τ. The full Fock state wavefunction which describes the n-particle state of a hadron with 4-momentum $P^\mu = (P^+, P^-, \vec{P}_\perp)$ and constituents with momenta

$$k^\mu = \left(k^+, k^-, \vec{k}_\perp\right) = \left(xP^+, \frac{(x\vec{P}_\perp + \vec{k}_\perp)^2 + m^2}{x}, x\vec{P}_\perp + \vec{k}_\perp\right) \tag{3.6}$$

and spin projection λ_i is

Table 2 Time-ordered perturbation theory

Equal t	Equal $\tau = t + z$
$k^0 = \sqrt{\vec{k}^2 + m^2}$ $\left(\begin{matrix}\text{particle}\\ \text{mass shell}\end{matrix}\right)$	$k^- = \dfrac{k_\perp^2 + m^2}{k^+}$ $\left(\begin{matrix}\text{particle}\\ \text{mass shell}\end{matrix}\right)$
$\sum \vec{k}$ conserved	$\sum \vec{k}_\perp, k^+$ conserved
$\mathcal{M}_{ab} = V_{ab}$	$\mathcal{M}_{ab} = V_{ab}$
$+\sum_c V_{ac} \dfrac{1}{\sum_a k^0 - \sum_c k^0 + i\epsilon} V_{cb}$	$+\sum_c V_{ac} \dfrac{1}{\sum_a k^- - \sum_c k^- + i\epsilon} V_{cb}$
n! time-ordered contributions	$k^+ > 0$ only
Fock states $\psi_n(\vec{k}_i)$	Fock states $\psi_n(\vec{k}_{\perp i}, x_i)$
$\sum_{i=1}^n \vec{k}_i = \vec{P} = 0$	$x = \dfrac{k^+}{P^+}$, $\sum_{i=1}^n x_i = 1$, $\sum_{i=1}^n \vec{k}_{\perp i} = 0$
	$(0 < x_i < 1)$
$\mathcal{E} = P^0 - \sum_{i=1}^n k_i^0$	$\mathcal{E} = P^+\left(P^- - \sum_{i=1}^n k_i^-\right)$
$= M - \sum_{i=1}^n \sqrt{k_i^2 + m_i^2}$	$= M^2 - \sum_{i=1}^n \left(\dfrac{k_\perp^2 + m^2}{x}\right)_i$

$$\tau_n = \psi_n\left(x_i, k_{\perp i};\ \lambda_i\right) \prod_{\text{fermions}} \frac{u\left(x_i P^+, x_i \vec{P}_\perp + \vec{k}_{\perp i}\right)_{\lambda_i}}{\sqrt{x_i}} \tag{3.7}$$

$$\cdot \prod_{\text{gluons}} \frac{\varepsilon\left(x_i P^+, x_i \vec{P}_\perp + \vec{k}_{\perp i}\right)_{\lambda_i}}{\sqrt{x_i}}$$

Note that $\psi_n(x_i, \vec{k}_{\perp i};\ \lambda_i)$ is independent of P^+, $\vec{P}_\perp$. The general normalization condition is

$$\sum_n \int \left[d^2k_\perp\right] \int [dx] \left|\psi_n(x_i, \vec{k}_{\perp i};\ \lambda_i)\right|^2 = 1 \tag{3.8}$$

where by momentum conservation

$$\left[d^2k_\perp\right] = 16\,\pi^3 \delta^2\left(\sum_{i=1}^n \vec{k}_{\perp i}\right) \prod_{i=1}^n \frac{d^2k_{\perp i}}{16\,\pi^3} \tag{3.9}$$

and

$$[dx] = \delta\left(1 - \sum_{i=1}^{n} x_i\right) \prod_{i=1}^{n} dx_i \tag{3.10}$$

In the non-relativistic limit the equal $\tau = t + z/c$ and equal time t theories coincide. For example, for the Fock state wavefunction in the rest system we can identify

$$x = \frac{k^0 + k^3}{M} \cong \frac{m}{M} + \frac{k^3}{M} \tag{3.11}$$

and the off-shell light-cone energy is

$$\mathcal{E} = P^+\left[P^- - \sum_{i=1}^{n} k^-\right] = M^2 - \sum_{i=1}^{n}\left(\frac{k_\perp^2 + m^2}{x}\right)_i \tag{3.12}$$

$$\cong 2M\left[\mathcal{E}_{NR} - \sum_{i=1}^{n}\left(\frac{k_\perp^2 + k_3^2}{2m}\right)_i\right]$$

Thus, in the non-relativistic limit, the hydrogen atom wavefunction is

$$\psi_{1s} = \frac{C}{\left[k_\perp^2 + \left(m_e - xM\right)^2 + \alpha^2 m_e^2\right]^2} \tag{3.13}$$

Light-cone perturbation theory rules can be derived by either evaluating standard equal-time time-ordered perturbation theory for an observer in a fast moving Lorentz frame (the "infinite momentum" method), [43] or more directly, by quantizing at equal τ. The LCPTh rules are: [19,44]

(1) For each Feynman diagram assign particle 4-momentum k^μ such that $k^+, \vec{k}_\perp$ is conserved at each of the n vertices. (This is the analogue of 3-momentum conservation.) Since all particles are on the (positive energy) mass shell ($k^2 = m^2$) we have

$$k^- = \frac{k_\perp^2 + m^2}{k^+} > 0 \tag{3.14}$$

(2) Construct all time orderings (up to n!) such that $k^+ > 0$ for all particles.

(3) For each intermediate state assign a propagator

$$\frac{1}{\sum_{\text{initial}} k_i^- - \sum_{\text{intermediate}} k_i^- + i\varepsilon} \tag{3.15}$$

and a factor $1/k^+$ for each internal line. (This is the analogue of $1/\left(\sum_{\text{initial}} E_i - \sum_{\text{intermediate}} E_i + i\varepsilon\right)$ and $1/(2E)$ in TOPTh.)

(4) For each loop integrate

$$\int \frac{d^2k_\perp}{2(2\pi)^3} \int_0^\infty dk^+ \tag{3.16}$$

and sum over intermediate state spins and polarization.

(5) The vertex factors depend on the theory. In the case of $g\phi^3$ interaction, assign a factor g at each vertex. In gauge theories the gluon-fermion vertices are

$$g\bar{u}\not{\varepsilon}u,\ -g\bar{v}\not{\varepsilon}v,\ g\bar{u}\not{\varepsilon}v,\ -g\bar{v}\not{\varepsilon}u \quad . \tag{3.17}$$

The trigluon and quartic-gluon vertices are given in Table I.

(6) Finally, there are instantaneous gluon contributions in $A^+ = 0$ gauge:

$$\frac{\gamma^+ \ldots \gamma^+}{(k^+)^2} \tag{3.18}$$

(analogous to Coulomb interactions) and instantaneous fermion contributions $\gamma^+/2k^+$ (the remnant of backward-moving "Z-graph" fermion lines). For example, the electron-electron scattering diagrams of Fig.5b give

$$\mathcal{M}_{ee\to ee} = e^2 \frac{\bar{u}\gamma^\mu u\ \bar{u}\gamma^\nu u}{k^+ D} d_{\mu\nu} + e^2 \frac{u\gamma^+ u\ u\gamma^+ u}{(k^+)^2} \tag{3.19}$$

where the polarization sum is

$$d^{\mu\nu} = \sum_{\lambda=1,2} \varepsilon_\lambda^\mu \varepsilon_\lambda^\nu, \quad \varepsilon^+ = 0, \quad k\cdot\varepsilon = 0 \tag{3.20}$$

and the light-cone and energy denominator is

$$D = p_a^- - k^- - p_c^- + i\varepsilon \quad . \tag{3.21}$$

Similarly, the Compton scattering diagrams of Fig.5c give

$$\mathcal{M}_{\gamma e\to\gamma e} = e^2 \sum_{\lambda=1,2} \frac{\bar{u}\not{\varepsilon}_c u_\lambda\ \bar{u}_\lambda \not{\varepsilon}_a u}{p^+ D} + e^2 \frac{\bar{u}\not{\varepsilon}_c\ \gamma^+ \not{\varepsilon}_a u}{2p^+} \tag{3.22}$$

$$D = k_a^- + p_\perp^{\prime\,2} - p^- + i\varepsilon$$

(This is analogous to the decomposition of the Feynman propagator $(\not{p} - m + i\varepsilon)^{-1}$ into positive and negative frequency components.)

Calculations in light-cone perturbation theory are often surprisingly simple since one can usually choose Lorentz frames for the external particles such that only a few time-orderings need to be considered. All the variables have a direct physical interpretation. The formalism is also ideal for computing helicity amplitudes directly without trace projection techniques. A list of all the gluon fermion vertices which are required as gauge theory calculations is given in Tables I and II of Ref. 19.

It is straightforward to implement ultraviolet renormalization in light-cone perturbation theory. We define truncated wavefunctions ψ^κ and a truncated Hamiltonian H^κ such that all intermediate states with $|\mathcal{P}| > \kappa^2$ are excluded. [45] Thus κ^{-1} is analogous to the lattice spacing in lattice field theory. Since QCD is renormalizable the effects of the neglected states are accounted for by the use of the running coupling constant $\alpha_s(\kappa^2)$ and running mass $m(\kappa^2)$, as long as κ^2 is sufficiently large compared to all physical mass thresholds. Completeness implies

$$\sum_{n,\lambda_i} \int \left[d^2k_\perp\right] \int [dx] |\psi_n^\kappa(x_i, k_{\perp i}; \lambda_i)|^2 = 1 - \mathcal{O}\left(\frac{m^2}{\kappa^2}\right) \tag{3.23}$$

The equation of state for the meson or baryon wavefunction in QCD is a set of coupled multiparticle equations (see Fig.5d):

$$\left[M^2 - \sum_{i=1}^{n} \left(\frac{k_\perp^2 + m^2}{x}\right)_i\right] \psi_n^\kappa = \sum_{n'} V_{nn'}^\kappa \, \psi_{n'}^\kappa \tag{3.24}$$

where M^2 is the eigenvalue and $V_{nn'}$ is the set of diagonal (from instantaneous gluon and fermion exchange) and off-diagonal (from the 3 and 4 particle vertices) momentum-space matrix elements dictated by the QCD rules. Because of the κ cutoff the equations truncate at finite n,n'. In analogy to non-relativistic theory, one can imagine starting with a trial wavefunction for the lowest $|q\bar{q}\rangle$ or $|qqq\rangle$ valence state of a meson or baryon and iterating the equations of motion to determine the lowest eigenstate Fock state wavefunctions and mass M. Invariance under changes in the cutoff scale provides an important check on the consistency of the results. Note that the general solution for the hadron wavefunction in QCD is expected to have Fock state components with arbitrary numbers of gluons and quark-antiquark pairs.

The two-particle "valence" light-cone Fock state wavefunction for mesons or positronium can also be related to the Bethe-Salpeter wavefunction evaluated at equal τ:

$$\int \frac{dk^-}{2\pi} \psi_{BS}(k;p) = \frac{u(x_1, \vec{k}_\perp)}{\sqrt{x_1}} \frac{\bar{v}(x_2, -\vec{k}_\perp)}{\sqrt{x_2}} \psi(x_i, \vec{k}_\perp) \tag{3.25}$$

$$+ \text{ negative energy components,}$$

where ψ satisfies an exact bound state equation [19]

$$\left[M^2 - \frac{k_\perp^2 + m_1^2}{x} - \frac{k_\perp^2 + m_2^2}{x_2}\right] \psi(x_i, \vec{k}_{\perp i}) \tag{3.26}$$

$$= \int_0^1 dy \int \frac{d^2\ell_\perp}{16\pi^3} \tilde{K}\left(x_i, \vec{k}_{\perp i}; y_i, \vec{\ell}_{\perp i}; M^2\right) \psi(y_i, \vec{\ell}_{\perp i})$$

The kernel $\tilde{K}$ is computed from the sum of all two-particle-irreducible contributions to the two-particle scattering amplitude. For example, the equation of motion for the $|e^+e^-\rangle$ Fock state of positronium reduces in the non-relativistic limit to $\left(k_\perp, \ell_\perp \sim \mathcal{O}(\alpha m),\ x = x_1 - x_2 \sim O(\alpha)\right)$ $M^2 = 4m^2 + 4m\varepsilon$

$$\left\{\varepsilon - \frac{k_\perp^2 + x^2 m^2}{m}\right\} \psi(x_i, k_\perp) \tag{3.27}$$

$$= (4x_1x_2) \int_{-1}^{1} dy \, m \int \frac{d^2\ell_\perp}{(2\pi)^3} \left[\frac{-e^2}{(\vec{k}_\perp - \vec{\ell}_\perp)^2 + (x-y)^2 m^2}\right] \psi(y_i, \ell_\perp)$$

The non-relativistic solution is ($\beta = \alpha m/2$) [19]

$$\psi(x_1,k_\perp) = \sqrt{\frac{m\beta^3}{\pi}}\ \frac{64\pi\beta\, x_1x_2}{\left[k_\perp^2 + (x_1-x_2)^2m^2 + \beta^2\right]^2}\begin{cases}\dfrac{u_+\bar v_+ - u_+\bar v_+}{\sqrt{2\,x_1x_2}}\\[2ex] \dfrac{u_+\bar v_+}{\sqrt{x_1x_2}}\end{cases} \tag{3.28}$$

for para and ortho states respectively.

More generally, we can make an (approximate) connection between the equal-time wavefunction of a composite system and the light-cone wavefunction by equating the off-shell propagator $\mathscr{E} = M^2 - \left(\sum_{i=1}^n k_i\right)^2$ in the two frames:

$$\mathscr{E} = \begin{cases} M^2 - \left(\sum_{i=1}^n q^o_{(i)}\right)^2, \quad \sum_{i=1}^n q_i = 0 \ \text{[C.M.]} \\[2ex] M^2 - \sum_{i=1}^n \left(\dfrac{k_\perp^2 + m^2}{x}\right)_i, \quad \sum \vec k_{\perp i} = 0, \quad \sum x_i = 1 \ \text{[L.C.]}\end{cases} \tag{3.29}$$

In addition we can identify

$$x_i = \frac{k_i^+}{p^+} \doteq \frac{(q^o + q^3)_i}{\sum_{j=1}^n q^o_{(j)}}, \quad \vec k_{\perp i} \doteq \vec q_{\perp i} \tag{3.30}$$

For a relativistic two particle state with a wavefunction which is a function of the off-shell variable $\mathscr{E}$ only, then we can identify ($m_1 = m_2 = m$, $x = x_1 - x_2$) [27]

$$\psi_{L.C.}\left(\frac{k_\perp^2 + m^2}{1 - x^2} - m^2\right) \doteq \psi_{C.M.}(\vec q^{\,2}) \tag{3.31}$$

In the non-relativistic limit, this corresponds to the identification $\vec q_\perp = \vec k_\perp$, $q_3^2 = x^2m^2$.

IV. MEASURES OF HADRONIC WAVE FUNCTIONS

A. Form Factors of Composite Systems

If we could solve the QCD equation of motion Eq. (3.24) for the light-cone wavefunctions ψ_n of a hadron then we could (in principle) calculate all of its electromagnetic properties. For example, to compute the elastic form factors $\langle p|J^\mu(0)|p+q\rangle$ of a hadron we choose the Lorentz frame [46]

$$p^\mu = (p^+,p^-,\vec p_\perp) = \left(P^+, \frac{M^2}{P^+}, \vec 0_\perp\right) \tag{4.1}$$

$$q^\mu = (q^+,q^-,\vec q_\perp) = \left(0, \frac{2p\cdot q}{p^+}, \vec q_\perp\right)$$

where $p^2 = (p+q)^2 = M^2$ and $-q^2 = Q^2 = q^2$. Then the only time ordering which contributes to the $\langle p|J^+|p+q\rangle$ matrix element is where the photon attaches directly to the $e_j\bar{u}_j\gamma^+u_j$ currents of the constituent quarks. The spin averaged form factor is [46,19] (see Fig.6a)

$$F(Q^2) = \sum_n \sum_j e_j \int [dx] \left[d^2k_\perp\right] \sum_{\lambda_i} \psi_n^{*\kappa}(x_i, \vec{k}'_{\perp i}; \lambda_i)\ \psi_n^{\kappa}(x_i, \vec{k}_{\perp i}; \lambda_i) \qquad (4.2)$$

where $\vec{k}'_j = \vec{k}_j + (1 - x_j)\vec{q}_\perp$ for the struck quark and $\vec{k}'_i = \vec{k}_i - x_i\vec{q}_\perp$ $(i \neq j)$ for the spectator quarks. (The $-x_i\vec{q}_\perp$ terms occur because the arguments $\vec{k}'_i$ are calculated relative to the direction of the final state hadron.) We choose $\kappa^2 \gg Q^2, M^2$. We note here the special advantage of light-cone perturbation theory: the current J^+ is diagonal in the Fock state basis.

Because of Eq. (3.23) the form factor is normalized to 1 at zero momentum transfer. We can also compute the helicity flip form factors in the same manner. [19,47] For example, the anomalous moment $a = F_2(0)$ of any spin 1/2 system can be written [47]

$$\frac{a}{M} = -\sum_j e_j \int [dx] \left[d^2k_i\right] \psi^{*\kappa}_{p\uparrow} \sum_{i\neq j} x_j \left(\frac{\partial}{\partial k_i^1} + i\frac{\partial}{\partial k_i^2}\right) \psi^{\kappa}_{p\downarrow} \quad . \qquad (4.3)$$

Explicit calculations of the electron anomalous moment in QED using this result are given in Ref. 47. We notice that in general all Fock states ψ_n^κ contribute to the anomalous moment of a system, although states with κ^2 much larger than the mean off-shell energy $\langle\mathcal{E}\rangle$ are not expected to be important. The general result (4.3) also includes the effects of the Lorentz boost of the wavefunction from p^μ to $(p+q)^\mu$. In particular, the Wigner spin rotation contributes to $F_2(q^2)$ and the charge radius $F_1'(q^2)$ in the $q^2 \to 0$ limit and can only be neglected in the limit of non-relativistic binding $\langle\mathcal{E}\rangle \ll M^2$. This effect gives non-trivial relativistic corrections [48] to nuclear magnetic moment calculations based on simple additivity $\vec{\mu} = \left\langle \sum_j \vec{\mu}_j \right\rangle$.

B. Form Factors of Mesons

Results such as Eqs. (4.2) and (4.3) are formally exact but useless unless we have complete knowledge of the hadronic or nuclear wave function. However, by making use of the impulse approximation and the smallness of the QCD running coupling constant, we can calculate features of elastic and inelastic large momentum transfer processes [19] without explicit knowledge of the wavefunction. For example consider the $|q\bar{q}\rangle$ Fock state component contribution to the pion form factor. Choosing $\kappa^2 = Q^2$, we have

$$F_\pi(Q^2) = \int_0^1 dx \int^Q \frac{d^2k_\perp}{16\pi^3}\, \psi^{*Q}(x, \vec{k}_\perp)\, \psi^Q\left(x, \vec{k}_\perp + (1-x)\vec{q}_\perp\right) \qquad (4.4)$$

$$+ \text{higher Fock state contributions} \quad .$$

The bound state wavefunctions are peaked at low transverse momentum, i.e., small off-shell energy $\mathcal{E}$. Thus the leading contribution at large Q^2 come from the regimes (a) $\vec{k}_\perp^2 \ll \vec{q}_\perp^2$ and (b) $\left(\vec{k}_\perp + (1-x)\vec{q}_\perp\right)^2 \ll \vec{q}_\perp^2$. Thus

$$F_\pi^{(a)}(Q^2) \simeq \int_0^1 dx\ \phi(x,Q)\ \psi^Q\left(x, (1-x)\vec{q}_\perp\right) \qquad (4.5)$$

where [19]

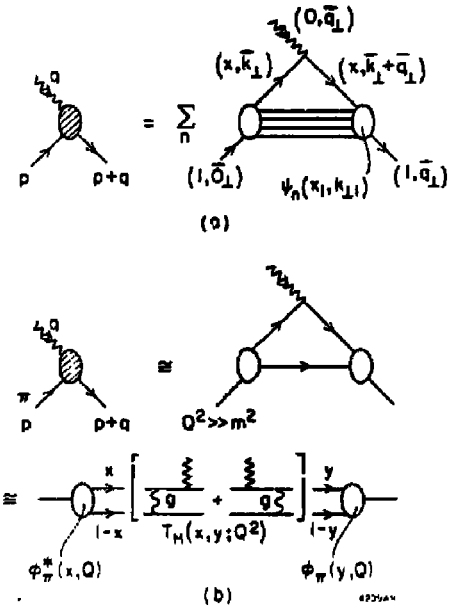

Fig. 6 (a) Calculation of current matrix elements in light-cone perturbation theory. (b) Valence Fock state contribution to the large momentum transfer meson form factor. T_H is computed for zero mass quarks q and $\bar{q}$ parallel to the pion momentum.

$$\phi(x,Q) \equiv \int^{Q} \frac{d^2k}{16\pi^3}\, \psi^Q(x,k_\perp) \quad . \tag{4.6}$$

If we simply iterate the one-gluon exchange kernel V_1 in the equation of motion for ψ, then for $q_\perp^2 \gg \langle k_\perp^2 \rangle$

$$\psi^Q\big(x,(1-x)q_\perp\big) \cong \int_0^1 dy \int^{Q} \frac{d^2k_\perp}{16\pi^3}\, \frac{V_1\big(x,(1-x)q_\perp;y,k_\perp\big)\psi^Q(y,k_\perp)}{-q_\perp^2(1-x)/x} \tag{4.7}$$

$$\cong \int_0^1 dy\, \frac{V_1\big(x,(1-x)q_\perp;y,0_\perp\big)}{-q_\perp^2(1-x)/x}\, \phi(y,Q) \quad .$$

Thus we can write the gluon exchange contribution to the form factor in the form; [11],19] (see Fig.6b)

$$F_\pi(Q^2) = \int_0^1 dx\, dy\, \phi^*(y,Q)\, T_H(x,y;\, Q)\, \phi(y,Q) \tag{4.8}$$

where

$$T_H = \frac{16\pi C_F \alpha_s(Q^2)}{Q^2}\left[\frac{e_1}{(1-y)(1-x)} + \frac{e_2}{xy}\right] \tag{4.9}$$

is the "hard scattering amplitude" for scattering collinear constituents q and $\bar{q}$ from the initial to the final direction. The color factor is $C_F = (n_c^2-1)/2n_c =$

4/3. The "distribution amplitude" $\phi(x,Q)$ is the amplitude for finding the $|q\bar{q}\rangle$ Fock state in the pion collinear up to the scale Q. (It is analogous to the wavefunction at the origin in non-relativistic calculations.) The distribution amplitude enters universally in all large momentum transfer exclusive amplitudes and is a process-independent measure of the valence quark distribution in each hadron; its (logarithmic) dependence on Q^2 can be determined directly from the operator product expansion or the light-cone or from an evolution equation, as we discuss below.

Thus the simplest estimate for the asymptotic behavior of the meson form factor is $F_\pi(Q^2) \sim \alpha_s(Q^2)/Q^2$. To see if this is correct we must examine the higher order corrections: [19]

(1) Contributions from higher particle number Fock states $|q\bar{q}g\rangle$, $|q\bar{q}q\bar{q}\rangle$, etc. are power-law suppressed since (in light-cone gauge) the numerator couplings cannot compensate the extra fall-off in Q^2 from the extra energy denominators.

(2) All infrared singularities and contributions from soft ($\ell_\perp \to 0$) gluons cancel in color singlet matrix elements. (It is interesting to note that the quark (Sudakov) form factor falls faster at large Q^2 than $F_\pi(Q^2)$.)

(3) Vertex and vacuum polarization corrections to the T_H are higher order in $\alpha_s(Q^2)$ since we choose $\kappa^2 = Q^2$. The effective argument of α_s in T_H is $Q^2 = xyQ^2$ or $(1-x)(1-y)Q^2$ corresponding to the actual momentum transfer carried by the gluon.

(4) By definition, $\phi(x,\kappa^2)$ sums all (reducible) contributions from low momentum transfer gluon exchange in the $q\bar{q}$ wavefunction. Hard gluon contributions with $|\mathcal{E}| > \kappa^2$ and the irreducible (cross-graph, etc.) give contributions to T_H which are higher order $\alpha_s(Q^2)$. By analyzing the denominators in T_H one can show that the natural $\mathcal{E}$ cutoff for $\phi(x,\kappa)$ which minimizes higher order contributions is $\kappa^2 = Q_x^2 = Q^2 \min\left\{\frac{x}{1-x}, \frac{1-x}{x}\right\}$.

(5) Although T_H is singular at $x \to 0,1$, the endpoint behavior of $\phi(x,Q^2) \sim x^\epsilon$, $(1-x)^\epsilon$ ($\epsilon > 0$) is sufficient to render this region harmless.

C. The Meson Distribution Amplitude

The essential prediction of QCD for the pion form factor is the power-law behavior [8] $F_\pi \sim 1/Q^2$, with logarithmic corrections from the explicit powers of $\alpha_s(Q^2)$ in T_H and the Q^2 dependence of the distribution amplitudes $\phi(x,Q^2)$.

The variation of ϕ with Q^2 comes from the upper limit of the $\vec{k}_\perp$ integration (since $\psi \sim 1/k_\perp^2$) and the renormalization scale dependence:

$$\phi^Q(x,\vec{k}_\perp) = \frac{Z_2(Q)}{Z_2(Q_0)}\,\psi^{Q_0}(x,\vec{k}_\perp) \tag{4.10}$$

due to the vertex and self-energy insertions. Thus

$$Q^2 \frac{\partial}{\partial Q^2}\phi(x,Q) = \frac{Q^2}{16\pi^2}\psi^Q(x,\vec{q}_\perp) + \frac{d}{d\,\log Q^2}\log Z_2(Q^2)\;\phi(x,Q) \quad . \tag{4.11}$$

To order $\alpha_s(Q^2)$ we can compute $Q^2\psi$ from one-gluon exchange (as in Eq. (4.7)), and $d\,\log Z_2(Q^2)/d\,\log Q^2 = \alpha_s(Q^2)\gamma_P/4\pi$. Setting $\phi(x,Q) = x(1-x)\,\tilde{\phi}(x,Q) = x_1x_2\tilde{\phi}$, we obtain an "evolutional equation" [19]

$$x_1x_2Q^2\frac{\partial}{\partial\,\log Q^2}\tilde{\phi}(x_i,Q) = \frac{\alpha_s(Q^2)}{4\pi}\int_0^1 [dy]\;V(x_i,y_i)\;\phi(y,Q) \tag{4.12}$$

where

$$V(x_1,y_1) = 2C_F\left\{x_1y_2\,\theta(y_1-x_1)\left(\delta_{h_1\bar{h}_2}+\frac{\Delta}{y_1-x_1}\right)+(1\leftrightarrow 2)\right\} \tag{4.13}$$

($\delta_{h_1\bar{h}_2}=1$ when the q and $\bar{q}$ helicities are opposite) and

$$\Delta\tilde{\phi}(y_1,Q) = \tilde{\phi}(y_1,Q) - \tilde{\phi}(x_1,Q) \quad . \tag{4.14}$$

The $\tilde{\phi}(x_1,Q)$ subtraction is due to the $\gamma_F\phi$ term — i.e., the infrared dependence at $y_1 = x_1$ is cancelled for color singlet hadrons. Thus given the initial condition $\phi(x_1,Q_0)$, perturbation theory determines the evolution of $\phi(x,Q)$ for $Q > Q_0$. The solution to the evolution equation is [19]

$$\phi(x_1,Q) = x_1x_2\sum_{n=0}^{\infty} a_n(Q_0^2)\,C_n^{3/2}(x_1-x_2)(\log Q^2/\Lambda^2)^{-\gamma_n} \tag{4.15}$$

where the Gegenbauer polynomials $C_n^{3/2}$ (orthogonal on $\int [dx]x_1x_2$) are eigenfunctions of $V(x_1,y_1)$. The corresponding eigenvalues are the "non-singlet" anomalous dimensions:

$$\gamma_n = \frac{C_F}{\beta_0}\left[1+4\sum_{2}^{n+1}\frac{1}{k}-\frac{2\delta_{h_1\bar{h}_2}}{(n+1)(n+2)}\right] \geq 0 \quad . \tag{4.16}$$

These results can also be derived by using the operator product expansion for the distribution amplitude. [49] By definition

$$\phi(x,Q) = \Lambda^+\int\frac{dz^-}{2\pi}\,e^{ixz^-/2}\,\langle 0|\bar{\psi}(z)\psi(0)|\pi\rangle^Q\Big|_{z^+=0,\ z^2=-z_\perp^2=\mathcal{O}(-1/Q^2)} \tag{4.17}$$

(Λ^+ is the positive energy spinor projection operator). The relative separation of the q and $\bar{q}$ thus approaches the light-cone $z^2 = 0$ as $Q^2 \to \infty$. Equation (4.16) then follows, by expanding $\psi(z)\psi(0)$ in local operators.

The coefficients a_n are determined from $\phi(x_1,Q_0)$:

$$a_n\left(\log\frac{Q^2}{\Lambda^2}\right)^{-\gamma_n} = \frac{2(2n+3)}{(2+n)(1+n)}\int_{-1}^{1} d(x_1-x_2)\,C_n^{3/2}(x_1-x_2)\,\phi(x_1,Q_0) \quad . \tag{4.18}$$

For $Q^2 \to \infty$, only the leading $\gamma_0 = 0$ term survives

$$\lim_{Q^2\to\infty}\phi(x,Q) = a_0x_1x_2 \tag{4.19}$$

where

$$\frac{a_0}{6} = \int_0^1 dx\,\phi(x,Q) = \int_0^1 dx\int^Q\frac{d^2k_\perp}{16\pi^3}\,\psi^Q(x,k_\perp) \tag{4.20}$$

is the meson wavefunction at the origin as measured in the decay $\pi \to \mu\nu$:

$$\frac{a_0}{6} = \frac{1}{2\sqrt{n_c}}f_\pi \quad . \tag{4.21}$$

More generally, the leptonic decay ($\rho^0 \to e^+e^-$, etc.) of each meson normalizes its distribution amplitude by the "sum rule"

$$\int_0^1 dx\, \phi_M(x,Q) = \frac{f_M}{2\sqrt{n_c}} \quad , \tag{4.22}$$

independent of Q. The fact that $f_\pi \neq 0$ implies that the probability of finding the $|q\bar{q}\rangle$ Fock state in the pion is non-zero. In fact all the Fock states wavefunctions $\psi_n^\kappa(x_i, \vec{k}_{\perp i})(|\vec{\mathcal{C}}| < \kappa^2)$ are well-defined, even in the infrared limit $x_i \to 0$ (since $|\vec{\mathcal{C}}| \sim \langle k_\perp^2\rangle/x_i$ and $\langle k_\perp^2\rangle$ is non-zero for a state of finite radius).

The pion form factor at high Q^2 can thus be written [11,19,50]

$$F_\pi(Q^2) = \int_0^1 dx\, \phi^*(x,Q) T_H(x,y;\, Q)\, \phi(y,Q) \tag{4.23}$$

$$T_H = \frac{16}{3\pi} \frac{\alpha_s\big((1-x)(1-y)Q^2\big)}{(1-x)(1-y)Q^2} \quad .$$

Thus

$$F_\pi(Q^2) = \left|\sum_{n=0} a_n \log^{-\gamma_n} Q^2/\Lambda^2\right|^2 \frac{16\pi}{3} \frac{\alpha_s(\bar{Q}^2)}{Q^2} \times \left[1 + \mathcal{O}\left(\frac{\alpha_s(Q^2)}{\pi}\right) + \mathcal{O}\left(\frac{\kappa^2}{Q^2}\right)\right] \tag{4.24}$$

where $\bar{Q}^2 \cong \langle(1-x)(1-y)\rangle Q^2$. Finally, for the asymptotic limit where only the leading anomalous dimension contributes: [51]

$$\lim_{Q^2 \to \infty} F_\pi(Q^2) = 16\pi f_\pi^2 \frac{\alpha_s(Q^2)}{Q^2} \quad . \tag{4.25}$$

The analysis of the $F_{\pi\gamma}(Q^2)$ form factor, measureable in $ee \to ee\pi^0$ reactions, proceeds in a similar manner (see Fig.1a). An interesting result is [19]

$$\alpha_s(Q^2) = \frac{F_\pi(Q^2)}{4\pi Q^2 |F_{\pi\gamma}(Q^2)|^2}\left[1 + \mathcal{O}\left(\frac{\alpha_s(Q^2)}{\pi}\right)\right] \tag{4.26}$$

which provides a definition of α_s independent of the form of the distribution function ϕ_π. Higher order corrections to $F_\pi(Q^2)$ and $F_{\pi\gamma}(Q^2)$ are discussed in Ref. 50.

D. Large Momentum Transfer Exclusive Processes [19]

The meson form factor calculation which we outlined above is the prototype for the calculation of the QCD hard scattering contribution for the whole range of exclusive processes at large momentum transfer. Away from possible special points in the x_i integrations (see below) a general hadronic amplitude can be written to leading order in $1/Q^2$ as a convolution of a connected hard-scattering amplitude T_H convoluted with the meson and baryon distribution amplitudes:

$$\phi_M(x,Q) = \int^{|\mathcal{E}|<Q^2} \frac{d^2k_\perp}{16\pi^2}\, \psi^Q_{q\bar{q}}(x,\vec{k}_\perp) \quad , \tag{4.27a}$$

and

$$\phi_B(x_i,Q) = \int^{|\mathcal{E}|<Q^2} [d^2k_\perp]\, \psi_{qqq}(x_i,\vec{k}_{\perp i}) \quad . \tag{4.27b}$$

The hard scattering amplitude T_H is computed by replacing each external hadron line by massless valence quarks each collinear with the hadrons momentum $p_i^\mu \cong x_i\, p_H^\mu$. For example, the baryon form factor at large Q^2 has the form [9,19] (See Fig.2a and Fig.7.)

$$G_M(Q^2) = \int [dx][dy]\, \phi^*(y_i,\tilde{Q})\, T_H(x,y;\, Q^2)\, \phi(s,\tilde{Q}) \tag{4.28}$$

where T_H is the $3q + \gamma \to 3q'$ amplitude. (The optimal choice for $\tilde{Q}$ is discussed in Ref. 19.) For the proton and neutron we have to leading order ($C_B = 2/3$)

$$T_p = \frac{128\pi^2\, C_B^2}{\left(Q^2 + M_0^2\right)^2}\, T_1 \tag{4.29}$$

$$T_n = \frac{128\pi^2\, C_B^2}{3\left(Q^2 + M_0^2\right)^2}\, \left[T_1 - T_2\right] \tag{4.30}$$

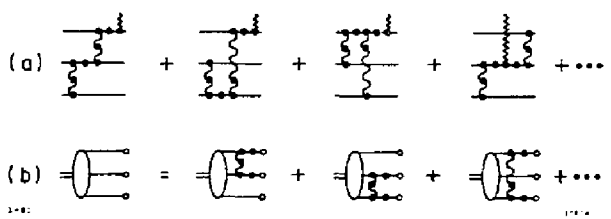

Fig. 7 (a) Leading contributions to T_H for the baryon form factors corresponding to the four terms of Eqs. (4.31) and (4.32), respectively. (b) Contributions to the kernel for the evolution of the baryon distribution amplitude.

where

$$T_1 = -\frac{\alpha_s(x_3y_3Q^2)\ \alpha_s\left((1-x_1)(1-y_1)Q^2\right)}{x_3(1-x_1)^2\ y_3(1-y_1)^2} + \frac{\alpha_s(x_2y_2Q^2)\ \alpha_s\left((1-x_1)(1-y_1)Q^2\right)}{x_2(1-x_1)^2\ y_2(1-y_1)^2} \tag{4.31}$$

$$- \frac{\alpha_s(x_2y_2Q^2)\ \alpha_s(x_2y_2Q^2)}{x_2x_3(1-x_3)\ y_2y_3(1-y_1)} \quad ,$$

and

$$T_2 = -\frac{\alpha_s(x_1y_1Q^2)}{x_1x_3(1-x_1)}\frac{\alpha_s(x_3y_3Q^2)}{y_1y_3(1-y_3)} \quad . \tag{4.32}$$

T_1 corresponds to the amplitude where the photon interacts with the quarks (1) and (2) which have helicity parallel to the nucleon helicity, and T_2 corresponds to the amplitude where the quark with opposite helicity is struck. The running coupling constants have arguments $\hat{Q}^2$ corresponding to the gluon momentum transfer of each diagram. Only large Q^2 behavior is predicted by the theory; we utilize the parameter M_0 to represent the effect of power-law suppressed terms from mass insertions, higher Fock states, etc.

The Q^2-evolution of the baryon distribution amplitude can be derived from the operator product expansion of three quark fields or from the gluon exchange kernel, in parallel with the derivation of (4.12). The baryon evolution equation to leading order in α_s is [19]

$$x_1x_2x_3\left|\frac{\partial}{\partial\zeta}\tilde{\phi}(x_i,Q) + \frac{3}{2}\frac{C_F}{\beta_0}\tilde{\phi}(x_i,Q)\right| = \frac{C_B}{\beta_0}\int_0^1 [dy]\, V(x_i,y_i)\,\tilde{\phi}(y_i,Q) \quad . \tag{4.33}$$

Here $\phi = x_1x_2x_3\tilde{\phi}$, $\zeta = \log(\log Q^2/\Lambda^2)$ and (see Fig. 7b)

$$V(x_i,y_i) = 2x_1x_2x_3\sum_{i\neq j}\theta(y_i-x_i)\,\delta(x_k-y_k)\,\frac{y_j}{x_j}\left(\frac{\delta_{h_i\bar{h}_j}}{x_i+x_j} + \frac{\Delta}{y_i-x_i}\right) \tag{4.34}$$

$$= V(y_i,x_i) \quad .$$

The infrared singularity at $x_i = y_i$ is cancelled because the baryon is a color singlet. The evolution equation has the general solution

$$\phi(x_i,Q) = x_1x_2x_3\sum_{n=0}^{\infty} a_n\,\tilde{\phi}_n(x_i)\left(\log\frac{Q^2}{\Lambda^2}\right)^{-\gamma_n^B} \quad . \tag{4.35}$$

The leading (polynomial) eigensolution $\tilde{\phi}_n(x_i)$ and corresponding baryon anomalous dimensions are given in Refs. 19 and 52. Thus at large Q^2, the nucleon magnetic form factors have the form [9,19]

$$F_M(Q^2) \to \frac{\alpha_s^2(Q^2)}{Q^4}\sum_{n,m} b_{nm}\left(\log\frac{Q^2}{\Lambda^2}\right)^{-\gamma_n^B-\gamma_n^B}\left[1 + \mathcal{O}\left(\alpha_s(Q^2), \frac{m^2}{Q^2}\right)\right] \quad . \tag{4.36}$$

We can also use this result to obtain results for ratios of various baryon and isobar form factors assuming isospin or SU(3)-flavor symmetry for the basic wavefunction structure. Results for the neutral weak and charged weak form factors assuming standard SU(2) × U(1) symmetry are given in Ref. 46.

As we see from Eq. (4.28), the integration over x_i and y_i have potential endpoint singularities. However, it is easily seen that any anomalous contribution (e.g., from the region $x_2,x_3 \sim \mathcal{O}(m/Q)$, $x_1 \sim 1 - \mathcal{O}(m/Q)$) is asymptotically suppressed at large Q^2 by a Sudakov form factor arising from the virtual correction to the $\bar{q}vq$ vertex when the quark legs are near-on-shell ($p^2 \sim \mathcal{O}(mQ)$). [19,54] This Sudakov suppression of the endpoint region requires an all orders resummation of perturbative contributions, [57] and thus the derivation of the baryon form factors is not as rigorous as for the meson form factor, which has no such endpoint singularity.

The most striking feature of the QCD prediction (4.36) is the $1/Q^4$ power-law behavior of G_M^p as G_M^n. The power-law dependence [8] reflects:

(1) The essential scale-invariance of the qq scattering subprocesses within T_H.

(2) The fact that the minimal Fock state of a baryon is the 3-quark state.

We will discuss the phenomenology of the baryon form factors and the resulting constraints on the baryon wavefunction in Sec. VI.

In the case of hadron scattering amplitudes A+B → C+D, photoproduction, Compton scattering, etc., the leading hard scattering QCD contribution at large momentum transfer $Q^2 = tu/s$ has the form [19] (helicity labels and suppressed)(see Fig.8)

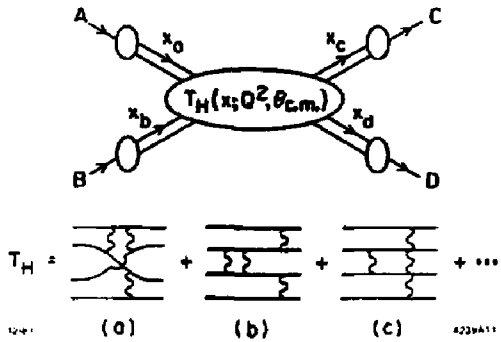

Fig. 8 QCD contributions to meson-meson scattering at large momentum transfer. Diagram (c) corresponds to the Landshoff pinch singularity which is suppressed by quark form factor effects.

$$\mathcal{M}_{A+B\to C+D}(Q^2,\theta_{c.m.}) = \int [dx]\phi_C(x_c,\tilde{Q})\ \phi_D(x_d,\tilde{Q})\ T_H(x_i;\ Q^2,\theta_{c.m.}) \qquad (4.37)$$

$$\times\ \phi_A(x_a,\tilde{Q})\ \phi_B(x_b,\tilde{Q}) \quad .$$

The essential behavior of the amplitude is determined by T_H, computed where each hadron is replaced by its (collinear) quark constituents. We note again that T_H is "collinear irreducible," i.e., the transverse momentum integrations of all reducible loop integration are restricted to $k_\perp^2 > \mathcal{O}(Q^2)$ since the small $k_\perp$ region is already contained in ϕ. If the internal propagators in T_H are all far-off-shell $\mathcal{O}(Q^2)$ (as in Fig.8a) then a perturbative expansion in $a_s(Q^2)$ can be carried out. However, this is not true for all hadron-hadron scattering amplitudes since on can have multiple quark-quark scattering processes which allow near-on-shell propagation in intermediate states at finite values of the x_i. [17] The classic example is meson-meson scattering, where two pairs of quarks scatter through the same angle (see Fig.7c). However, the near-on-shell region of integration is again suppressed by Sudakov factors. (Physically this suppression occurs because the near-on-shell quarks must scatter without radiating gluons.) A model calculation by MUELLER [10] for $\pi-\pi$ scattering in QCD (using an exponentiated form of the Sudakov form factor) shows that the leading contribution comes in fact from the off-shell region $|k^2| \sim \mathcal{O}(Q^2)^{1-c}$ where $c = (2c+1)^{-1}$, $c = 8C_F/(11 - 2/3\ n_f)$ (for four flavors $c \cong 0.281$). This region gives the contribution [10]

$$\mathcal{M}_{\pi\pi\to\pi\pi} \sim \mathcal{O}(Q^2)^{-3/2 - c\ln(2c+1/2c)} \qquad (4.38)$$

$$\cong (Q^2)^{-1.922}$$

compared to $(Q^2)^{-2}$ from the hard scattering $|k^2| \sim \mathcal{O}(Q^2)$ region.

Thus, even when pinch singularities are present, the far-off-shell hard scattering quark and gluon processes dominate large momentum transfer hadron scattering amplitudes. Given this result, we can abstract some general QCD features common to all exclusive processes at large momentum transfer:

(1) All of the non-perturbative bound state physics is isolated in the process-independent distribution amplitudes.

(2) The nominal power-law behavior of an exchange amplitude is $(1/Q)^{n-4}$ where n is the number of external elementary particles (quarks, gluons, leptons, photons in T_H). This immediately implies the dimensional counting rules: [8]

$$\frac{d\sigma}{dt}(A+B \to C+D) \sim \left(\frac{1}{Q^2}\right)^{n-2} f(\theta_{c.m.}) \tag{4.39}$$

where $n = n_A + n_B + n_C + n_D$, and

$$F_H(Q^2) \sim \left(\frac{1}{Q^2}\right)^{n_H - 1} \tag{4.40}$$

where F_H is the helicity-conserving [18,19] form factor. These power-law predictions are modified by (a) the Q^2-dependence of the factors of α_s in T_H, (b) the Q^2-evolution of the distribution amplitudes and (c) a possible small power associated with the almost complete Sudakov suppression of pinch singularities in hadron-hadron scattering. The dimensional-counting rules appear to be experimentally well-established for a wide variety of processes (see Ref. 19 and Fig.9):

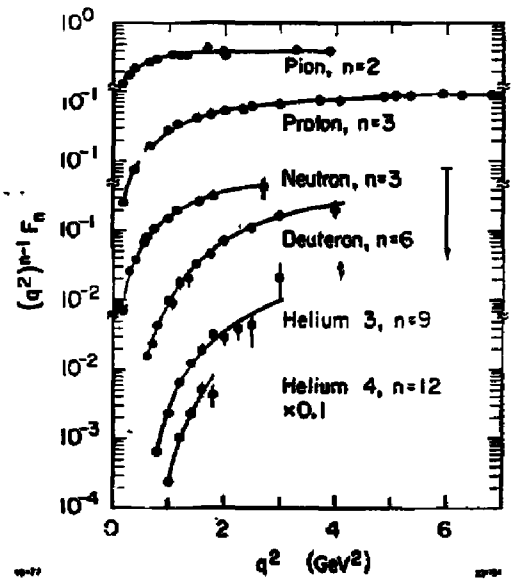

Fig. 9 Hadronic form factors multiplied by $(Q^2)^{n-1}$. (From Ref. 1.)

$$G_M(Q^2) \sim (Q^2)^{-2} \quad , \quad F_\pi(Q^2) \sim (Q^2)^{-1} \tag{4.41}$$

and

$$\frac{d\sigma}{dt}(\gamma p \to \pi p) \sim (Q^2)^{-7} \tag{4.42}$$

$$\frac{d\sigma}{dt}(\pi p \to \pi p) \sim (Q^2)^{-8}$$

$$\frac{d\sigma}{dt}(pp \to pp) \sim (Q^2)^{-10}$$

$$\frac{d\sigma}{dt}(\gamma p \to \gamma p) \Big/ \frac{d\sigma}{dt}(\gamma p \to \pi p) \sim Q^2$$

at fixed $\theta_{c.m.}$. The application to $\gamma\gamma \to M\bar{M}$ processes is discussed in Sec. IV-E.

(3) Since the distribution amplitudes ϕ_M and ϕ_B are $L_z = 0$ angular momentum projections of the hadronic wavefunctions, the sum of the quark spin along the hadron's momentum equals the hadron spin: [18]

$$\sum_{i \in H} S_i^z = S_H^z \tag{4.43}$$

(In contrast, in inclusive reactions there are any number of non-interacting quark and gluon spectators, so that the spin of the interacting constituents is only statistically related to the hadron spin — except possibly at the edge of phase-space $x \sim 1$.) Furthermore, since all propagators in T_H are hard, the quark and hadron masses can be neglected at large Q^2 up to corrections of order $\sim m/Q$. The vector gluon interactions conserve quark helicity when all masses are neglected. Thus total quark helicity is conserved in T_H at large Q^2. Combining this with (4.43), we have the QCD selection rule:

$$\sum_{\text{initial}} \lambda_H = \sum_{\text{final}} \lambda_H \tag{4.44}$$

i.e., total hadron helicity is conserved up to corrections of order $\mathcal{O}(m/Q)$.

Hadron helicity conservation thus applies for all large momentum transfer exclusive amplitudes involving light meson and baryons. Notice that the photon spin is not important: QCD predicts that $\gamma p \to \pi p$ is proton helicity conserving at fixed $\theta_{c.m.}$, $s \to \infty$, independent of the photon polarization. Exclusive amplitudes which involve hadrons with quarks or gluons in higher orbital angular momentum states are also suppressed by powers of the momentum transfer. An important corollary of this rule is that helicity-flip form factors are suppressed, e.g.:

$$F_{2p}(Q^2) \Big/ F_1(Q^2) \sim \mathcal{O}(m^2/Q^2) \quad . \tag{4.45}$$

The helicity rule, Eq. (4.44), is one of the most characteristic features of QCD, being a direct consequence of the gluon's spin. A scalar or tensor gluon-quark coupling flips the quark's helicity. Thus, for such theories, helicity may or may not be conserved in any given diagram contributing to T_H, depending upon the number of interactions involved. Only for a vector theory, like QCD, can we have a helicity selection rule valid to all orders in perturbation theory.

The study of timelike hadronic form factors using e^+e^- colliding beams can provide very sensitive tests of this rule, since the virtual photon in $e^+e^- \to \gamma^* \to h_A\bar{h}_B$ always has spin ± 1 along the beam axis at high energies. Angular momentum conservation implies that the virtual photon can "decay" with one of only two possible angular distributions in the center of momentum frame: $(1 + \cos^2\theta)$ for $|\lambda_A - \lambda_B| = 1$, and $\sin^2\theta$ for $|\lambda_A - \lambda_B| = 0$ where $\lambda_{A,B}$ are the helicities of hadron $h_{A,B}$. Hadronic helicity conservation, Eq. (4.44), as required by QCD greatly restricts the

possibilities. It implies that $\lambda_A + \lambda_B = 0$ (since the photon carries no "quark helicity"), or equivalently that $\lambda_A - \lambda_B = 2\lambda_A = -2\lambda_B$. Consequently, angular momentum conservation requires $|\lambda_A| = |\lambda_B| = 1/2$ for baryons, and $|\lambda_A| = |\lambda_B| = 0$ for mesons; furthermore, the angular distributions are now completely determined:

$$\frac{d\sigma}{d\cos\theta}(e^+e^- \to B\bar{B}) \propto 1 + \cos^2\theta \quad \text{(baryons)} \tag{4.46}$$

$$\frac{d\sigma}{d\cos\theta}(e^+e^- \to M\bar{M}) \propto \sin^2\theta \quad \text{(mesons)} \tag{4.47}$$

We emphasize that these predictions are far from trivial for vector mesons and for all baryons. For example, one expects distributions like $1 + \alpha\cos^2\theta$, $-1 < \alpha < 1$, in theories with a scalar or tensor gluon. So simply verifying these angular distributions would give strong evidence in favor of a vector gluon.

The power-law dependence in s of these cross sections is also predicted in QCD, using the dimensional counting rule. Such "all orders" predictions for QCD allowed processes are summarized in Table III.

Table III Exclusive channels in e^+e^- annihilation. The $h_A\bar{h}_B\gamma^*$ couplings in allowed processes are $-ie(p_A - p_B)^\mu F(s)$ for mesons, $-ie\bar{v}(p_B)\gamma^\mu G(s)u(p_A)$ for baryons, and $-ie^2\varepsilon_{\mu\nu\rho\sigma}p_M^\rho\varepsilon^\sigma p_\gamma^\nu F_{M\gamma}(s)$ for meson-photon final states. Similar predictions apply to decays of heavy-quark vector states, like the $\psi,\psi',\ldots$, produced in e^+e^- collisions.

	$e^+e^- \to h_A(\lambda_A)\,\bar{h}_B(\lambda_B)$	Angular Distribution	$\frac{\sigma(e^+e^- \to h_A\bar{h}_B)}{\sigma(e^+e^- \to \mu^+\mu^-)}$
Allowed in QCD	$e^+e^- \to \pi^+\pi^-, K^+K^-$	$\sin^2\theta$	$\frac{1}{4}\lvert F(s)\rvert^2 \sim c/s^2$
	$\rho^+(0)\rho^-(0), K^{*+}K^{*-}$	$\sin^2\theta$	$\frac{1}{4}\lvert F(s)\rvert^2 \sim c/s^2$
	$\pi^0\gamma(\pm1), \eta\gamma, \eta'\gamma$	$1 + \cos^2\theta$	$(\pi\alpha/2)s\lvert F_{M\gamma}(s)\rvert^2 \sim c/s$
	$e^+e^- \to p(\pm\tfrac{1}{2})\bar{p}(\mp\tfrac{1}{2}), n\bar{n}, \ldots$	$1 + \cos^2\theta$	$\lvert G(s)\rvert^2 \sim c/s^4$
	$p(\pm\tfrac{1}{2})\bar{\Delta}(\mp\tfrac{1}{2}), \bar{n}\Delta, \ldots$	$1 + \cos^2\theta$	$\lvert G(s)\rvert^2 \sim c/s^4$
	$\Delta(\pm\tfrac{1}{2})\bar{\Delta}(\mp\tfrac{1}{2}), \gamma^*\gamma^*, \ldots$	$1 + \cos^2\theta$	$\lvert G(s)\rvert^2 \sim c/s^4$
Suppressed in QCD	$e^+e^- \to \rho^+(0)\rho^-(\pm1), \pi^+\rho^-, K^+K^{*-}, \ldots$	$1 + \cos^2\theta$	$< c/s^3$
	$\rho^+(\pm1)\rho^-(\pm1), \ldots$	$\sin^2\theta$	$< c/s^3$
	$e^+e^- \to p(\pm\tfrac{1}{2})\bar{p}(\pm\tfrac{1}{2}), p\bar{n}, \Delta\bar{\Delta}, \ldots$	$\sin^2\theta$	$< c/s^5$
	$p(\pm\tfrac{1}{2})\bar{\Delta}(\pm\tfrac{1}{2}), \Delta\bar{n}, \ldots$	$1 + \cos^2\theta$	$< c/s^5$
	$\Delta(\pm\tfrac{1}{2})\bar{\Delta}(\pm\tfrac{1}{2}), \ldots$	$\sin^2\theta$	$< c/s^5$

Processes suppressed in QCD are also listed there; these all violate hadronic helicity conservation, and are suppressed by powers of m^2/s in QCD. This would not necessarily be the case in scalar or tensor theories.

The exclusive decays of heavy quark atoms ($\psi,\psi',\ldots$) into light hadrons can also be analyzed in QCD. [18] The decay $\psi \to p\bar{p}$ for example proceeds via diagrams such as those in Fig.2b. Since ψ's produced in e^+e^- collisions must also have spin 1 along the beam direction and since they can only couple to light quarks via gluons, all the properties listed in Table III apply to ψ, ψ', Υ, Υ',... decays as well. There are considerable experimental data for the ψ and ψ' decays. [55]

Perhaps the most significant tests are the decays $\psi,\psi' \to p\bar{p}, n\bar{n}, \ldots$. The predicted angular distribution $1 + B^2 \cos^2\theta$ is consistent with published data. [35] This is important evidence favoring a vector gluon since scalar or tensor gluon theories would predict a distribution of $\sin^2\theta + \mathcal{O}(\alpha_s)$. Dimensional counting rules can be checked by comparing the ψ and ψ' rates into $p\bar{p}$, normalized by the total rates into light-quark hadrons so as to remove dependence upon the heavy-quark wavefunctions. Theory predicts

$$\frac{BR(\psi \to p\bar{p})}{BR(\psi' \to p\bar{p})} \sim \left(\frac{M_{\psi'}}{M_\psi}\right)^8 \tag{4.48}$$

where

$$BR(\psi \to p\bar{p}) \equiv \frac{\Gamma(\psi \to p\bar{p})}{\Gamma(\psi \to \text{light-quark hadrons})} \quad . \tag{4.49}$$

Existing data suggest a ratio $(M_{\psi'}/M_\psi)^n$ with $n \sim 6 \pm 3$, in good agreement with QCD.

Many more examples of exclusive reactions which test the basic scaling laws and spin structure of QCD are discussed in Refs. 18 and 19. The essential point is that exclusive reactions have the potential for isolating the QCD hard-scattering subprocesses in situations where the helicities of all the interaction constituents are controlled. In contrast, in inclusive reactions the absence of restrictions on the spectator quark and gluons allows only a statistical correlation between the constituent and hadronic helicities.

E. Two-Photon Processes [12]

One of the most important applications of perturbative QCD is to the two-photon processes $d\sigma/dt\ (\gamma\gamma \to M\bar{M})$, $M = \pi,\kappa,\rho,\omega$ at large $s = (k_1 + k_2)^2$ and fixed $\theta_{c.m.}$. These reactions, which can be studied in $e^+e^- \to e^+e^-M\bar{M}$ processes, provide a particularly important laboratory for testing QCD since these "Compton" processes are, by far, the simplest calculable large-angle exclusive hadronic scattering reactions. As we discuss below, the large-momentum-transfer scaling behavior, the helicity structure, and often even the absolute normalization can be rigorously computed for each two-photon channel.

Conversely, the angular dependence of the $\gamma\gamma \to M\bar{M}$ amplitudes can be used to determine the shape of the process-independent meson "distribution amplitudes," $\phi_M(x,Q)$, the basic short-distance wavefunctions which control the valence quark distributions in high momentum transfer exclusive reactions.

A critically important feature of the $\gamma\gamma \to M\bar{M}$ amplitude is that the contributions of LANDSHOFF [17] pinch singularities are power-law suppressed at the Born level -- even before taking into account Sudakov form factor suppression. There are also no anomalous contributions from the $x \sim 1$ endpoint integration region. Thus, as in the calculation of the meson form factors, each fixed-angle helicity amplitude can be written to leading order in $1/Q$ in the factorized form [$Q^2 = p_T^2 = tu/s$; $\tilde{Q}_x = \min(xQ,(1-x)Q)$] (see Fig.9):

$$\mathcal{M}_{\gamma\gamma \to M\bar{M}} = \int_0^1 dx \int_0^1 dy\ \phi_{\bar{M}}(y,\tilde{Q}_y)\ T_H(x,y;\ s,\theta_{c.m.})\ \phi_M(x,\tilde{Q}_x) \tag{4.50}$$

where T_H is the hard-scattering amplitude $\gamma\gamma \to (q\bar{q})(q\bar{q})$ for the production of the valence quarks collinear with each meson and $\phi_M(x,Q)$ is the (process-independent) distribution amplitude for finding the valence q and $\bar{q}$ with light-cone fractions of the meson's momentum, integrated over transverse momenta $k_\perp < Q$. The contribution of nonvalence Fock states are power-law suppressed. Further, the spin-selection rule (4.44) of QCD predicts that vector mesons M and $\bar{M}$ are produced with opposite helicities to leading order in $1/Q$ and all orders in $\alpha_s(Q^2)$.

Dimensional counting [8] predicts that for large s, $s^4\, d\sigma/dt$ scales at fixed t/s or $\theta_{c.m.}$, up to factors of $\ln s/\Lambda^2$.

Some forty diagrams contribute to the hard-scattering amplitudes for $\gamma\gamma \to M\bar{M}$ (for nonsinglet mesons). These can be derived from the four independent diagrams in Fig.10b by particle interchange. The resulting amplitudes for helicity zero mesons are:

$$\left.\begin{matrix} T_{++} \\ T_{--} \end{matrix}\right\} = \frac{16\pi\alpha_s}{3s}\,\frac{32\pi\alpha}{x(1-x)y(1-y)}\left[\frac{(e_1-e_2)^2 s}{1-\cos^2\theta_{c.m.}}\right] \tag{4.51}$$

$$\left.\begin{matrix} T_{+-} \\ T_{-+} \end{matrix}\right\} = \frac{16\pi\alpha_s}{3s}\,\frac{32\pi\alpha}{x(1-x)y(1-y)}\left[\frac{(e_1-e_2)^2(1-a)}{1-\cos^2\theta_{c.m.}} + \frac{e_1e_2 a\big(y(1-y)+x(1-x)\big)}{a^2-b^2\cos^2\theta_{c.m.}}\right] \tag{4.52}$$

where $\left.\begin{matrix} a \\ b \end{matrix}\right\} = (1-x)(1-y) \pm xy$, the subscripts ++,--,... refer to photon helicities, and e_1, e_2 are the quark charges (i.e., the mesons have charges $\pm(e_1 - e_2)$).

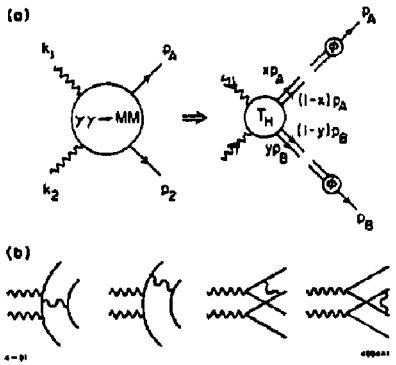

Fig. 10 (a) Factorized structure of the $\gamma\gamma \to M\bar{M}$ amplitude in QCD at large momentum transfer. The T_H amplitude is computed with quarks collinear with the outgoing mesons. (b) Diagram contributing to $T_H(\gamma\gamma \to M\bar{M})$ to lowest order in α_s.

To compute the $\gamma\gamma \to M\bar{M}$ amplitude $\mathcal{M}_{\lambda\lambda}$, (Eq.(4.50)), we now need only know the x-dependence of the meson's distribution amplitude $\phi_M(x,Q)$; the overall normalization of ϕ_M is fixed by the 'sum rule' ($n_c = 3$)

$$\int_0^1 dx\ \phi_M(x,Q) = \frac{f_M}{2\sqrt{3}} \tag{4.53}$$

where f_M is the meson decay constant as determined from leptonic decays. Note that the dependence in x and y of several terms in $T_{\lambda\lambda}$, is quite similar to that appearing in the meson's electromagnetic form factor (4.23):

$$F_M(s) = \frac{16\pi\alpha_s}{3s}\int_0^1 dx\,dy\,\frac{\phi_M^*(x,\tilde{Q}_x)\,\phi_M^*(y,\tilde{Q}_y)}{x(1-x)\ y(1-y)} \tag{4.54}$$

when $\phi_M(x,Q) = \phi_M(1-x,Q)$ is assumed. Thus much of the dependence on $\phi(x,Q)$ can be removed from $\mathcal{M}_{\lambda\lambda}$, by expressing it in terms of the meson form factor — i.e.,

$$\left.\begin{matrix}\mathcal{M}_{++}\\ \mathcal{M}_{--}\end{matrix}\right\} = 16\pi\alpha\, F_M(s)\left[\frac{\langle(e_1-e_2)^2\rangle}{1-\cos^2\theta_{c.m.}}\right] \tag{4.55}$$

$$\left.\begin{matrix}\mathcal{M}_{+-}\\ \mathcal{M}_{-+}\end{matrix}\right\} = 16\pi\alpha\, F_M(s)\left[\frac{\langle(e_1-e_2)^2\rangle}{1-\cos^2\theta_{c.m.}} + 2\langle e_1e_2\rangle\, g\left[\theta_{c.m.};\,\phi_M\right]\right] \tag{4.56}$$

up to corrections of order α_s and m^2/s. Now the only dependence on ϕ_M, and indeed the only unknown quantity, is in the θ-dependent factor

$$g\left[\theta_{c.m.};\,\phi_M\right] = \frac{\displaystyle\int_0^1 dx\,dy\,\frac{\phi_M^*(x,\bar{Q})\;\phi_M^*(y,\bar{Q})}{x(1-x)\;y(1-y)}\,\frac{a\left[y(1-y)+x(1-x)\right]}{a^2-b^2\cos^2\theta_{c.m.}}}{\displaystyle\int_0^1 dx\,dy\,\frac{\phi_M^*(x,\bar{Q})\;\phi_M^*(y,\bar{Q})}{x(1-x)\;y(1-y)}} \quad . \tag{4.57}$$

The spin-averaged cross section follows immediately from these expressions:

$$\frac{d\sigma}{dt} = \frac{2}{s}\frac{d\sigma}{d\cos\theta_{c.m.}} = \frac{1}{16\pi s^2}\frac{1}{4}\sum_{\lambda\lambda'}|\mathcal{M}_{\lambda\lambda'}|^2 \tag{4.58}$$

$$= 16\pi\alpha^2\left|\frac{F_M(s)}{s}\right|^2\left\{\frac{\langle(e_1-e_2)^2\rangle^2}{\left(1-\cos^2\theta_{c.m.}\right)^2}+\frac{2\langle e_1e_2\rangle\langle(e_1-e_2)^2\rangle}{1-\cos^2\theta_{c.m.}}\right.$$
$$\left.\times\, g\left[\theta_{c.m.};\,\phi_M\right]+2\langle e_1e_2\rangle^2\, g^2\left[\theta_{c.m.};\,\phi_M\right]\right\} \quad .$$

In Fig.11 the spin-averaged cross sections (for $\gamma\gamma \to \pi\pi$) are plotted for several forms of $\phi_M(x,Q)$. At very large energies, the distribution amplitude evolves to the form

$$\phi_M(x,Q) \underset{Q\to\infty}{\longrightarrow} \sqrt{3}\, f_M\, x(1-x) \quad , \tag{4.59}$$

and the predictions (curve (a)) become exact and parameter-free. However, this evolution with increasing Q^2 is very slow (logarithmic), and at current energies ϕ_M could be quite different in structure, depending upon the details of hadronic binding. Curves (b) and (c) correspond to the extreme examples $\phi_M \propto [x(1-x)]^{1/4}$ and $\phi_M \propto \delta(x-1/2)$, respectively. Remarkably, the cross section for charged mesons is essentially independent of the choice of ϕ_M, making this an essentially parameter-free prediction of perturbative QCD. By contrast, the predictions for neutral helicity-zero mesons are quite sensitive to the structure of ϕ_M. Thus we can study the x-dependence of the meson distribution amplitude by measuring the angular dependence of this process.

The cross sections shown in Fig.8 are specifically for $\gamma\gamma \to \pi\pi$, where the pion form factor has been approximated by $F_\pi(s) \sim 0.4\ \mathrm{GeV}^2/s$. The $\pi^+\pi^-$ cross section is quite large at moderate s:

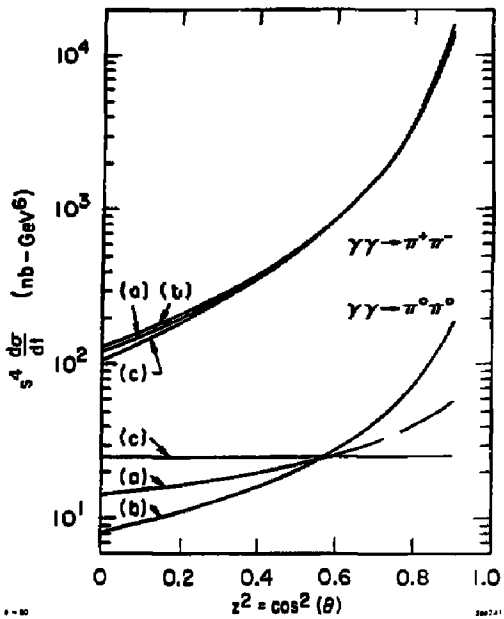

Fig. 11 QCD predictions for $\gamma\gamma \to \pi\pi$ to leading order in QCD. The results assume the pion form factor parameterization $F_\pi(s) \sim 0.4\ \text{GeV}^2/s$. Curves (a), (b) and (c) correspond to the distribution amplitudes $\phi_M = x(1-x)$, $[x(1-x)]^{1/4}$, and $\delta(x-1/2)$, respectively. Predictions for other helicity zero mesons are obtained by multiplying with the scale constants given in Ref. 15.

$$\frac{\frac{d\sigma}{dt}(\gamma\gamma \to \pi^+\pi^-)}{\frac{d\sigma}{dt}(\gamma\gamma \to \mu^+\mu^-)} \sim \frac{4|F_\pi(s)|^2}{1-\cos^4\theta_{c.m.}} \sim \frac{0.6\ \text{GeV}^4}{s^2} \quad \text{at} \quad \theta_{c.m.} = \pi/2 \tag{4.60}$$

Similar predictions are possible for other helicity-zero mesons. The normalization of $\gamma\gamma \to M\bar{M}$ relative to the $\gamma\gamma \to \pi\pi$ cross section is completely determined by the ratio of meson decay constants $(f_M/f_\pi)^4$ and by the flavor-symmetry of the wavefunctions, provided only that ϕ_M and ϕ_π are similar in shape. Note that the cross section for charged ρ's with helicity zero is almost an order of magnitude larger than that for charged π's.

Finally notice that the leading order predictions (Eq. (4.58)) have no explicit dependence on α_s. Thus they are relatively insensitive to the choice of renormalization scheme or of a normalization scale. This is not the case for either the form factor or the two-photon annihilation amplitude when examined separately. However, by combining the two analyses as in Eq. (4.58) we obtain meaningful results without computing $O(\alpha_s)$ corrections. The corresponding calculations for helicity-one mesons are given in Ref. 12. Hadronic helicity conservation implies that only helicity-zero mesons can couple to a single highly virtual photon. So F_{M_1}, the transverse form factor, cannot be measured experimentally. For simplicity we will assume that the longitudinal and transverse form factors are equal to obtain a rough estimate of the $\gamma\gamma \to \rho_L\rho_L$ cross section (Fig.12). Again we see strong dependence on ϕ_{M_1} for all angles except $\theta_{c.m.} \sim \pi/2$, where the terms involving g_1 vanish. Consequently, a measurement of the angular distribution would be very sensitive to the x-dependence of ϕ_{M_1}, while measurements at $\theta_{c.m.} = \pi/2$ determine $F_{M_1}(s)$. Notice also that the number of charged ρ-pairs (with any helicity) is much larger than the number of neutral ρ's, particularly near $\theta_{c.m.} = \pi/2$. The cross sections are again quite large with

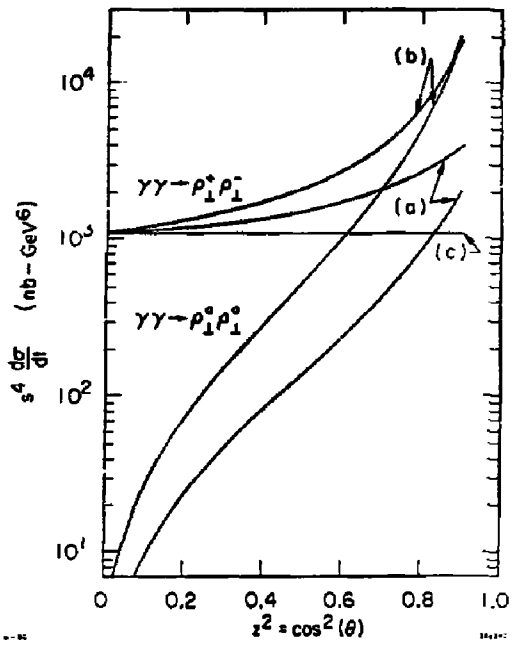

Fig. 12 QCD predictions for $\gamma\gamma \to \rho_\perp\rho_\perp$ with opposite helicity ± 1 to leading order in QCD. The normalization given here assumes that the ρ distribution amplitude is helicity independent.

$$\left.\frac{d\sigma/dt\left(\gamma\gamma \to \rho_\perp^+\rho_\perp^-\right)}{d\sigma/dt\left(\gamma\gamma \to \mu^+\mu^-\right)}\right|_{\theta_{c.m.} = \frac{\pi}{2}} \sim \frac{5\ \text{GeV}^4}{s^2} \quad . \tag{4.61}$$

Results for other mesons are given in Ref. 12.

The $\gamma\gamma \to M\bar{M}$ and $\gamma^*\gamma \to M$ processes thus provide detailed checks of the basic Born structure of QCD, the scaling behavior of the quark and gluon propagators and interactions, as well as the constituent charges and spins. Conversely, the angular dependence of the $\gamma\gamma \to M\bar{M}$ amplitudes can be used to determine the shape of the process-independent distribution amplitude $\phi_M(x,Q)$ for valence quarks in the meson $q\bar{q}$ Fock state. The $\cos\theta_{c.m.}$-dependence of the $\gamma\gamma \to M\bar{M}$ amplitude determines the light cone x-dependence of the meson distribution amplitude in much the same way that the x_{Bj} dependence of deep inelastic cross sections determines the light-cone x-dependence of the structure functions (quark probability functions) $G_{q/M}(x,Q)$.

The form of the predictions given here are exact to leading order in $\alpha_s(Q^2)$. Power-law $(m/Q)^2$ corrections can arise from mass insertions, higher Fock states, pinch singularities and nonperturbative effects. In particular, the predictions are only valid when s-channel resonance effects can be neglected. It is likely that the background due to resonances can be reduced relative to the leading order QCD contributions if one measures the two-photon processes with at least one of the photons tagged at moderate spacelike momentum q^2, since resonance contributions are expected to be strongly damped by form factor effects. In contrast, the leading order QCD $\gamma_1\gamma_2 \to M\bar{M}$ amplitudes are relatively insensitive to the value of q_1^2 or q_2^2 for $|q_1^2| \ll s$.

Finally, we note that the amplitudes given above have simple crossing properties. In particular, we can immediately analyze the Compton amplitude $\gamma M \to \gamma M$ in the

region t large enough with s >> |t| in order to study the leading Regge behavior in the large momentum transfer domain. In the case of helicity ±1 mesons, the leading contribution to the Compton amplitude has the form (s >> |t|)

$$\mathcal{M}_{\gamma M \to \gamma M} = 16\pi\alpha F_{M_\perp}(t)\left(e_1^2 + e_2^2\right) \qquad (4.62)$$

$$(\lambda_\gamma = \lambda'_\gamma\,, \quad \lambda_M = \lambda'_M)$$

which corresponds to a fixed Regge singularity at J = 0. [56] In the case of helicity zero mesons, this singularity actually decouples, and the leading J-plane singularity is at J = -2.

V. DEEP INELASTIC LEPTON SCATTERING

The crucial evidence that the electromagnetic current within hadrons is carried by point-like spin 1/2 quarks comes from deep-inelastic electron, muon and neutrino scattering. At large momentum transfer, $Q^2 \geq 2$ GeV^2 the lepton-nucleon inelastic cross section displays a scale-invariant behavior consistent with the simplest type of impulse approximation — where the electron scatters directly against point-like quark constituents of the target. [57] The deviations which are observed at very large Q^2 are consistent with the color radiative corrections predicted by QCD. In addition at low values of Q^2, there is evidence for power law "higher twist" corrections associated with coherent multiquark processes, interference effects, and final state corrections — quite in analogy to the corrections to impulse approximation expected in nuclear physics inelastic breakup calculations.

The Fock state representation we discussed in Sec. III provides a particularly simple and elegant basis for calculating the deep inelastic cross section in QCD. We first consider the forward Compton amplitude $\gamma^* p \to \gamma^* p$ with virtual photon mass $q^2 = -Q^2 < 0$, and then calculate the $ep \to eX$ cross section from the absorptive part. An ideal Lorentz frame is

$$p = \left(p^+, p^-, \vec{p}_\perp\right) = \left(p^+, \frac{M^2}{p^+}, \vec{0}_\perp\right) \qquad (5.1)$$

$$q = \left(q^+, q^-, q_\perp\right) = \left(0, \frac{2p\cdot q}{p^+}, \vec{q}_\perp\right) \qquad (5.2)$$

with $q^2 = -Q^2$ and $p \cdot q = M\nu$. For the diagram 13b which has no final state interactions, the (light-cone) energy denominator between the photon interactions is

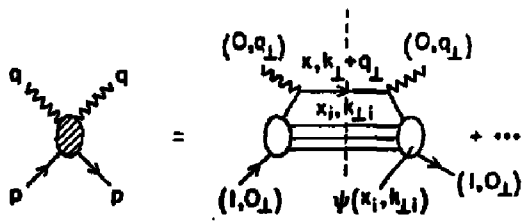

Fig. 13 Calculation of the forward virtual Compton amplitude. Diagram (b) gives the impulse approximation, neglecting final state and multiquark interactions.

$$D = M^2 + 2M\nu - \frac{(\vec{k}_1 + \vec{q}_1)^2 + m^2}{x} - \sum_{i\neq 1}\left(\frac{k_i^2 + m^2}{x}\right)_i + i\varepsilon \qquad (5.3)$$

where m is the struck quark mass, and the sum over i ≠ 1 gives the spectator quark and gluon contributions. For states with

$$|\mathcal{E}| = \left|M^2 - \sum_i \left(\frac{k_\perp^2 + m^2}{x}\right)_i\right| \ll 2M\nu \text{ and } k_\perp^2 \ll Q^2$$

we can write

$$D \cong 2M\nu - \frac{Q^2}{x} + i\varepsilon \tag{5.4}$$

$$\mathrm{Im}D^{-1} = \frac{x\pi}{2M\nu}\,\delta\left(x - \frac{Q^2}{2M\nu}\right) \tag{5.5}$$

i.e., the electron scattering on a quark with light-cone momentum fraction

$$x \equiv \frac{k^o + k^3}{p^o + p^3} \cong \frac{Q^2}{2M\nu} = x_{Bj} \tag{5.6}$$

The corresponding impulse approximation cross section is ($x \to x_{Bj}$)

$$\frac{d}{dQ^2\,dx}(lp \to l'X) = \sum_q G_{q/p}(x,Q)\,\frac{d\sigma}{dQ^2}(lq \to l'q)\Big|_{p_q = xp} \tag{5.7}$$

where [21]

$$G_{q/p}(x,Q) = \sum_{n\geq 3}\int^Q \left[d^2k_\perp\right][dx]\,|\psi_n^Q(x,k_\perp)|^2\,\delta(x - x_q) \tag{5.8}$$

gives the probability distribution for finding the quark with fractional light-cone momentum collinear up to the scale $k_\perp^2 < Q^2$, $|\mathcal{E}| < 2M\nu$. Unlike large momentum transfer exclusive amplitudes, all Fock states contribute to the inclusive cross section. The subprocess cross section $d\sigma/dQ^2(lq \to l'q)$ is evaluated for a quark collinear with the proton momentum $p_q^+ = xp^+$, $\vec{k}_\perp \simeq 0$. Since all the loop corrections to the subprocess cross section are hard ($k_\perp^2 \geq O(Q^2)$), it can be developed as a power series in $\alpha_s(Q^2)$. Thus the only correction to perfect scale-invariance of $d\sigma/dx\,dQ^2$ at large Q^2 and fixed x_{Bj} comes from the Q^2 dependence of the probability distribution $G(x,Q^2)$. This in turn can only arise from the wavefunction renormalization or from contributions $\psi_n \sim O(1/k_\perp)$ at large $k_\perp$. In QCD these occur only from the perturbative processes $q \to qg$, and $g \to gg$, $g \to q\bar{q}$, as illustrated in Fig.14.

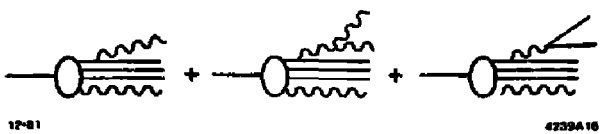

12-81 4239A16

Fig. 14 Contributions to the hadron Fock state wavefunction which give $\psi \sim 1/k_\perp$ at large $k_\perp$ and thus structure function evolution.

In parallel to the derivation of the evolution equation for the distribution amplitude, we then can derive evolution equation for the distributions $G_{q/H}(x,Q^2)$ and $G_{g/H}(x,Q^2)$ of the form [58,59]

$$\frac{\partial}{\partial \log Q^2} G(x,Q) = \frac{\alpha_s(Q^2)}{2\pi} \int_x^1 P\left(\frac{x}{y}\right) G(y,Q) \frac{dy}{y} \tag{5.9}$$

For example, for the "non-singlet" distribution

$$G_{q/H}(x,Q) - G_{\bar{q}/H}(x,Q) = G_{q/H}(x,Q) - G_{\bar{q}/H}(x,Q) \tag{5.10}$$

we have to lowest order in $\alpha_s(Q^2)$, ($C_F = 4/3$)

$$P_{q/q}(z) = C_F \left(\frac{1+z^2}{1-z}\right)_+ = C_F \left[\frac{1+z^2}{1-z} - \delta(1-z) \int_0^1 dx \frac{1+x^2}{1-x}\right] \tag{5.11}$$

(The subtraction term, which ensures finite behavior at $x_g = 0$, arises from the wavefunction renormalization, as in Eq. (4.14)). The Q^2 dependence can be displayed most simply by taking moments:

$$M_n(Q^2) = \int_0^1 G(x,Q^2)\, x^n dx \tag{5.12}$$

Then

$$M_n^{NS} = M_n^{NS}(Q_0^2) \left(\frac{\log Q^2/\Lambda^2}{\log Q_0^2/\Lambda^2}\right)^{-\gamma_n} \tag{5.13}$$

where the γ_n are defined in Eq. (4.16). The higher order corrections to the Q^2-evolution of M_n are discussed in Refs. 1 and 2. A critical feature [21] is the fact that the higher loop corrections (e.g., from the higher Fock states) are constrained kinematically to $k_\perp^2 < (1-y)Q^2 < (1-x)Q^2$, where y is labelled in the figure; i.e., the evolution is reduced at large x and for large n. A detailed discussion is given in Ref. 41.

Equation (5.7) displays an essential feature of the QCD predictions for inclusive reactions: the factorization of the physical cross section into a hard-scattering subprocess cross section, controlled by short-distance perturbative QCD, convoluted with structure functions $G(x,Q^2)$ which contain the long distance hadronic bound state dynamics. Notice that the Q^2-evolution of $G(x,Q)$ is also completely specified by the perturbative QCD processes and is independent of the nature of the target.

All the corrections to the perturbative QCD impulse approximation from final state interactions, finite $k_\perp^2$ effects, interference contributions, mass corrections, etc. are of higher order in $1/Q^2$, at least when analyzed using perturbative methods. In the operator product analysis these contributions correspond to matrix elements of "higher twist" operators which have non-minimal dimensions. The most important higher twist terms for deep inelastic lepton scattering are expected to correspond to processes where the lepton scatters on multiparticle clusters in the target (qq, $q\bar{q}$, virtual mesons, qg, etc.). We thus obtain a sum of contributions (see Fig.15): [15]

$$\frac{d\sigma}{dQ^2 dx}(\ell H \to \ell' X) = \sum_{a \in H} G_{a/H}(x) \frac{d\sigma}{dQ^2}(\ell a \to \ell a)\Big|_{p_a = xp_H} \tag{5.14}$$

where, in general $d\sigma_a/dQ^2$ falls in Q^2 according to the compositeness of a:

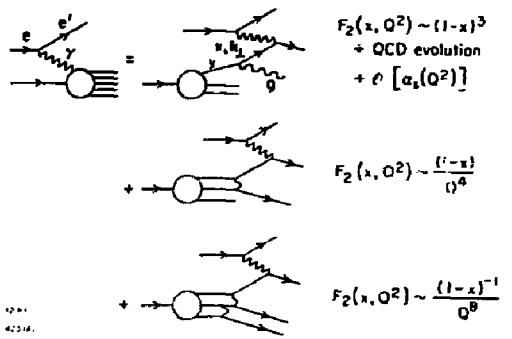

Fig. 15 QCD contributions to inelastic electron-nucleon scattering, including radiative and higher twist (diquark, triquark) corrections.

$$\frac{d\sigma}{dQ^2}(ea \to e'a) \sim \frac{4\pi\alpha^2}{Q^4} |F_a(Q^2)|^2 \tag{5.15}$$

For example, the "diquark" eqq → eqq gives a contribution to ep → eX of relative order $(m^2/Q^2)^2$. Since the qq can carry a large fraction of the proton's momentum, this contribution can be significant at large x. For a guide to this effect one can use the spectator counting rule: [60,8]

$$G_{a/H}(x) \underset{x \to 1}{\sim} (1-x)^{2n_s-1} \tag{5.16}$$

where n_s is the minimum number of spectator quarks (or gluons) in the Fock state required to stop at x → 1. The minimal Fock states containing a gives the dominant contribution.

The simplified rule (5.16) can be derived from minimally connected tree graph diagrams, ignoring spin effects, or from simple phase space considerations if one ignores the spectator quark masses [61] (see Sec. VI). Using this simple counting we can then classify the contributions to the hadron structure functions, as illustrated in Fig.15. The diquark contribution is expected to give a large contribution to the longitudinal structure function since it acts coherently as a boson current. The order $\alpha_s(Q^2)$ contribution from the hard gluon radiative corrections with $k_\perp^2 > (1-x)Q^2$ also gives a significant contribution to σ_L.

A detailed derivation of the behavior of structure functions at x ~ 1 from perturbative QCD is given in Ref. 21. At x ~ 1 all of the hadron's momentum must be carried by one quark, and each quark and gluon quark and gluon propagator which transfers this momentum becomes far off-shell:

$$k^2 \sim \mathcal{O}\left(-\frac{k_\perp^2 + m^2}{1-x}\right) \quad .$$

Perturbative QCD predictions thus become relevant. An important result is that at large x the struck quark tends to have the same helicity as the target nucleon: [21,62]

$$G_{q^\uparrow/p^\uparrow} \sim (1-x)^3; \qquad G_{q^\downarrow/p^\uparrow} \sim (1-x)^5 \tag{5.17}$$

This type of spin correlation is consistent with the SLAC-Yale polarized electron/polarized target data. Combined with the SU(6) symmetry of the nucleon wavefunction

this implies that the leading quark in the proton is five times more likely to be an up quark than a down quark, and thus [62] $\left(F_2 = \sum_q e_q^2 x G_{q/n}\right)$

$$F_{2n}(x,Q^2)/F_{2p}(x,Q^2) \xrightarrow[x\sim 1]{} 3/7 \tag{5.18}$$

For the case of mesons, the perturbative QCD gluon exchange prediction is [63]

$$G_{q/m} \sim (1-x)^2 \tag{5.19}$$

In addition, the same QCD analysis predicts a large C/Q^2 contribution to the meson longitudinal structure function (see Fig.3b): [22,64]

$$F_L^\pi(x,Q^2) = \frac{2x^2}{Q^2} C_F \int_{\sim m^2/(1-x)}^{Q^2} dk^2 \, \alpha_s(k^2) \, F_\pi(k^2) \tag{5.20}$$

which numerically is $F_L \sim x^2/Q^2$ in GeV^2 units. This contribution, which can dominate leading twist quark distributions in mesons is normalized in terms of the meson distribution amplitude, which in turn is normalized by the pion form factor.

The dominance of the longitudinal structure functions in the fixed W limit for mesons is an essential prediction of perturbative QCD. Perhaps the most dramatic consequence is in the Drell-Yan process $\pi p \to \ell^+\ell^- X$; one predicts [22] that for fixed pair mass Q, the angular distribution of the ℓ^+ (in the pair rest frame) will change from the conventional $(1 + \cos^2\theta_+)$ distribution to $\sin^2(\theta_+)$ for pairs produced at large x_L. A recent analysis of the Chicago-Illinois-Princeton experiment [65] at FNAL appears to confirm the QCD high twist prediction with about the expected normalization. Striking evidence for the effect has also been seen in a Gargamelle analysis [66] of the quark fragmentation functions in $\nu p \to \pi^+\mu^- X$. The results yield a quark fragmentation distribution into positive charged hadrons which is consistent with the predicted form: $dN^+/dzdy \sim B(1-z)^2 + (C/Q^2)(1-y)$ where the $(1-y)$ behavior corresponds to a longitudinal structure function. It is also crucial to check that the $e^+e^- \to HX$ cross section becomes purely longitudinal ($\sin^2\theta$) at large z at moderate Q^2. [62]

The results (5.17) and (5.19) for $G_{q/B}$ and $G_{q/M}$ give the behavior of the leading QCD contribution to the structure function before QCD evolution is applied; e.g., the results are valid for $F_2(x,Q^2)$ at Q^2 of order of $\langle k_\perp^2\rangle_H$. The large Q^2 behavior is determined by the evolution equations (5.9), taking account of the phase space limits of the radiated gluons at $x \sim 1$. [41]

VI. THE PHENOMENOLOGY OF HADRONIC WAVEFUNCTIONS

Thus far, most of the phenomenological tests of QCD have focused on the dynamics of quark and gluon subprocesses in inclusive high momentum transfer reactions. The Fock state wavefunction $\psi_n^\uparrow(x_i, \vec{k}_{\perp i}; \lambda_i)$ which determine the dynamics of hadrons in terms of their quark and gluon degrees of freedom are also of fundamental importance. If these wavefunctions were accurately known then an extraordinary number of phenomena, including decay amplitudes, exclusive processes, higher twist contributions to inclusive phenomena, structure functions, and low transverse momentum phenomena (such as diffractive processes, leading particle production in hadron-hadron collisions and heavy flavor hadron production) could be interrelated. Conversely, these processes can provide phenomenological constraints on the Fock state wavefunctions which are important for understanding the dynamics of hadrons in QCD. In addition, as we discuss in Sec. VII, the structure of nuclear wavefunctions in QCD is essential for understanding the syntheses of nuclear physics phenomenology with QCD.

A. Measures of Hadron Wavefunctions

As we have shown in Sec. III the central measures of the hadron wavefunctions are the distribution amplitudes

$$\phi(x_i,Q) = \int^Q \left[d^2k_\perp\right] \psi_v^Q(x_i,\vec{k}_{\perp i}) \tag{6.1}$$

which control high momentum transfer form factors and exclusive processes:

$$\mathcal{M} \cong \Pi\, \phi \otimes T_H \tag{6.2}$$

and the quark and gluon structure functions

$$G_{q/H}(x,Q) = \sum_n \int^Q \left[d^2k_\perp\right] |\psi_n(x_i,k_{\perp i})|^2 \delta(x - x_q) \tag{6.3}$$

which control high momentum transfer inclusive reactions

$$d\sigma \cong \sum C \otimes d\hat{\sigma} \tag{6.4}$$

Examples are shown in Figs.1 through 3. A summary of the basic properties, logarithmic evolution, and power law behavior of these quantities is given in Table IV.

The exclusive formula (6.2) also includes applications to large momentum transfer multiparticle production [68,8] $e^+e^- \to H_1 \ldots H_n$ with $p_i \cdot p_j \sim \mathcal{O}(Q^2)$, and the elastic and inelastic weak and electromagnetic form factors. We also note that hard scattering higher twist subprocesses to inclusive reactions such as $\gamma q \to Mq$, $gq \to Mq$, $q\bar{q} \to M\bar{q}$, $qq \to B\bar{q}$., etc. are absolutely normalized in terms of the distribution amplitudes. [69] In particular, some amplitudes such as $\gamma q \to \pi q$, $q\bar{q} \to \pi g$ and $gq \to \pi q$ can be rigorously related to the pion form factor since the same integral

$$\int_0^1 \frac{dx}{1-x}\, \phi_\pi(x,Q) \tag{6.5}$$

enters in each of the quantities. [70] The p_T^{-6} processes [24] $gq \to Mq$ (see Fig.3a) and $q\bar{q} \to Mg$ are particularly interesting and important in high-p_T meson production processes such as $pp \to MX$ since the meson is produced directly in the subprocess without the necessity for quark or gluon jet fragmentation. In fact, the contributions of standard p_T^{-4} scaling processes such as $qq \to qq$, $gq \to gq$, and $gg \to gg$ to hadron production are strongly suppressed by two to three orders of magnitude because of the suppression of jet fragmentation $D_{M/q}(z)$ at large momentum fraction z and the fact that the subprocesses must occur at a significantly larger momentum transfer than that of the triggered particle. [71]

Despite much effort there is at this time no systematic understanding of high p_T hadron production in QCD. A comprehensive attack must take into account not only the leading twist subprocesses and directly coupled higher twist contributions such as those listed above, but also the effects of initial state multiple scattering effects. One of the most important experiments which could clarify the nature of these effects is the measurement of the ratio of direct photon to meson at high p_T: $(x_T = 2p_T/\sqrt{s})$

$$R_{\gamma/\pi}(x_T,s,\theta_{c.m.}) = \frac{d\sigma}{d^3p/E}(pp \to \gamma X) \Big/ \frac{d\sigma}{d^3p/E}(pp \to \pi X) \tag{6.6}$$

Table IV Comparison of exclusive and inclusive cross sections

Exclusive Amplitudes	Inclusive Cross Sections
$\mathcal{M} \sim \prod \phi(x_i,Q) \otimes T_H(x_i,Q)$	$d\sigma \sim \prod G(x_a,Q) \otimes d\hat{\sigma}(x_a,Q)$
$\phi(x,Q) = \int^Q \left[d^2k_\perp\right] \psi^Q_{val}(x,k_\perp)$	$G(x,Q) = \sum_n \int^Q \left[d^2k_\perp\right][dx]' \psi^Q_n(x,k_\perp)^2$
Measure ϕ in $\gamma\gamma \to M\bar{M}$	Measure G in $\ell p \to \ell X$
$\sum_{i\in H} \lambda_i = \lambda_H$	$\sum_{i\in H} \lambda_i \neq$
EVOLUTION	
$\frac{\partial\phi(x,Q)}{\partial \log Q^2} = \alpha_s \int [dy] V(x,y)\phi(y)$	$\frac{\partial G(x,Q)}{\partial \log Q^2} = \alpha_s \int dy\ P(x/y)G(y$
$\lim_{Q\to\infty} \phi(x,Q) = \prod_i x_i \cdot C_{flavor}$	$\lim_{Q\to\infty} G(x,Q) = \delta(x)\ C$
POWER LAW BEHAVIOR	
$\frac{d\sigma}{dx}(A+B \to C+D) \cong \frac{1}{s^{n-2}} f(\theta_{CM})$	$\frac{d\sigma}{d^2p/E}(AB \to CX) \cong \sum \frac{(1-x_T)^{2n_s-1}}{(Q^2)^{n_{act}-2}} f(\theta_{CM})$
$n = n_A + n_B + n_C + n_D$	$n_{act} = n_a + n_b + n_c + n_d$
T_H: expansion in $\alpha_s(Q^2)$	$d\hat{\sigma}$: expansion in $\alpha_s(Q^2)$
COMPLICATIONS	
End point singularities Pinch singularities High Fock states	Multiple scales Phase-space limits on evolution Heavy quark thresholds Heavy twist multiparticle processes Initial and final state interactions

For example, if leading twist QCD processes dominate these reactions then $R_{\gamma/\pi} \sim f(x_T) \sim (1-x_T)^{-2}$ at $\theta_{c.m.} \sim \pi/2$. If directly-coupled processes such as $gq \to \gamma q$ dominate the meson production then one predicts $R_{\gamma/\pi} \sim p_T^4$ at fixed x_T and $\theta_{c.m.}$ [72] Measurements of this ratio in nuclear targets are important for clarifying the contribution of final state multiple scattering processes.

The photon probe plays a crucial role in high-p_T hadron reactions since the photon couples directly to the quark and gluon subprocesses at short distances. The most dramatic example of these point-like phenomena is the recent observations at PETRA [6-8] of high transverse momentum hadrons in $\gamma\gamma$ collisions. The results at $p_T \geq 3$ GeV appear to be consistent with the scale invariant QCD prediction [73]

$$\frac{d\sigma(\gamma\gamma \to \text{jet} + \text{jet})}{d\sigma(\gamma\gamma \to \mu^+\mu^-)} = 3\sum e_q^4, \quad q = u,d,s,c \qquad (6.7)$$

$$\left[1 + \mathcal{O}\left(\frac{\alpha_s(p_T^2)}{\pi}\right)\right]$$

These results also indicate that, unlike typical meson-induced reactions, an incident photon often produces high p_T hadronic jets without leaving hadronic energy in the beam fragmentation direction. [74] One also expects analogous results for directly coupled photons in $\gamma p \to HX$ and $\gamma p \to$ Jet + X reactions. The point-like behavior of on-shell photons is in direct contrast to the predictions of vector meson dominance models.

A surprising feature of QCD is that even a hadron can produce jets at large p_T without beam fragmentation. [70] For example, the existence of high twist subprocesses such as $Mq \to gq$ and $Mg \to q\bar{q}$ leads to high p_T jet events in meson-induced collisions $Mp \to$ Jet + Jet + X where there is no hadronic energy left in the meson beam fragmentation direction (see Fig.3c). The inclusive cross section, which scales as p_T^{-6} at fixed x_T and $\theta_{c.m.}$, is absolutely normalized to the meson form factor. As in the case of the photon-induced reactions, the directly coupled meson has no associated color radiation or structure function evolution. An experimental search for these unique and highly kinematically constrained events is very important in order to confirm the presence of these subprocesses which involve the direct coupling of meson $q\bar{q}$ Fock state to quarks and gluons at short distance.

In general, we can replace any direct photon interaction by a direct-coupled meson interaction in the subprocess cross section by the replacement $\alpha \to \frac{1}{2} F_\pi(p_T^2)$. Furthermore, one can compute direct-coupled processes which isolate the valence Fock state of baryons, e.g., $pp \to pX$ (production of isolated large p_T protons via the $qq \to pq$ subprocesses), and reactions $pp \to qqX$ (from $\bar{q}p \to qq$) (see Fig.3b), $pp \to qqqX$ (from $gq \to qqq$) etc., each of which produce jets at high p_T without beam spectators or fragmentation.

B. Constraints on the Pion and Proton Valence Wavefunction [27]

The central unknown in the QCD analysis of hadronic matrix elements is the hadron wavefunction in the non-perturbative domain $\kappa^2 \gtrsim 1\ \text{GeV}^2$. For illustration we shall assume that in this region the ψ_n fall off exponentially in the off-shell energy:

$$\psi_n^\kappa(x_i, k_{\perp i}) = A_n\, e^{b^2 \mathcal{M}_n^2} \qquad (6.8)$$

$$\mathcal{M}_n^2 = M^2 - \sum_{i=1}^{n} \left(\frac{k_i^2 + m^2}{x}\right)_i < 0 \qquad (6.9)$$

The parameterization is taken to be independent of spin; the full wavefunction is then obtained by multiplying by free spinors $u/\sqrt{k^+}$. The form (6.8) has the advantage of analytic simplicity: for example, the resulting baryon distribution amplitude at small κ is

$$\phi(x_i, \kappa) = A_\phi\, x_1 x_2 x_3\, e^{-b_3^2 \sum_{i=1}^{3} \frac{m_i^2}{x_i}} \qquad (6.10)$$

At large κ, ϕ is determined from the evolution equation (4.33). At very large $k_\perp$ the ψ_n for non-valence Fock states should match onto the power law fall-off $k_\perp^{-1}$

predicted by perturbative QCD. It should be emphasized that the form (6.8) is chosen just for simplicity. An equally plausible parameterization is $_n \sim A_n \mathcal{E}_n^{-p}$ with $p = 3$, which is suggested by the Schroedinger equation assuming linear potential and the correspondence given in Eq. (3.41).

In the case of the pion we can derive two important constraints on the valence wavefunction from the $\pi \to \mu\nu$ and $^0 \to \gamma\gamma$ decay amplitudes:

$$\int \frac{d^2k_\perp}{16\pi^3} \int_0^1 dx\, \psi^\kappa(x,k_\perp) = \frac{f_\pi}{2\sqrt{n_c}} \left[1 + \mathcal{O}\left(\frac{m_\pi^2}{\kappa^2}\right)\right] \tag{6.11}$$

and [27]

$$\psi^\kappa(x,k_\perp = 0) \frac{Z_2(m_\pi^2)}{Z_2(\kappa^2)} = \frac{\sqrt{n_c}}{f_\pi} \tag{6.12}$$

The derivation of the second constraint assumes that the radius of the pion is much smaller than its Compton length:

$$m_q^2, m_\pi^2 << \frac{6}{R_\pi^2} \quad . \tag{6.13}$$

Let us now assume the form

$$\psi^\kappa_{q\bar{q}} \propto e^{-b_V^2 \left(\frac{k_\perp^2 + m^2}{x(1-x)}\right)}, \quad (\kappa^2 < 1\ \mathrm{GeV}^2) \tag{6.14}$$

where

$$-\frac{d}{dQ^2} F_\pi^V(Q^2)\Big|_{Q^2=0} = \frac{1}{6}\left(R_\pi^{q\bar{q}}\right)^2 = b_V^2 \tag{6.15}$$

is the contribution to the slope of the meson form factor from the valence Fock state (see Eq. (4.2)). The two conditions (6.11) and (6.12) then determine $R_\pi^{q\bar{q}} = 0.42$ fm, and [27]

$$P^\kappa_{q\bar{q}/\pi} = \int^\kappa \frac{d^2k_\perp}{16\pi^3} \int_0^1 dx \left|\psi^\kappa_{q\bar{q}/\pi}(x,\vec{k}_\perp)\right|^2 = \frac{1}{4}\left(\frac{Z_2(\kappa^2)}{Z_2(m_\pi^2)}\right)^2 \leq \frac{1}{4} \quad . \tag{6.16}$$

Thus the probability that the pion contains only the valence Fock state at small κ^2 is less than 1/4. Furthermore, the radius of the valence state turns out to be smaller than that of the total state: $R_\pi^{expt} \cong 0.7$ fm. One can also verify that the bound $P_{q\bar{q}/\pi} \leq 1/4$ is also true for power law wavefunctions $\psi \sim \mathcal{E}^{-p}$, $p > 2$.

The existence of other Fock states at equal τ in the pion is to be expected considering the fact that its quark and gluon constituents are relativistic. The existence of large m_ρ/m_π and m_Δ/m_N spin splittings (due to transverse-polarized gluon exchange) also implies that there is a non-zero gluon component intrinsic to both meson and nucleon bound states.

In the case of the baryon wavefunction, one can obtain non-trivial constraints on the form of the 3-quark valence wavefunction by making a simultaneous analysis

of the proton and neutron form factors and the $\psi \to p\bar{p}$ decay amplitude, assuming the ψ decays via a 3-gluon intermediate state (see Fig.6). The observed angular distribution [53] for $\psi \to p\bar{p}$ is in fact consistent with the predicted form $1 + \beta^2 \cos^2\theta$ (where β is the nucleon velocity) and is a non-trivial check of hadron helicity conservation for exclusive processes in QCD.

The $\psi \to p\bar{p}$ ratio is given to leading order in α_s by (Fig.1b) [18]

$$\frac{\Gamma(\psi \to 3g \to p\bar{p})}{\Gamma(\psi \to 3g \to \text{all})} \to 3.2 \times 10^6 \, \alpha_s^3(s) \, \frac{|\vec{p}_{CM}|}{\sqrt{s}} \, \frac{\langle T \rangle^2}{s^4} \tag{6.17}$$

here $|p_{CM}|/\sqrt{s} \simeq .4$, $s = 9.6$ GeV^2, and

$$\langle T \rangle = \int_0^1 [dx][dy] \, \frac{\phi^*(y_i, s)}{y_1 y_2 y_3} \, \frac{x_1 y_3 + x_3 y_1}{\left[x_1(1-y_1) + y_1(1-x_1)\right]\left[x_3(1-y_3) + y_3(1-x_3)\right]}$$

$$\times \frac{\phi(x_i, s)}{x_1 x_2 x_3} \tag{6.18}$$

is a well defined function of the baryon distribution amplitude. In the case of the nuclear form factors (see Eqs. (4.31, 4.32)) it is important to use the correct argument for each α_s in the hard scattering amplitude T_H corresponding to the actual momentum transfer which flows through each exchanged gluon in Fig.7b. This effect is expected to yield the most important contribution to next to leading order in α_s and is an integral part of the QCD predictions. It is interesting to note that if $\phi_B = A_\phi x_1 x_2 x_3$ and if all the α_s have the same argument (which is, in fact, the situation in the asymptotic $Q^2 \to \infty$ limit [9,19]) then Eqs. (4.28-4.32) give $\lim_{Q^2 \to \infty} G_M^p(Q^2)/G_M^n(Q^2) = 0$. However, the fact that α_s is not a constant and has different arguments for each diagram in T_H allows one to obtain empirically consistent results for the normalization [75] of $G_M^p(Q^2)$, $G_M^n(Q^2)$ and the $\psi \to p\bar{p}$ decay rate. To first approximation one requires [27]

$$\frac{\alpha_s(x_i y_i Q^2)}{\alpha_s\left((1-x_i)(1-y_i)Q^2\right)} \cong \frac{\alpha_s(Q^2/9)}{\alpha_s(4Q^2/9)} \sim 1.5 \text{ to } 2.0 \text{ at } Q^2 \cong 10 \text{ GeV}^2 \quad . \tag{6.19}$$

The QCD predictions (4.28-4.30) for the proton and neutron form factors are only valid at large Q^2 where the effects of mass corrections, higher Fock states and finite transverse momentum can be neglected. In order to understand these effects we extend the parameterization of the 3 quark valence Fock state contribution by using $(Q^2 + M_0^2)^{-2}$ in the denominators of (4.29, 4.30) and replacing $\alpha_s(Q^2) \to \alpha_s(Q^2 + M^2) = 4\pi/\beta_0 \log\left((Q^2 + M^2)/\Lambda^2\right)$ to reflect the fact that at low Q^2 the transverse momenta intrinsic to the bound state wavefunctions flow through all the propagators.

Although we have not tried to optimize the parameterizations, a typical fit which is compatible with the proton and neutron form factors (see Fig.16) and $\psi \to p\bar{p}$ decay data are $M_0 \cong 1.5$ GeV, $\mu \cong 450$ MeV, $m_q \cong 300$ MeV, and $\Lambda = 280$ MeV, so that $\alpha_s(Q^2 = 10 \text{ GeV}^2) \cong 0.29$. (Analyses [50] of higher order QCD corrections to the meson form factors suggest that one can identify the Λ used here with $\Lambda_{\overline{MOM}} = 2.16 \, \Lambda_{\overline{MS}}$.) The computed radius of the 3-quark valence state (computed from G_M^p via Eq. (4.2)) is, however, quite small: $R_V \cong 0.3$ fm, and the valence Fock state probability is $P_{qqq/p} \gtrsim 1/4$. If this preliminary analysis is correct, then, as in the meson case, the valence state is much smaller in transverse size than the physical hadron (which receives contributions to its charge radius from all Fock states).

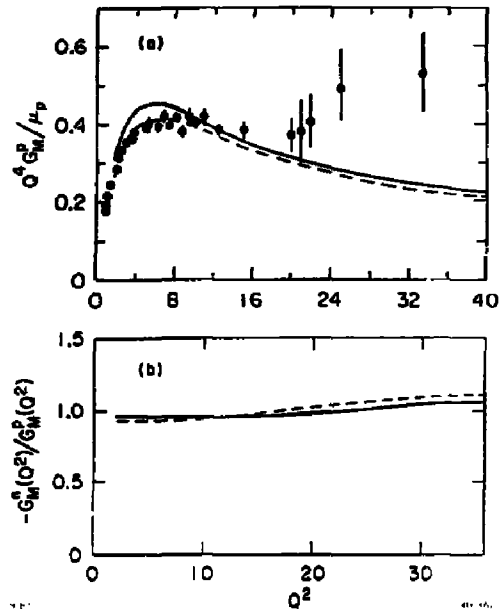

Fig. 16 Fit to nucleon form factor data described in the text. (From Ref. 27.)

The most crucial prediction from this analysis is that $Q^4 G_M^p(Q^2)$ should decrease by a factor of 2 for $Q^2 = 10$ to $Q^2 = 40$ GeV^2, a trend not at all indicated by the data! Further measurements of $G_M(Q^2)$ are clearly crucial in order to check this essential prediction of asymptotic freedom.

Given the above parameterization of the nucleon valence Fock state we can use Eq. (5.8) to compute the 3-quark non-perturbative contribution to the proton structure function at large x (see Fig.17)

$$G^v_{q/p}(x,Q_0^2) = x(1-x)^3 \, e^{-2m^2b^2\left(\frac{1}{x}+\frac{2}{1-x}\right)} \qquad (6.20)$$

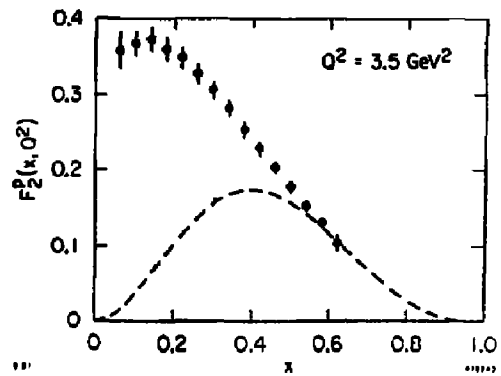

Fig. 17 Predicted valence quark contribution to the proton structure function. Evolution and higher Fock states are not included. (From Ref. 27.)

Since $4\ m^2b^2 \sim 0.05$, the exponential factor is not very important away from the edge of phase space and so it is difficult to distinguish between the non-perturbative and $(1-x)^3$ perturbative contributions at large x (see Sec. V). Higher Fock states $|qqqg\rangle$, $|qqq\ q\bar{q}\rangle$ are expected to give the dominant contribution at lower x. Despite the freedom in this parameterization it is reassuring that one can simultaneously fit a number of diverse nucleon properties with QCD formulae and parameters which are in the expected range.

At low Q^2 the exact formula (4.2) can be used as a further constraint on the baryon Fock states. Eventually one hopes to extend the predictions to other domains of baryon phenomenology such as the baryon decay amplitude in grand unified models and the normalization of higher twist subprocess contributions to inelastic lepton-nucleon scattering.

C. Quark Jet Diffractive Excitation [30]

The fact that the wavefunction of a hadron is a superposition of (infrared and ultraviolet finite) Fock amplitudes of fixed particle number but varying spatial and spin structure leads to the prediction of a novel effect in QCD. [30] We first note that the existence of the decay amplitude $\pi \to \mu\nu$ requires a finite probability amplitude for the pion to exist as a quark and diquark at zero transverse separation:

$$\psi(x, \vec{r}_\perp = 0) = \sqrt{4\pi}\ \sqrt{n_c}\ x(1-x) f_\pi \tag{6.22}$$

In a QCD-based picture of the total hadron-hadron cross section, the components of a color singlet wavefunction with small transverse separation interact only weakly with the color field, and thus can pass freely through a hadronic target while the other components interact strongly. A large nuclear target will thus act as a filter removing from the beam all but the short-range components of the projectile wavefunction. The associated cross section for diffractive production of the inelastic states described by the short range components is then equal to the elastic scattering cross section of the projectile on the target multiplied by the probability that sufficiently small transverse separation configurations are present in the wavefunction. In the case of the pion interacting in a nucleus one computes the cross section

$$\left.\frac{d\sigma}{dx\ d^2r_\perp}\right|_{r_\perp^2 \sim 0} \cong \sigma_{el}^{\pi A}\ 12\pi\ f_\pi^2\ x^2(1-x)^2 \tag{6.23}$$

corresponding to the production of two jets just outside the nuclear volume. The x distribution corresponds to $d\sigma/d\cos\theta \sim \sin^2\theta$ for the jet angular distribution in the $q\bar{q}$ center of mass. By taking into account the absorption of hadrons in the nucleus at $\vec{r}_\perp \neq 0$ one can also compute the $k_\perp$ distribution of the jets and the mass spectrum of the diffractive hadron system. Details are given in Ref. 30.

D. The "Unveiling" of the Hadronic Wavefunction and Intrinsic Charm

The renormalizability of QCD implies that all of the dynamics of the hadron wavefunctions $\psi_n^k(x_i, \vec{k}_{\perp i})$ at scales κ^2 much larger than mass thresholds is completely contained in the structure of the running coupling constant $\alpha_s(\kappa^2)$ and running mass $m(\kappa^2)$ and the quark and gluon external line renormalization constants. Nevertheless, the fact that there are different hadronic scales and thresholds in QCD does imply non-trivial dynamical structure of the wavefunctions. In the case of Compton scattering, $\gamma p \to \gamma p$, the energy denominators (see Eq. (5.3)) are a function of $2M\nu - \mathcal{M}_n^2$, so that the cross section is sensitive to wavefunctions up to the scale $\kappa^2 \sim 2M\nu$.

As an example of the change of wavefunction physics with the resolution scale let us consider a deuteron target. For very low $\kappa^2 \ll 2M\varepsilon_{B.E.}$ the deuteron acts as a coherent object. At the scale $\kappa^2 \gg 2M\varepsilon_{B.E.}$, the wavefunction corresponds to a n-p bound state. As the scale increases to $\kappa^2 \gtrsim 1$ GeV^2, the quark degrees of freedom become relevant and the deuteron wavefunction in QCD must be described in terms of six quark (and higher) Fock states: [76]

$$|D\rangle = a|(uud)_1(ddu)_1\rangle + b|(uud_8(ddu)_8\rangle + c|(uuu)_1(ddd)_1\rangle + d|(uuu)_8(ddd)_8\rangle + \ldots \tag{6.24}$$

The first component corresponds to the usual n-p structure of the deuteron. The second component corresponds to "hidden color" or "color polarized" configurations where the three-quark clusters are in color-octets, but the overall state is a color-singlet. The last two components are the corresponding isobar configurations. If we suppose that at low relative momentum the deuteron is dominated by the n-p configuration, then quark-quark scattering via single gluon exchange generates the color polarized states (b) and (d) at high $k_\perp$; i.e., there must be mixing with color-polarized states in the deuteron wavefunction at short distances. [67]

The deuteron's Fock state structure is thus much richer in QCD than it is in nuclear physics where the only degrees of freedom are hadrons.

It is interesting to speculate on whether the existence of these new configurations in normal nuclei could be related to the repulsive core of the nucleon-nucleon potential, [76] and the enhancement [77] of parity-violating effects in nuclear capture reactions. One may also expect that there are resonance states with nuclear quantum numbers which are dominantly color-polarized. The mass of these states is not known. It has also been speculated [78] that such long-lived states could have an anomalously large interaction cross section, and thus account for the JUDEK [79] anomaly in cosmic ray and heavy ion experiments. [80] Independent of these speculations, it is clearly important that detailed high-resolution searches for these states be conducted, particularly in inelastic electron scattering and tagged photon nuclear target experiments, such as $\gamma d \to \gamma d$ scatter at large angles.

The structure of the photon's Fock states in QCD is evidently richer than that expected in the vector meson dominance model. [81] For example, consider the one-gluon exchange correction to the $\gamma \to q\bar{q}$ vertex. For $\ell_\perp^2 > \mathcal{O}(\kappa^2)$ the vertex correction renormalizes the point-vertex. For the soft domain $\ell_\perp^2 < \mathcal{O}(\kappa^2)$ one expects large corrections which eventually by dispersion theory correspond to the usual ρ, ω, ϕ, ... interpolating fields. The soft corrections thus give the usual hadron-like component of real photon interactions. Nevertheless, the point-like component survives at any momentum scale, [81] producing point-like corrections to photon shadowing, $J = 0$ fixed pole phenomena in the Compton amplitude, and the "anti-scaling" QCD structure function of the photon. [13] As the resolution scale κ^2 increases past the heavy quark thresholds, one adds the $\gamma \to c\bar{c}$, $b\bar{b}$, etc. components to the photon's wavefunctions.

It is also interesting to consider the dynamical changes to the nucleon wavefunction as one passes heavy quark thresholds. For $\kappa^2 > 4m_c^2$ the proton Fock state structure contains charm quarks, e.g., states $|p\rangle \sim |uud\,c\bar{c}\rangle$. We can distinguish two types of contributions to this Fock state. [31] (1) The "extrinsic" or interaction-dependent component generated from quark self energy diagrams as shown in Fig.18b – a component which evolves by the usual QCD equations with the photon mass scale Q^2; and (2) the "intrinsic" or interaction-independent component which is generated by the QCD potential and equations of motion for the proton, as in Fig.18a – a component which contributes to the proton Fock state without regard to QCD evolution. Since the intrinsic component is maximal for minimum off-shell energy

$$\mathcal{M} = M^2 - \sum_i \left[(k_\perp^2 + m^2)/x\right]_i$$

the charm quarks tend to have the largest momentum fraction x in the Fock state. (This also agrees with the physical picture that all the constituents of a bound state tend to have the same velocity in the rest frame, i.e., strong correlations in rapidity.) Thus, heavy quarks (though rare) carry most of the momentum in the Fock state in which they are present — in contrast to the usual parton model assumption that non-valence sea quarks are always found at low x. One can also estimate using the bag model and perturbative QCD that the probability of finding intrinsic charm in the proton is ~1-2%. [82]

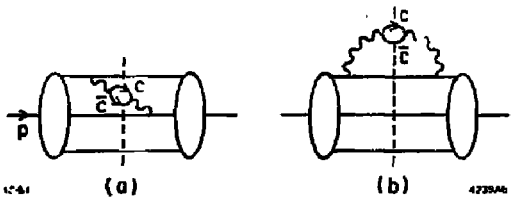

Fig. 18 Intrinsic (a) and extrinsic (b) contributions to the proton $|uudc\bar{c}\rangle$ Fock state.

The diffractive dissociation of the proton's intrinsic charm state [30,31] provides a simple explanation why charmed baryons and charmed mesons which contain no valence quarks in common with the proton are diffractively produced at large x_L with sizeable cross sections at ISR energies. Further discussion may be found in Ref. 31.

VII. THE SYNTHESIS OF QCD AND NUCLEAR PHYSICS

In this section we will discuss applications of quantum chromodynamics to nuclear physics where the basic quark and gluon substructure of hadrons plays an essential role at the nuclear level. [83] Because of asymptotic freedom we can make detailed predictions for nuclear form factors and nuclear scattering processes at large momentum transfer, as well as predict the asymptotic short-distance features of the nucleon-nucleon interaction and nuclear wavefunctions. [84,85] We shall also discuss areas where QCD places constraints on or actually conflicts with standard nuclear physics models. In particular, the fact that the nuclear wavefunction has "hidden color" Fock components [86] implies that the conventional meson and nucleon degrees of freedom of nuclear physics are not sufficient to fully describe nuclei in QCD.

A. The Deuteron Form Factor and Nuclear States at Short Distances

The most direct application of perturbative quantum chromodynamics to nuclei is the structure of the Fock state wavefunctions and the form factors of nuclei at large momentum transfer. In analogy with the meson and nucleon form factor calculations discussed in Secs. III and VI we can write the deuteron form factor at large momentum transfer in the factorized form (see Fig.19): [85]

$$F_D(Q^2) = \int_0^1 [dx] \int_0^1 [dy]\, \phi_D^*(x_i,Q)\, T_H(x_i,y_i;\, Q)\, \phi_D(y,Q) \qquad (7.1)$$

where $T_H \sim [\alpha_s(Q^2)/Q^2]^5$ is computed from the sum of hard scattering diagrams $6q + \gamma^* \to 6q$ where the initial and final quarks are collinear with the initial and final deuteron momentum p and $p+q$, respectively. The distribution amplitude

$$\phi_D(x_i;\, Q) = \int^{\phi} \left[d^2k_\perp\right] \psi_{6q}(x_i, k_{\perp i}) \qquad (7.2)$$

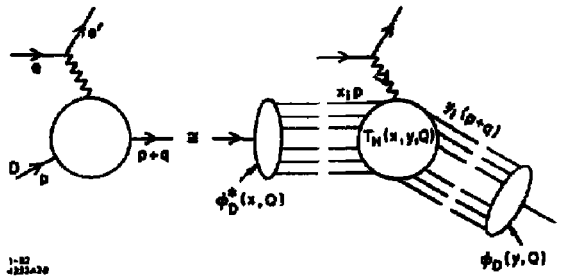

Fig. 19 QCD factorization of the deuteron form factor at large momentum transfer. T_H is computed for six quarks collinear with the incident and final directions.

is defined in terms of the deuteron's six-quark valence wavefunction evaluated at equal time on the light cone. As in the case of the meson and baryon distribution amplitudes, the log Q^2 dependence of ϕ_D is determined from an evolution equation of the form (4.33) where to leading order in $a_s(Q^2)$, the interaction kernel is determined from the sum of single gluon exchange amplitudes.

Because of the helicity-selection rules, the leading form factor of the deuteron corresponds to the helicity zero — helicity zero electron deuteron scattering amplitude:

$$F_D(Q^2) = \sqrt{A_D(Q^2)} \quad .$$

The other deuteron form factors are suppressed by at least one extra power of Q^2. As in the case of the meson form factors, the leading deuteron form factor is not affected by endpoint singularities in the x_i and y_i integration. Thus asymptotically, to leading order in m^2/Q^2 and $a_s(Q^2)$ we have

$$F_D(Q^2) = \left[\frac{a_s(Q^2)}{Q^2}\right]^5 \sum_{n,m=0}^{\infty} d_{nm} \left[\log \frac{Q^2}{\Lambda^2}\right]^{-\gamma_n^D - \gamma_m^D} \tag{7.3}$$

where the deuteron anomalous dimensions γ_n^D can be computed from the eigenvalues of the evolution equation for $\phi_D(x_i,Q)$ or the operator product expansion for six fermion fields near the light cone.

The nominal QCD power law prediction $F_D(Q^2) \sim (Q^2)^{-5}$ at large Q^2 is consistent with the dimensional counting rule [8] $F(Q^2) \sim (Q^2)^{n-1}$ where n is the minimum number of elementary constituents in the Fock state. The prediction thus reflects the QCD substructure of the nucleus and the essential scale-invariance of the renormalizable quark interactions in the tree graphs for T_H. A comparison with data [87] for π, p, n, D, H_e^3 and H_e^4 is shown in Fig.9.

As we have indicated in Fig.20, the deuteron form factor receives contributions from six quark wavefunction components which are in both the standard color $|(uud)_1(udd)_1\rangle$ and "hidden color" $|(uud)_8(udd)_8\rangle$ configurations (see Sec. VI). It should be emphasized that the QCD equation of state for ψ_{6q} automatically leads to mixed color components, at least at short distances. For example, if we impose the boundary condition that the deuteron is effectively an n - p bound state at large distances then the one gluon exchange kernel in the evolution equation for $\phi_D(x,Q)$ automatically leads to hidden color components at large Q^2.

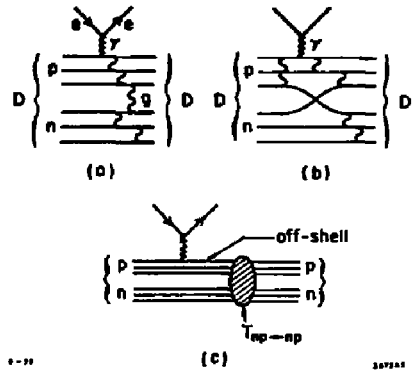

Fig. 20 Hard-scattering contributions to the deuteron form factor. The contributions of diagram (a) require an internal hidden color state. Diagram (b) corresponds to quark interchange. Diagram (c) shows the relationship of the deuteron form factor to the N-N off-shell scattering amplitude.

The perturbative structure of the QCD equation of state for ψ_D at large $k_\perp$ also determines the power law and anomalous dimension structure of the valence wavefunction. [47] For example, if one quark has large $k_\perp$ relative to the deuteron, then $\psi_D(x_i,k_\perp) \sim (k_\perp^2)^{-1}$. On the other hand, if we consider the deuteron as two nucleon clusters, then at large transverse separation we have

$$\psi_D(x_i,k_{\perp i}) \sim \left(\frac{1}{k_{\perp N}^2}\right)^5 \tag{7.4}$$

This power law reflects the fact that the effective nucleon-nucleon interaction large momentum transfer is $T_{np\to np} \sim (1/Q^2)^4$, which is again consistent with dimensional counting.

The specific connection of the asymptotic deuteron form factor to the nucleon-nucleon interaction is as follows: [84] the deuteron form factor is the probability amplitude for the deuteron to remain intact after absorbing a large momentum transfer $n \to p+q$. If we consider the deuteron to be a loosely bound n - p system, with each constituent sharing almost equally the deuteron-four momentum, then each nucleon scatters from $\sim p/2$ to $\sim(p+q)/2$. The coupling of the electromagnetic current to the struck nucleon is effectively point-like as in the case of deep inelastic scattering at large q^2, since the intermediate nucleon state $(p/2 + q)^2 \sim q^2/2$ is far-off-shell. The required n - p scattering amplitude (evaluated at $t = q^2/4 = u$, with one leg space-like at $p_N^2 = q^2/2$) scales at $T_{np\to np} \sim (1/Q^2)^4$. This scaling, combined with the off-shell propagator then gives the results $F_D(Q^2) \sim (Q^2)^{-5}$. The normalization of $F_D(Q^2)$ can then be related to the non-relativistic deuteron wavefunction at the origin (see Ref. 84). It should be emphasized that the relativistic calculation of the deuteron form factor is incompatible with the conventional nuclear physics parameterization [88]

$$F_D(Q^2) = F_N(Q^2)\ F_{Body}(Q^2) \quad . \tag{7.5}$$

In the case of (static) non-relativistic models this form removes the structure of the struck nucleon. Equation (7.5) is, however, incorrect in the large Q^2 domain since the struck nucleon cannot be on-shell both before and after the interaction with the electromagnetic current.

B. Reduced Form Factors [84]

For a general nucleus, the asymptotic power behavior for the minimal helicity-conserving form factor is $F_A(Q^2) \sim (Q^2)^{1-3A}$ reflecting the fact that one must pay

a penalty of $\alpha_s(Q^2)/(Q^2)$ to move each quark constituent from p to p+q. The fact that the momentum transfer must be partitioned among the constituent: implies that the asymptotic domain increases with the nuclear number A.

However, as we shall now show, the introduction of the reduced form factor $F_A(Q^2)$ will allow interesting QCD predictions to be made even at relatively low momentum transfers. The basic idea is as follows: the deuteron from factor $F_D(Q^2)$ is the probability amplitude for the nucleus to remain intact after absorbing momentum transfer Q. Clearly $F_D(Q^2)$ must fall at least as fast as $G_M^p(Q^2/4) \cdot G_M^n(Q^2/4)$ since each nucleon must change momentum from p/2 to (p+q)/2 and stay intact. Thus we should define the "reduced form factor" $f_D(Q^2)$ via

$$F_D(Q^2) \equiv F_N^2\left(\frac{Q^2}{4}\right) f_D(Q^2) \tag{7.6}$$

Note that $f_D(Q^2)$ must itself decrease at large Q^2 since it can be identified as the probability amplitude for the n-p system to remain a ground state deuteron. In fact, the dimensional counting rules $F_D(Q^2) \sim (Q^2)^{-5}$, $F_N(Q^2) \sim (Q^2)^{-2}$ implies the asymptotic behavior $f_D(Q^2) \sim (Q^2)^{-1}$. This is precisely what one expects for a composite of two elementary systems once the nucleon structure has been removed.

We can also understand the origin of the simple result for $f_D(Q^2)$ from T_H diagrams such as Fig.20c where a gluon immediately transfers momentum $1/2\ q^\mu$ to the other nucleon. Such diagrams give contributions of the form

$$F_D(Q^2) \cong F_N^2\left(\frac{Q^2}{4}\right) \frac{\alpha_s(Q^2/4)}{1+Q^2/m^2} \tag{7.7}$$

The mass parameter can be estimated from the corresponding parameters in the meson and nucleon form factors and is expected to be small, $m^2 \cong 0.3\ GeV^2$. The comparison of the data for $f_D(Q^2)$ with the prediction $(Q^2 + 0.3\ GeV^2)\ f_D(Q^2) \to$ const. is given in Fig.21. Remarkably, the predicted flat behavior for $Q^2 f_D(Q^2)$ appears to be accurate from Q^2 below 1 GeV^2 out to the limits of the data. The prediction is also verified at larger Q^2 when one uses inelastic deuteron form factor data at fixed mass $(p+q)^2$.

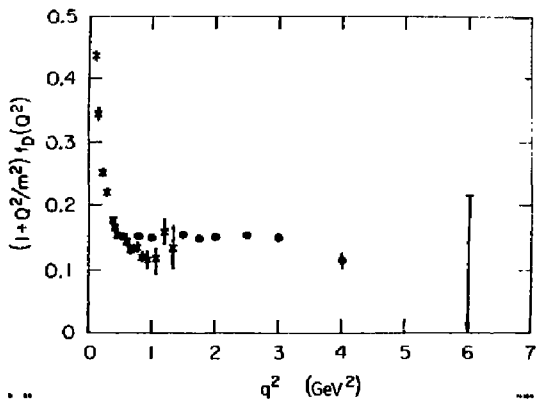

Fig. 21 Comparison of deuteron form factor data with the QCD prediction $(1+Q^2/m^2)f_D(Q^2) \to$ const. at large Q^2. The data are from Ref. 87.

In general, we can define reduced nuclear form factors [84]

$$f_A(Q^2) \equiv \frac{F_A(Q^2)}{\left[F_N(Q^2/A^2)\right]^A} \tag{7.8}$$

QCD then predicts the power behavior $f_D(Q^2) \sim (Q^2)^{1-A}$ (as if the nucleons were elementary). Comparisons with data for H_e^3 and H_e^4 are given in Ref. 87. The definition of the reduced form factor takes into account the correct partitioning of the nuclear momenta, and thus to first approximation represents the nuclear form factor in the limit of point-like nucleon constituents. One can also extend the definition to reduced elastic nuclear scattering amplitudes

$$t_A(Q^2) \equiv \frac{T_A(Q^2)}{\left[F_N(Q^2/A^2)\right]^A} \tag{7.9}$$

e.g., in meson-deuteron elastic scattering at large momentum transfer. It should be of interest to see whether a consistent parameterization of nuclear amplitudes can be obtained if in each nuclear scattering process, reduced "point" amplitudes are defined by dividing out all of the constituent nucleon form factors at the correct partitioned momentum. Again, we emphasize that the standard method based on Eq. (7.5) is invalid in a relativistic theory. The measurements of hadron-nucleus elastic scattering are also interesting from the standpoint of testing basic QCD scattering mechanisms. [84] For example, the $K^+ - A$ scattering amplitude should scale as $A+Z$ at large momentum transfers if the scattering is dominated by u-quark interchange.

C. The Nucleon-Nucleon Interaction at Short Distances

The basic measure of the nuclear force is nucleon-nucleon scattering. As we have discussed in Sec. IV, two general features of the N - N amplitude at large momentum transfer can be predicted from perturbative QCD: hadron helicity conservation and power law scaling at fixed angle. In general there are five independent parity-conserving and time reversal invariant helicity amplitudes. The QCD selection rules [18] $h_{initial} = h_{final}$ implies that $\mathcal{M}(++ \to +-)$ and $\mathcal{M}(-- \to ++)$ are power law suppressed relative to $\mathcal{M}(++ \to ++)$, $\mathcal{M}(+- \to +-)$, $\mathcal{M}(-+ \to +-)$. The helicity conserving amplitudes thus are predicted in first approximation to scale as $\mathcal{M}_{\Delta h = 0} \sim (Q^2)^{-4}$, yielding the dimensional counting prediction

$$s^{10} \frac{d\sigma}{dt}(s,\theta_{cm}) = F(\theta_{cm}) \tag{7.10}$$

for nucleon-nucleon scattering at fixed angle and $s \gg M^2$. More precisely, the nominal power-law is slightly modified by the Landshoff pinch singularity contributions and the logarithm factors from 10 powers of $\alpha_s(Q^2)$ and the anomalous dimensions of the distribution amplitudes. Remarkably, the $pp \to pp$ data is consistent (within a factor ~2) with the fixed angle scaling predicted by (7.10) as the cross section falls more than 4 decades in the range $4 < p_T^2 < 12$ GeV^2, $38^o < \theta_{cm} < 90^o$. (See Fig.22.) The simplest interpretation of the results is that the variation of $\alpha_s(Q^2)$ is very slow in this domain, as in the case of the $Q^6 G_M(Q^2)$ scaling of the nucleon form factors. The presence of the Landshoff pinch singularities, however, could act to compensate for the fall-off of α_s. In addition, there is some evidence [90] that the data is systematically oscillating about the $s^{10}d\sigma/dt$ const prediction, possibly suggesting the presence of an interfering subasymptotic amplitude.

The computation of the angular dependence and normalization of each of the helicity-conserving N - N amplitudes in QCD is a formidable task since, even to

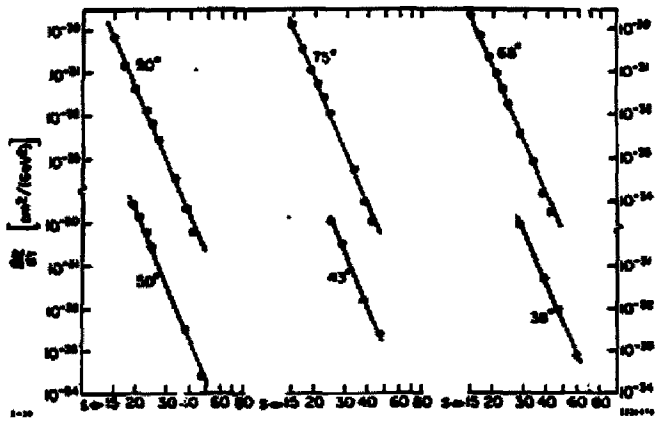

Fig. 22 Differential cross sections for pp → pp scattering at large center of mass angles. The straight lines correspond to the predicted power-law fall-off at $1/s^{10}$. The data compilation is from Ref. 89.

lowest order in α_s, there are of the order of 3×10^6 connected Feynman diagrams in which five gluons interact with six quarks; [91] in addition a detailed representation of the Sudakov suppression is needed in order to integrate over the Landshoff singularities. [92] Considerable phenomenological progress has, however, been made simply by assuming that the dominant diagrams involve quark interchange; [15] i.e., exchange of the common valence quarks. This ansatz seems to yield a good approximation to the observed large angle meson-baryon and baryon-baryon scattering amplitude angular distributions, as well as the correct crossing behavior between the hadronic amplitudes, including $pp \to pp$ to $p\bar{p} \to \bar{p}p$. A useful analytic form for the interchange amplitude in terms of light-cone Fock state wavefunctions is given in Ref. 93. A simple model for the quark interchange amplitude for $pp \to pp$ which has such properties is $\mathcal{M} \propto G_M^p(t)G_M^p(u)$.

The most sensitive tests of the hard scattering QCD prediction involve the polarization effects. The spin asymmetry A_{NN} is defined as

$$A_{NN} = \frac{\frac{d\sigma}{dt}(\uparrow\uparrow) + \frac{d\sigma}{dt}(\downarrow\downarrow) - \frac{d\sigma}{dt}(\uparrow\downarrow) - \frac{d\sigma}{dt}(\downarrow\uparrow)}{\frac{d\sigma}{dt}(\uparrow\uparrow) + \frac{d\sigma}{dt}(\downarrow\downarrow) + \frac{d\sigma}{dt}(\uparrow\downarrow) + \frac{d\sigma}{dt}(\downarrow\uparrow)} \quad . \tag{7.11}$$

which measures the difference of cross sections when both nucleons are polarized parallel to the normal ($\hat{x}$) of the scattering plane or are anti-parallel. Similarly refers to the polarization asymmetry where the initial spins are polarized the laboratory beam direction ($\hat{z}$) versus anti-parallel spins, and A_{SS} refers initial spins polarized (sideways) along the third direction ($\hat{y}$).

For the scattering of identical particles at 90° all amplitudes involving a single helicity flip vanish, e.g., $(++ \to +-)$. This implies the sum rule [97,98]

$$A_{NN} - A_{LL} - A_{SS} = 1 \quad (\theta_{c.m.} = 90^\circ) \quad . \tag{7.12}$$

If in addition the double-flip amplitude $(++ \to --)$ vanishes, as in the case of the perturbative QCD predictions, then we have $A_{NN} = -A_{SS}$ (all angles) and the above sum rule becomes

$$2A_{NN} - A_{LL} = 1 \quad (\theta_{c.m.} = 90^{o}) \tag{7.13}$$

The striking CRABB et al., Argonne measurements for A_{NN} (see Fig.23) can now be combined with preliminary results [96] for A_{LL} at 90° and $p_{lab} = 11.75$ GeV ($p_T \cong 2.4$ GeV): $2A_{NN} - A_{LL} \cong 2(0.58 \pm 0.04) - (0.18 \pm 0.09) = 0.98 \pm 0.17$, which is consistent with helicity conservation. On the other hand, it should be noted that the change of A_{NN} is very rapid: $A_{NN} \cong 0.05$ at $\theta_{c.m.} \leq 60^{o}$ to $A_{NN} \cong 0.60$ at $\theta_{c.m.} \geq 70^{o}$, which is in marked contrast to the generally smooth behavior predicted from calculations of T_H for proton-proton scattering. For example, hard scattering diagrams with only quark interchange (see, e.g., Fig.20b) between the nucleons (which gives a good representation of the pp → pp angular distribution and crossing to $p\bar{p} \to p\bar{p}$) leads to the simple predition [97,98]

$$A_{NN} = -A_{LL} = -A_{SS} = 1/3 \quad (\theta_{c.m.} = 90^{o}) \quad . \tag{7.14}$$

with a very slow variation (≤2%) over all $\theta_{c.m.}$. Diagrams with quark interchange plus gluon exchange between nucleons give a smaller value for A_{NN}. [99] The angular distribution predicted for diagrams with only gluon exchange is incompatible with the large angle data; furthermore, if these amplitudes are normalized to the small angle regime then they are negligible at 90°. [19]

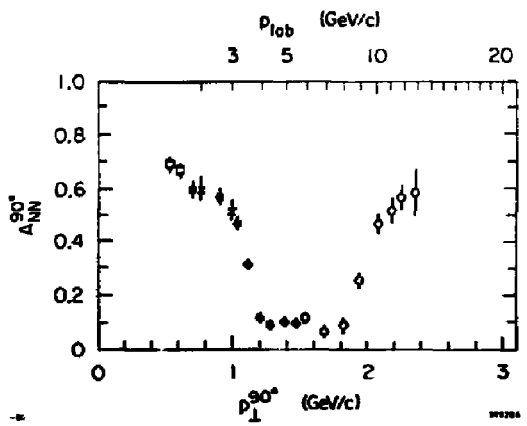

Fig. 23 Data for the spin asymmetry A_{NN} (normal to the scattering plane) for pp scattering at 90° as a function of p_{lab} and p_T. From Ref. 95.

At this stage, there does not seem to be a convincing explanation of the nucleon-nucleon polarization effects at large angle. [100] It seems possible that whatever interference of amplitudes causes the oscillation of $d\sigma/dt$ around the smooth s^{-10} behavior can also lead to striking interference effects in the polarization correlations. [90,97] One possibility is that the quark interchange amplitude is asymptotically dominant, but that in the present experimental range there is significant interference with multi-Regge exchange contributions. [97] An important point is that the Landshoff pinch contribution for pp → pp scattering includes three sequential qq → qq scatterings each at approximately the same momentum transfer $\hat{t} \sim 1/9$. Since $|\hat{t}| < 1.1$ GeV^2 is not very large, ordinary Reggeon exchange could still be playing a role in the quark-quark scattering amplitude. Unfortunately, the introduction of such contributions necessarily includes extra parameters and considereble model-dependence. Nevertheless, a simple estimate of the rotating phase associated with triple Regge exchange is consistent with the interference pattern indicated by the pp → pp large angle data. [91]

D. Continuity of Nuclear Physics and Quantum Chromodynamics

The syntheses of nuclear dynamics with QCD is clearly an important and fascinating fundamental problem in hadron dynamics. The short distance structure of the nucleon-nucleon interaction as determined by perturbative QCD must join smoothly and analytically with the large distance constraints (meson-exchange dynamics) of the N - N potential. The length scale of QCD is comparable with the inverse nucleon radius so it is difficult to find a specific domain where nuclear physics can be studied in isolation from QCD.

The grand goal of QCD would be to actually derive the nuclear force from fundamental QCD interactions. The difficulty is that the nucleon-nucleon interaction in QCD is a remnant of the color forces and is analogous in complexity to calculating the molecular force between neutral atoms, e.g., positronium. The basic ingredients are quark interchange which is evidently related at long distances to pion and other meson exchange, and multiple gluon exchange, which despite the zero mass of the gluon must have an inverse range shorter than the mass of the lowest lying gluonium state. It is possible that numerical results for the N - N potential will eventually be obtained from lattice gauge theory calculations. Model calculations of these exchange forces have also been given in the context of bag [101] and potential models. [102]

The constraints of asymptotic QCD behavior, especially its power-law scaling and helicity selection rules have only begun to be exploited. For example, dispersion relations and superconvergent relations for the nuclear-nuclear helicity amplitudes should yield sum rules and constraints on hadronic couplings and their spectra. One could try to enforce a form of duality which equates the $q\text{-}\bar{q}\text{-}g$ exchange amplitudes with the sum over meson-exchange degrees of freedom. However, this cannot be strictly correct since the existence of hidden color configurations — whether mixed with ordinary nuclear states or appearing as resonance excitations — implies that duality in terms of the low-lying hadrons cannot be a true identity.

One missing ingredient in nuclear physics model calculations of meson exchange amplitudes and currents is the form of the effective off-shell meson-nucleon-nucleon vertices. In principle, the effective form factors of these couplings is determined by QCD. Let us return to the form of the ultraviolet regularized QCD Lagrangian density discussed in Sec. II. If the cutoff κ^2 is comparable to hadronic scales then extra contributions will be generated in the effective Lagrangian:

$$\mathscr{L}^{\kappa}_{QCD} = \mathscr{L}^{\kappa}_{0} + \frac{em(\kappa)}{\kappa^2}\ \bar{\psi}\sigma_{\mu\nu}\,\partial^{\mu}\,\psi A^{em}_{\nu} \qquad (7.15)$$

$$+ s\,\frac{f_{\pi}^2}{\kappa^2}\,\phi_{\pi}\overleftrightarrow{\partial^{\mu}}\,\phi_{\pi}\,A^{em}_{\mu}$$

$$+ e\,\frac{f_{\pi}^2}{\kappa^2}\,\bar{\psi}_N\,\gamma^{\mu}\,\psi_N\,A^{em}_{\mu}$$

$$+ \frac{f_p^2\,f_{\pi}}{\kappa^6}\,\partial_{\mu}\,\bar{\psi}_N\,\gamma_5\,\gamma^{\mu}\,\psi_N\,\phi_{\pi}$$

$$+ \ldots$$

where $\mathscr{L}^{\kappa}_{0}$ is the standard contribution and the higher twist terms of order κ^{-2}, κ^{-4}, ... are schematic representations of the quark Pauli form factor, the pion and nucleon Dirac form factors, and the π-N-N coupling. The pion and nucleon fields represent composite operators constructed and normalized from the valence Fock

amplitudes and the leading interpolating quark operators. Our main point for writing down Eq. (7.15) is just to estimate the effective asymptotic power law behaviors of the couplings, e.g., $F_{Pauli}^{quark} \sim 1/Q^2$, $F_\pi \sim f_\pi^2/Q^2$, $G_M \sim f_p^2/Q^4$ and the effective $\pi \bar{N} \gamma_5 N$ $F_{\pi NN}$ coupling: $F_{\pi NN}(Q^2) \sim M_N f_p^2 f_\pi / Q^6$. The net pion exchange amplitude thus falls off very rapidly at large momentum transfer $M_{NN \to NN}^{\pi} \sim (Q^2)^{-7}$, much faster than the leading quark interchange amplitude $M_{NN \to NN}^{q\bar{q}} \sim (Q^2)^{-4}$. Similarly, the vector exchange contributions give contributions $M_{NN \to NN}^{\rho} \sim (Q^2)^{-6}$.

Thus, meson exchange amplitudes and currents, even summed over their excited spectra do not contribute to the leading asymptotic behavior of the N - N scattering amplitudes or deuteron form factors, once proper account is taken of the off-shell form factors which control the meson-nucleon-nucleon vertices.

There is a further difficulty extending nuclear physics models based on an effective nucleon-nucleon-meson field theory. If one uses pointlike $\bar{N}\vec{\tau}N$ isospin invariant couplings of the nucleons to the rho meson then the theory is not renormalizable without the full apparatus of non-Abelian gauge theories, including triple ρ and four-point ρ meson couplings, and a spontaneous symmetry breaking mechanism to generate the ρ mass. We emphasize that a non-renormalizable field theoretic model requires a new cutoff in each order of perturbation theory and thus is not predictive.

In addition to the above problems, it is difficult to understand within the context of QCD the role of $N\bar{N}$ pair production contributions as conventionally used in nuclear physics model calculations of electromagnetic exchange currents, etc. Nucleon pair (i.e., $qqqq\bar{q}\bar{q}\bar{q}$) terms are far-off-shell and highly suppressed by off-shell form factors in QCD. On the other hand, anomalous "contact" terms are automatically generated in QCD time-ordered perturbation theory for the Z-graph term in the quark electromagnetic current. In the case of light-cone perturbation theory these are the instantaneous quark propagator terms described in Sec. III.

E. Structure Functions of Nuclei

If the nucleus were simply a loosely bound collection of nucleons, then the nuclear structure functions should reflect simple additivity:

$$G_{q/A}(x,Q) = Z\, G_{q/p}(x,Q) + (A-Z)\, G_{q/n}(x,Q) \tag{7.16}$$

$$G_{g/A}(x,Q) = A\, G_{g/N}(x,Q)$$

where $x = A\left(k^o + k^3/p_A^o + p_A^3\right)$ is the quark light-cone momentum fraction scaled to the nucleon momentum. The interesting physics is the derivation from simple additivity, which arises from the following sources:

(1) The nuclear structure functions $G_{q/A}$ and $G_{g/A}$ do not vanish at $x = 1$ but extend kinematically all the way out to $x = A$ where one quark or gluon has the entire available light-cone momentum of the nucleus. For $x \gtrsim 1$ this is related to ordinary fermi motion. At larger x the structure functions are sensitive to far-off-shell QCD dynamics. [84,103,104] Modulo logarithms, the power behavior of perturbative QCD contributions to the inclusive distributions is given by the spectator counting rule [60] (see Fig.24)

$$G_{a/A} = \frac{dN_{a/A}}{dx_a} \underset{x_a \to A}{=} C_{a/A}\, (A - x_a)^{2n_s - 1} \tag{7.17}$$

where n_s is the number of spectator (quark) constituents in the bound system A forced to carry small light-cone momentum fraction: $x_a \to 0$. The power law is

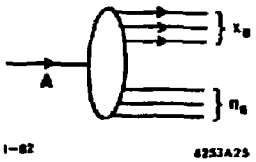

Fig. 24 Application of spectator counting rule to general composite or nuclear systems. The subsystem a has light-cone momentum fraction $x_a = k_a^+/p_a^+$. There are n_s quark spectators.

derived by simply counting the minimum number of off-shell propagators ($\mathcal{G} \to -\infty$ as $x \to x_{max}$) which are required to transfer all the momentum of A to a. Since the end result only depends on the number of spectators, it is easily shown that the system a can be a quark, gluon, or multiparticle cluster of constituents. However, the rule (7.17) holds only for the case where the helicities of a and A are identical; otherwise there are additional power-law suppressions. Examples of the spectator counting rule are $dN/dx \sim (1-x)^3$ for q/p, $(3-x)^{15}$ for q/H_e^3 and $(3-x)^{11}$ for p/H_e^3. These rules can be tested not only in deep inelastic lepton-nucleus scattering, but also in forward inclusive nuclear scattering reactions where hadrons are produced with large longitudinal momentum fractions; e.g., $dN/dx\ (A_1 + A_2 \to p+X) \sim dN/dx\ (P/A_1)$. [103,105] The data for large x for these reactions does appear to be generally consistent with the power-law fall-off predicted by QCD spectator counting. Further discussions and tests can be found in Refs. 83, 103, and 105. In the case of the deuteron (and other even spin nuclei) the mismatch between the quark and nuclear helicity implies that the deuteron structure function vanishes at the kinematic limit as [106] $F_{2D} \sim G_{q/D}(x) \sim (2-x)^{10}$ rather than $(2-x)^9$. (In each case, the power is logarithmically increased by QCD evolution.) One also expects an anomalous contribution to F_{LD} at $x \sim 2$ analogous to the pion longitudinal structure function. Such contributions cannot be obtained from simple convolutions of the nucleon structure functions with nuclear distributions. The testing of these predictions is, of course, difficult because of the rapid fall-off of the structure functions, and the necessity for high Q^2 in order to avoid higher twist contributions. As we have discussed in Sec. V, we expect, in general, a sum of impulse approximation contributions [84,107]

$$\frac{d\sigma}{dQ^2\,dx}(\ell A \to \ell' X) = \sum_a \frac{d\sigma}{dQ^2}(\ell a \to \ell' a)\,\frac{d\,N_{a/A}}{dx} \tag{7.18}$$

representing incoherent contributions, each of which correspond to lepton scattering on one quark or clusters of quarks in the nuclear target. We also note that the transverse momentum distributions $dN_{a/A}/d^2k_\perp$ can also be predicted from the perturbative QCD processes which control the high momentum tail of the bound state wavefunctions.

(2) The deviations from simple additivity of $G_{a/A}$ at $x \sim 0$ are related to the important question of whether the leading twist nucleon structure functions are shadowed; i.e., $F_{2A}(x,Q^2) \sim A^{\alpha(x,Q^2)} F_{2N}(x,Q^2)$ at large Q^2, with $\alpha(x,Q^2) < 1$ (see Fig.25). A simple duality argument [109] based on the assumption of continuity of the structure function at $x = x_{Bj} = Q^2/2M\nu \to 0$ with the photoabsorption cross section $\sigma_{\gamma A}(\nu)$ (which is shadowed because of coherent vector meson photoproduction processes) obviously implies shadowing of $F_{2A}(x,Q^2)$. However, as emphasized in Ref. 110, the QCD momentum sum rule then implies that a region of x must exist (probably at $x \sim m_\pi/M_N$) where the structure function obeys "anti-shadowing," i.e., $\alpha(x) > 1$. The existing data on lepton-nucleon scattering [108] clearly show shadowing at low x and low Q^2, but the data are not sufficient to demonstrate whether the shadowing occurs in the leading twist Bjorken-scaling contributions to the structure function, rather than in higher twist contributions associated with vector meson electroproduction.

There are several arguments which indicate that QCD actually predicts the absence of shadowing for the leading twist structure functions, i.e., $\alpha(x,Q^2) \cong 1$

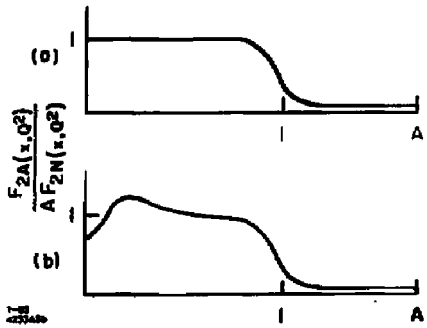

Fig. 25 Schematic representation of the deep inelastic nuclear structure function normalized to its nucleon components. (a) The case of zero shadowing. (b) Shadowing and anti-shadowing.

at $Q^2 \to \infty$ and fixed $x < 1$. Since shadowing is associated with initial state (Glauber) interactions, [20] let us consider the representative initial state contributions to the virtual photo-absorption cross section $\sigma_{\gamma^*}(x,Q^2)$ shown in Fig.26.

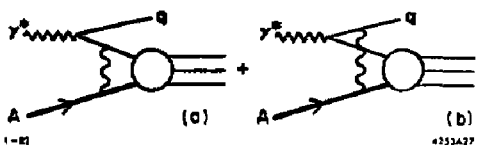

Fig. 26 Example of an initial state scattering correction to the nuclear photo-absorption cross section leading to Glauber corrections and shadowing of the nuclear structure functions. The contributions of (a) and (b) cancel for Q^2 large compared to the momentum transfer of the exchanged gluon.

At low Q^2, soft vector gluon exchange (finite transverse momentum $\ell_\perp$, and small light-cone momentum fraction $\ell^+ \sim \mathcal{O}(1/\sqrt{s})$ between the incident quark and the nuclear quark spectators gives an energy independent initial state correction to the photon-nucleus cross section as in meson-nucleus reactions. However, at high $Q^2 \gg \ell_\perp^2$, the contributions of Figs.26a and 26b exactly cancel — corresponding to the vanishing of the hadronic radius of the photon. A complimentary argument for the absence of shadowing corrections based on explicit consideration of coherent shadowing contributions and their damping at large Q^2 is given in Ref. 105.

(3) In addition to the above considerations, simple additivity of the nuclear structure functions will be violated by the fact that the nuclear Fock state spectrum is more complex than that of the individual nucleon. For example, the nuclear binding associated with meson exchange contributions leads to a modification to the sea quark and antiquark distributions in the nuclear structure functions. The number of strange quarks in the a-nucleus structure function may be different than the extrapolation from a nucleon target. We also emphasize that the existence of hidden color components in the Fock state expansion of the nuclear state also implies new contributions to the nuclear structure functions, particularly in the $x > 1$ far-off-shell domain.

The definitive experimental identification of additivity violating effects in the nucleus will also require a careful study of the nuclear target dependence of lepto-production channels, e.g., the reaction $eA \to eK^+X$ which is sensitive to the intrinsic strange quark composition of the nucleus, i.e., contributions not due to QCD evolution (see Sec. VI). The identification of specific $ed \to eN^*N^*$ channels in electron-deuteron scattering may be an important clue to the $\Delta\Delta$ and hidden color Fock states of the deuteron as in Eq. (6.24).

F. Nuclei as Probes of Particle Physics Dynamics

Thus far in this section we have discussed applications of QCD specific to the dynamics and structure of nuclei. Conversely, there are numerous examples where a nuclear target can be used as a tool to probe particular aspects of particle physics. We will only mention a few applications here.

(1) Parity violation in hadronic or nuclear processes. The exchange of a weak W or Z boson between the quarks of a hadron or nucleus leads to a high momentum component in the Fock state wavefunction

$$\Delta\psi(x,\vec{k}_\perp) \sim \frac{a}{k_\perp^2 + M_W^2}\,\phi\left(x, M_W^2\right) \tag{7.19}$$

as in the derivation of the distribution amplitude evolution equation. [19] The interference of these amplitudes with normal QCD contributions leads to parity violation in processes such as photodisintegration $\gamma d \to np$ and total hadronic cross sections. [111]

(2) The nucleus as a color filter. As we have discussed in Sec. VI, one can study a new class of diffractive dissociative jet production processes in nuclei which isolate the valence component of meson wavefunctions. [30] One can also use the A dependence of the nuclear cross section to separate central and diffractive mechanisms for heavy flavor production (open charm, etc.). [30,31]

(3) Nuclear corrections to inclusive QCD reactions. When a hadron traverses a nucleus, its Fock state structure would be expected to be modified by elastic and inelastic collisions. An analysis based on perturbative QCD is given in Ref. 20. We show that multiple scattering in the nucleus increases the transverse momentum fluctuations of the quark and gluon constituents in the hadron, implying a nuclear enhancement for the rate of hadron and photon production at large transverse momentum. At very large p_T the direct photon production cross section in nuclei should have the form

$$\frac{d\sigma}{d^3p/E}\,(pA \to \gamma X) = A\,\frac{d\sigma}{d^3p/E}\,(pN \to \gamma X)\left[1 + \mathcal{O}\left(\frac{A^{1/3}}{p_T^2}\right)\right] \quad . \tag{7.20}$$

In the case of the Drell-Yan cross section $d\sigma/dQ^2\,d^2Q_\perp\,(pA \to \mu^+\mu^- X)$ the transverse momentum $Q_\perp$ distribution of the produced lepton pair is predicted to broaden due to multiple scattering in the nucleus of the quarks in the initial state. Nevertheless, the integrated cross section $d\sigma/dQ^2\,(pA \to \mu^+\mu^- X)$ is proportional to A. Furthermore, as shown in Ref. 20, the light-cone x distribution of a fast quark is not effected by inelastic processes induced by multiple scattering in the nucleus as long as the quark momentum is large compared to a scale proportional to the length of the target. This effect is related to the formation zone analysis of LANDAU and POMERANCHUK [112] which shows that radiation from a classical current propagation between fixed target centers is limited at high energies.

(4) Propagation of quark and gluon jets in nuclear targets. In the conventional parton model picture based on the impulse approximation, the multiplicity of hadrons produced in deep inelastic lepton scattering or a nuclear target is expected to be identical to that on a single nucleon, since only one nucleon is "wounded" at large momentum transfer. In fact, the soft gluons radiated by the scattered quark jet in the deep inelastic process can interact in the nuclear target and produce extra associated multiplicity in the target-fragmentation and central rapidity regions. [113] As shown in Ref. 20 only fast quanta are prevented in QCD from interacting inelastically in a nuclear target. The study of the initial and final interactions of the hadrons and jets in nuclear target, specifically the modification of longitudinal and transverse momentum distributions, can provide important insights into the nature of QCD dynamics.

VIII CONCLUSIONS

In these lectures we have discussed the application of QCD to hadron and nuclear dynamics at short distances where asymptotic freedom allows a systematic perturbative approach. We have shown that it is possible to define the perturbative expansion in $\alpha_s(Q^2)$ in such a way as to avoid ambiguities due to choice of

renormalization scheme or scale, at least in the first non-trivial orders. [14] Our main emphasis in these lectures, however, has been on how to systematically incorporate the effects of the hadronic wavefunction in large momentum transfer exclusive and inclusive reactions — thus leading to a broader testing ground for QCD. We have particularly emphasized the Fock state wavefunctions $\psi_n(x_i, \vec{k}_{\perp i}; \lambda_i)$ which define the hadron or nuclear state in terms of its quark and gluon degrees of freedom at equal time on the light-cone. It is clear that a central problem of QCD is to determine not only the spectrum of the theory but also the basic bound state wavefunctions of the color singlet sector. Such solutions may be found in the near future using lattice numerical methods, particularly by quantizing at equal time on the light-cone, or by more direct attacks on the QCD equations of motion for the ψ_n, as discussed in Sec. III.

Even without explicit solutions for the ψ_n, we can make a number of basic and phenomenological statements concerning the form of the wavefunctions: [27]

(1) Given the ψ_n we can compute the single and multiple quark and gluon distribution amplitudes and structure functions which appear as the coefficient functions in the QCD predictions for high momentum transfer exclusive and inclusive reactions, including dynamical higher twist contributions. We have also emphasized general features of these distributions, including helicity selection rules, Lorentz properties, connections with the Bethe-Salpeter amplitudes, renormalization properties, and correspondence limits in the non-relativistic weak binding approximation.

(2) The perturbative structure of QCD leads to predictions for the high $k_\perp$, $x \to 1$ and far-off-shell behavior of the wavefunction. In particular, the large $k_\perp$ power-law behavior $\psi_V \sim k_\perp^{-2}$ of the valence wavefunctions and the $|\psi|^2 \sim k_\perp^{-2}$ behavior of the higher Fock state contributions leads to QCD evolution equations and light-cone operator product expansion for the essential measures of the wavefunctions, the distribution amplitudes $\phi_M(x,Q)$, $\phi_B(x_i,Q)$, $\phi_D(x_i,Q)$ and the structure functions. We have also emphasized the fact that the valence wavefunction behavior $\psi_V \sim k_\perp^{-2}$ implies that the high $k_\perp^2$ behavior of quark and gluon jet distributions $dN/dk_\perp^2$ is $\sim 1/k_\perp^4$, not exponential or gaussian.

(3) Important boundary values and constraints on hadronic wavefunctions are obtained from the weak and electromagnetic decay amplitudes, including $\phi \to B\bar{B}$. The meson and baryon distribution amplitudes are measureable in detail from the angular behavior of the $\gamma\gamma \to M\bar{M}$ and [114] $\gamma\gamma \to B\bar{B}$ amplitudes.

(4) By assuming simple analytic forms for the valence wavefunctions in the non-perturbative domain, we have found consistent parameterizations which are compatible with the data for hadron form factors, decay amplitudes, etc. An important feature which emerges from these studies is that the valence state is more compact in transverse dimensions than the physical hadron. Even at low momentum transfer scale, higher Fock states play an important role, i.e., there is no scale where the proton can be identified as a 3-quark valence state. This observation may be compatible with the traditional nuclear physics picture of the nucleon as a central core, surrounded by a light-meson cloud. [115]

(5) The fact that there is a finite probability for a hadron to exist as its valence state alone, implies the existence of a new class of "directly-coupled" semi-inclusive processes where a meson or baryon is produced singly at large transverse momentum, or interacts in a high-momentum transfer reactions without accompanying radiation or structure function evolution. [29] As in the case of directly-coupled photon reactions, the hadron can interact directly with quark and gluons in the short-distance subprocess, with a normalization specified rigorously in terms of the distribution amplitudes or form factors. Examples of these subprocesses are $q\bar{q} \to B\bar{q}$, $gq \to Mq$, $Mg \to q\bar{q}$, $B\bar{q} \to q\bar{q}$. We have also discussed an important contribution to the longitudinal meson structure function $F_L^M \sim C/Q^4$, involving direct-coupling of the meson, somewhat analogous to the photon-structure function. The finite probability for a meson to exist as a $q\bar{q}$ Fock state at small separation also implies a new class of diffractive dissociation processes. [30]

(6) The Fock state description of hadrons in QCD also has interesting implications for nuclear states, especially aspects involving hidden color configurations. More generally, we have emphasized the idea that the far-off-shell components of hadron wavefunctions can be "unveiled" as the energy resolution scale is increased. For example, the existence of heavy quark vacuum polarization processes within the hadronic bound state implies finite probabilities for hidden charm Fock states even in light mesons and baryons. The diffractive dissociations of these rare states appears to provide a natural explanation of the remarkable features of the charm production cross sections measured at the ISR. [31]

(7) We have also emphasized the importance of initial state interactions in all inclusive reactions involving hadron-hadron collisions. The initial state interactions disturb the color coherence, $k_\perp$ distributions, and at low energies the x-dependence on the incoming hadronic distributions. Despite these profound effects on the hadronic Fock states, many of the essential features of the QCD predictions still are retained. [20] We have also discussed many examples where a nuclear target can be used to analyze the propagation of quarks and gluons through a hadronic medium.

(8) In Sec. VII of these lectures we focussed on the role of QCD at nuclear dimensions and its implications for fundamental nuclear interactions. The existence of hidden color Fock state components in the nucleon wavefunction implies that the standard nucleon and meson degrees of freedom are not sufficient to describe nuclei. The mixing of the ground state of a nucleus with the extra hidden color states will evidently lower its energy and thus influence the nuclear magnetic moment, charge radius, and other properties. We expect that the hidden color components will be most significant in large momentum transfer nuclear processes and reactions such as the parity-violating terms in the photon-disintegration of the deuteron, which are sensitive to the structure of the nuclear wavefunction at short distances. Conversely, the new QCD degrees of freedom should also imply the existence of excited nuclear states which are predominantly of hidden color. These states may have narrow width if they are below the pion decay threshold. The six-quark excitation of the deuteron could possibly be found by a careful search for anomalous resonant structure in $\gamma d \to \gamma d$ scattering at large angles. Other speculations [86] concerning the phenomenology of these states are discussed in Sec. VI.

The fact that QCD is a viable theory for hadronic interactions implies that a fundamental description of the nuclear force is now possible. Although detailed work in the synthesis of QCD and nuclear physics is just beginning it is clear from the structure of QCD as a relativistic field theory that several traditional concepts of nuclear physics will have to be modified. These include conventional treatments of meson and baryon-pair contributions to the electromagnetic current and analyses of the nuclear form factor in terms of factorized on-shell nucleon form factors. On the other hand, the reduced nuclear form factors and scattering matrix elements discussed in Sec. VII give a viable prescription for the extrapolation of nuclear amplitudes to zero nucleon radius. There is the possibility that the present phenomenology of nuclear parameters will be significantly modified.

Independent of the specific dynamical theory, we have emphasized the utility of light-cone perturbation theory as an elegant but calculationally simple extension of non-relativistic quantum mechanics to the relativistic domain. The number of possible applications of this tool to nuclear physics [116] is extensive since quantization at equal time on the light-cone allows a consistent definition of relativistic Fock state wavefunctions, their equations of state, and a completely relativistic treatment of the dynamics of elementary and composite systems.

Thus, in summary, we have found that the testing ground of perturbative QCD where rigorous, definitive tests of the theory can be made can now be extended throughout a large domain of large momentum transfer exclusive and inclusive lepton, photon, hadron and nuclear reactions. With the possible exception of inclusive hadron production at large transverse momentum, a consistent picture of these reactions is now emerging. By taking into account the structure of hadronic wavefunctions, we have the opportunity of greatly extending tests of QCD, unifying the

short and long distance physics of the theory, and making an eventual synthesis with the realm of hadronic spectroscopy, low momentum transfer reactions and nuclear physics.

ACKNOWLEDGEMENTS

These lectures are based on recent work done in collaboration with G. P. Lepage (exclusive processes in QCD and light-cone perturbation theory); Tao Huang and G. P. Lepage (the structure of hadronic wavefunctions and their constraints); G. P. Lepage and P. B. Mackenzie (scheme and scale dependence in perturbative QCD); E. L. Berger and G. P. Lepage (calculable higher twist and direct subprocesses); and G. Bodwin and G. P. Lepage (initial and final state corrections to QCD processes). The lectures on the applications of QCD to nuclear physics were inspired by my collaborations with Benson T. Chertok, whose experimental and theoretical work greatly motivated this field.

I am also grateful to the organizers of this very productive summer school, Professors D. C. Fries and B. Zeitnitz.

REFERENCES

[1]Reviews of QCD are given in: A. J. Buras, Rev. Mod. Phys. 52, 199 (1980); A. H. Mueller, Phys. Rep. 73C, 237 (1981); E. Reya, Phys. Rep. 69, 195 (1981); G. Altarelli, Univ. of Rome preprint 701 (1978); W. Marciano and H. Pagels, Phys. Rep. 36C, 137 (1978); S. J. Brodsky and G. P. Lepage, Proceedings of the SLAC Summer Inst. on Particle Physics, 1979. See also "Perturbative Quantum Chromodynamics" (Tallahassee, 1981). AIP Proceedings No. 74, New York, 1981.

[2]For recent reviews of the phenomenology of QCD see A. J. Buras, FERMILAB-CONF-81/69-THY and A. H. Mueller, CU-TP-219 (1981), to be published in the Proc. of the 1981 International Symposium on Lepton and Photon Interactions at High Energies, Bonn, August 1981.

[3]S. Gupta and H. R. Quinn, SLAC-PUB-2763 (1981).

[4]H. D. Politzer, Phys. Rev. Lett. 30, 1346 (1973); D. J. Gross and F. Wilczek, Phys. Rev. Lett. 30, 123 (1973).

[5]See, e.g., Sau Lan Wu, DESY-81-071 (1981) and Proc. of the 1981 SLAC Summer Inst. on Particle Physics. See also the 1981 Proc. of the IVth Int. Colloq. on Photon-Photon Interactions, Paris (ed. G. London).

[6]TASSO Collaboration: R. Brandelik, et al., DESY Report 81/053 (1981). JADE Collaboration: W. Bartel, et al., DESY Report 81/048 (1981).

[7]PLUTO Collaboration: see W. Wagner, Proc. of the XXth Int. Conf. on High Energy Physics, Madison, 1980; Ch. Berger, et al., DESY preprint 81/051 (1981).

[8]S. J. Brodsky and G. R. Farrar, Phys. Rev. Lett. 31, 1153 (1973), and Phys. Rev. D11, 1309 (1975); V. A. Matveev, R. M. Muradyan and A. V. Tavkheldize, Lett. Nuovo Cimento 7, 719 (1973).

[9]S. J. Brodsky and G. P. Lepage, Phys. Rev. Lett. 43, 545, 1625(E) (1979). S. J. Brodsky, G. P. Lepage, S.A.A. Zaidi, Phys. Rev. D23, 1152 (1981).

[10]For a review of high momentum transfer exclusive processes and references, see A. H. Mueller, Ref. 1.

[11]S. J. Brodsky and G. P. Lepage, SLAC-PUB-2294, published in "Quantum Chromodynamics," Wm. Frazer and F. Henyey (eds.) (AIP, 1979), Phys. Lett. 87B, 359 (1979), S. J. Brodsky, Y. Frishman, G. P. Lepage, C. Sachrajda, Phys. Lett. 91B, 239 (1980). See also A. V. Efremov and A. V. Radyushkin, Rev. Nuovo Cimento 3, 1 (1980); Phys. Lett. 94B, 245 (1980). A. Duncan and A. Mueller, Phys. Rev. D21, 1636 (1980); Phys. Lett. 90B, 159 (1980). G. R. Farrar and D. R. Jackson, Phys. Rev. Lett. 43, 246 (1979); V. L. Chernyak and A. R. Vhitnishii, JETP Lett. 25, 11 (1977); G. Parisi, Phys. Lett. 43, 246 (1979); M. K. Chase, Nucl. Phys. B167, 125 (1980).

[12]S. J. Brodsky and G. P. Lepage, Phys. Rev. D24, 1808 (1981).

[13]E. Witten, Nucl. Phys. B120, 189 (1977). V. A. Bardeen and A. J. Buras, Phys. Rev. D20, 166 (1979).

[14]S. J. Brodsky, G. P. Lepage, P. B. Mackenzie (to be published).

[15]For early work on higher twist contributions see: R. Blankenbecler, S. J. Brodsky, J. F. Gunion, Phys. Rev. D18, 900 (1978), and D. Sivers, S. J. Brodsky, and R. Blankenbecler, Phys. Rep. 23C, 1 (1976) and references therein. Higher twist contributions to deep inelastic scattering were first discussed in detail by: R. Blankenbecler and I. A. Schmidt, Phys. Rev. D16, 1318 (1977); L. F. Abbott and R. M. Barnett, Annals Phys. 125, 276 (1980); G. R. Farrar and D. R. Jackson, Phys. Rev. Lett. 35 (1975). See also L. F. Abbott, E. L. Berger, R. Blankenbecler, and G. Kane, Phys. Lett. 88B, 157 (1979); L. F. Abbott, W. B. Atwood, and R. M. Barnett, Phys. Rev. D22, 582 (1980), and references therein. More general frameworks for dynamical higher twist contributions are given in W. E. Caswell, R. R. Horgan, S. J. Brodsky, Phys. Rev. D18, 2415 (1978); and H. D. Politzer, Nucl. Phys. B172, 349 (1980); and S. J. Brodsky and G. P. Lepage, Ref. 1. Specific QCD calculations are given in G. R. Farrar and G. C. Fox, Nucl. Phys. B167, 205 (1980); E. L. Berger, T. Gottschalk, and D. Sivers, Phys. Rev. D23, 99 (1981); E. L. Berger and S. J. Brodsky, Phys. Rev. Lett. 42, 940 (1979), Phys. Rev. D24, 2428 (1981); E. L. Berger, Phys. Lett. 89B, 241 (1980); R. L. Jaffe and M. Soldate, Phys. Lett. 105B, 467 (1981).

[16]For a review of experimental evidence on higher twist terms in deep inelastic scattering see C. Matteuzzi, SLAC-PUB-2827 (1981).

[17]P. V. Landshoff, Phys. Rev. D10, 1024 (1974); P. Cvitanovic, Phys. Rev. D10, 338 (1974); S. J. Brodsky and G. Farrar, Phys. Rev. D11, 1309 (1975).

[18]S. J. Brodsky and G. P. Lepage, Phys. Rev. D24, 2848 (1981).

[19]G. P. Lepage and S. J. Brodsky, Phys. Rev. D22, 2157 (1980).

[20]G. T. Bodwin, S. J. Brodsky and G. P. Lepage, Phys. Rev. Lett. 47, 1499 (1981).

[21]S. J. Brodsky and G. P. Lepage, Ref. 1; and S. J. Brodsky and G. P. Lepage, SLAC-PUB-2601 (1980), presented at the XXth Int. Conf. on High Energy Physics, Madison, Wisc. (1980).

[22]G. R. Farrar and D. R. Jackson, Ref. 15; E. L. Berger and S. J. Brodsky, Ref. 15.

[23]For an early discussion see T. A. DeGrand, Y. J. Ng, S.H.H. Tye, Phys. Rev. D16, 3251 (1977). The large $k_\perp$ behavior of hadronic wavefunctions in QCD is discussed by S. J. Brodsky, Y. Frishman, G. P. Lepage, C. Sachrajda, Ref. 11. See also S. J. Brodsky and G. P. Lepage, Ref. 1. These contributions are in principle normalizable in QCD using the methods of Ref. 19.

[24]E. L. Berger, T. Gottschalk, and D. Sivers, Ref. 15. G. Farrar and G. Fox, Ref. 15.

[25]G. Parisi, Phys. Lett. 43, 246 (1978). A. Duncan and A. H. Mueller, Ref. 11.

[26]See, e.g., S. J. Brodsky, F. E. Close, J. F. Gunion, Phys. Rev. D6, 177 (1972). G. Grammer, J. Sullivan, in Electrons in the Interactions of Hadrons (eds. A. Donaghue, G. Shaw), Plenum Press (1977). T. H. Bauer, R. D. Spital, D. R. Yennie, F. M. Pipkin, Rev. Mod. Phys. 50, 261 (1978).

[27]S. J. Brodsky, T. Huang, G. P. Lepage, SLAC-PUB-2540 (1980), and T. Huang, SLAC-PUB-2580 (1980), published in the Proceedings of the XXth Int. Conf. on High Energy Physics, Madison, Wisc. (1980). The parameterization of the hadronic wavefunctions presented here is preliminary; a complete discussion and final values will be given by S. J. Brodsky, T. Huang, and G. P. Lepage to be published.

[28]A more detailed discussion of the regularization procedure is given by G. P. Lepage et al., presented at the Banff Summer Institute on Particle Physics (1981).

[29]E. L. Berger and S. J. Brodsky, Phys. Rev. D24, 2428 (1981).

[30]G. Bertsch, S. J. Brodsky, A. S. Goldhaber and J. F. Gunion, Phys. Rev. Lett. 47, 297 (1981).

[31]S. J. Brodsky, P. Hoyer, C. Peterson, N. Sakai, Phys. Lett. 93B, 451 (1980). S. J. Brodsky, C. Peterson, N. Sakai, Phys. Rev. D23, 2745 (1981).

[32]For review and references see P. Langacker, Phys. Rep. 72, 185 (1981).

[33]P. Cvitanovic, Phys. Rev. D14, 1536 (1976).

[34]See, e.g., K. Callan, R. Dashen and D. Gross, "Quantum Chromodynamics," Proceedings of the 1978 La Jolla Summer Institute, Wm. Frazer and F. Henyey (eds.), AIP (1979).

[35]For reviews and references for inclusive process factorization see A. J. Buras, Ref. 1. For exclusive processes see Ref. 19 and A. H. Mueller, Ref. 1

[36]G. Parisi and R. Petronzio, Nucl. Phys. B154, 427 (1979).

[37]M. Dine and J. Sapirstein, Phys. Rev. Lett. 43, 668 (1979). K. G. Chetyrkin, A. L. Kataev, F. V. Trachov, Phys. Lett. 85B, 277 (1979).

[38]Alternatively we can choose a standard scheme such as $\overline{MS}$ to define $\alpha_s(Q^2)$.
[39]R. Barbieri, M. Caffo, R. Gatto, E. Remiddi, Phys. Lett. 95B, 93 (1980) and CERN preprint 3071 (1981).
[40]G. P. Lepage and P. B. Mackenzie, Cornell preprint CLNS/81-498 (1981).
[41]S. J. Brodsky and G. P. Lepage, Ref. 1; C. Carci and M. Greco, Phys. Lett. 92B, 175 (1980); D. Amati, A. Bassetto, M. Ciafaloni, G. Marchesini and G. Veneziano, Nucl. Phys. B137, 429 (1980); M. Ciafaloni, Phys. Lett. 95B, 113 (1980).
[42]P.A.M. Dirac, Rev. Mod. Phys. 21, 392 (1949).
[43]S. Weinberg, Phys. Rev. 150, 1313 (1966); L. Susskind and G. Frye, Phys. Rev. 165, 1535 (1968); J. P. Kogut and D. E. Soper, Phys. Rev. D1, 2901 (1970); J. D. Bjorken, J. B. Kogut, D. E. Soper, Phys. Rev. D3, 1382 (1971); S. J. Brodsky, R. Roskies and R. Suaya, Phys. Rev. D8, 4574 (1973).
[44]J. D. Bjorken, et al., Ref. 43.
[45]The regularization can be performed using Pauli-Villars regularization. See Ref. 28.
[46]S. D. Drell and T. M. Yan, Phys. Rev. Lett. 24, 181 (1970).
[47]S. J. Brodsky and S. D. Drell, Phys. Rev. D22, 2236 (1981).
[48]S. J. Brodsky and T. Huang (in preparation).
[49]S. J. Brodsky, Y. Frishman, G. P. Lepage, C. Sachrajda, Ref. 11.
[50]R. D. Field, R. Gupta, S. Otto, L. Chang, Nucl. Phys. B186, 429 (1981); F. M. Dittes and A. V. Radyushkin, Dubna preprint JINR-E2-80-688 (1980); M. Chase, Ref. 11; E. Braaten (private communication).
[51]G. R. Farrar and D. R. Jackson, Phys. Rev. Lett. 43, 246 (1979).
[52]M. Peskin, Phys. Lett. 88B, 128 (1979).
[53]S. J. Brodsky, G. P. Lepage and S.A.A. Zaidi, Phys. Rev. [illegible], 1152 (1981).
[54]A. Duncan and A. Mueller, Phys. Rev. D21, 636 (1980); Phys. Lett. 98B, 159 (1980); A. Mueller, Ref. 1
[55]I. Peruzzi, et al., Phys. Rev. D17, 2901 (1978).
[56]See, e.g., S. J. Brodsky, F. E. Close, J. F. Gunion, Phys. Rev. D5, 1384 (1972); D8, 3678 (1973).
[57]J. D. Bjorken, Phys. Rev. 163, 1767 (1967); 179, 1547 (1969).
[58]G. Altarelli and G. Parisi, Nucl. Phys. B126, 298 (1977). See also, V. N. Gribov and L. N. Lipatov, Sov. J. Nucl. Phys. 15, 483, 675 (1972); J. Kogut and L. Susskind, Phys. Rev. D9, 697, 706, 3391 (1974); L. N. Lipatov, Sov. J. Nucl. Phys. 20, 94 (1975).
[59]R. D. Field, published in "Quantum Chromodynamics," Wm. Frazer and F. Henyey (eds.) AIP (1979).
[60]R. Blankenbecler, S. J. Brodsky, Phys. Rev. D10, 2973 (1974).
[61]F. Martin and A. DeRujula, Phys. Rev. D2 1787 (1980).
[62]G. R. Farrar and D. R. Jackson, Phys. Rev. Lett. 35, 1416 (1975); A. I. Vainshtain and V. I. Zakharov, Phys. Lett. 72B, 368 (1978).
[63]Z. F. Ezawa, Nuovo Cimento 23A, 271 (1974).
[64]See also A. Duncan and A. Mueller, Ref. 54.
[65]K. J. Anderson, et al., Phys. Rev. Lett. 43, 1219 (1979).
[66]M. Haguenauer, et al., Phys. Lett. 100B, 185 (1981).
[67]S. J. Brodsky and G. P. Lepage, Proceedings of the Eugene Few Body Conference 1980, 247C (Nucl. Phys. A353, 1981).
[68]S. Gupta, Phys. Rev. D24, 1169 (1981).
[69]See references 21, 24, 15, and S. J. Brodsky, J. F. Gunion, R. Rückl, Phys. Rev. D18, 2469 (1978). J. Bagger and J. F. Gunion, U.C. Davis preprint 81/3 (1981).
[70]E. L. Berger and S. J. Brodsky, Phys. Rev. D24, 2428 (1981).
[71]S. D. Ellis, P. V. Landshoff, M. Jacob, Nucl. Phys. B108, 93 (1978); P. V. Landshoff and M. Jacob, Nucl. Phys. B113, 395 (1976).
[72]S. J. Brodsky, J. F. Gunion, R. Rückl, Ref. 69.
[73]S. J. Brodsky, T. DeGrand, J. F. Gunion, J. Weis, Phys. Rev. D19, 1418 (1979), Phys. Rev. Lett. 41, 672 (1978); Ch. Llewellyn-Smith, Phys. Lett. 79B, 83 (1978); S. M. Berman, J. D. Bjorken and J. B. Kogut, Phys. Rev. D4, 3378 (1971).
[74]W. Ochs and L. Stodolsky (private communication).
[75]A review of the form factor data is given by B. T. Chertok, CERN preprint PRINT-81-0318, to be published in the Proceedings of the 16th Rencontre de Moriond (1981).
[76]See Ref. 67 and references therein.
[77]A. P. Kobushkin, Yad. Fiz 28, 495 (1978).

[78]Y. M. Dubovik and A. P. Kobushkin, Kiev preprint ITF-78-85E (1978).
[79]B. Judek, Can. J. Phys. 46, 343 (1968), 50, 2082 (1972), Proceedings of the 14th Int. Cosmic Ray Conf., Vol. 79, p. 2343. F. M. Friedlander et al., LBL preprint 11136 (1980). Y. J. Karant, LBL preprint 9171 (1979). W. J. Romo and P.J.S. Watson, Phys. Lett. 88B, 354 (1979).
[80]S. J. Brodsky, SLAC-PUB-1497 (1974), published in the Proceedings of the Int. Conf. on Few Body Problems in Nuclear and Particle Physics, University of Laval, Quebec (1974).
[81]See, e.g., S. J. Brodsky, SLAC-PUB-2747 (1981) and W. R. Frazer, UCSD 10P10-222 (1981), published in the Proceedings of the 4th Int. Colloq. on Photon-Photon Interactions, University of Paris, 1981; and W. A. Bardeen, to be published in the Proceedings of the 1981 Int. Symp. on Lepton and Photon Interactions at High Energies, Bonn, August 1981.
[82]J. F. Donoghue and E. Golowich, Phys. Rev. D15, 3421 (1977).
[83]For related discussions see also S. J. Brodsky and G. P. Lepage, Ref. 67. S. J. Brodsky, SLAC-PUB-2395 (1979) published in the Proceedings of the Berkeley Workshop on Ultrarelativistic Nuclear Collisions 1979: 419. R. Blankenbecler, SLAC-PUB-2077 (1978) and SLAC-PUB-2667 (1981). M. Chemtob, Nucl. Phys. A339, 229 (1980); A314, 387 (1979), and Saclay preprint (1981).
[84]S. J. Brodsky and B. T. Chertok, Phys. Rev. Lett. 37, 269 (1976); Phys. Rev. D14, 3003 (1976). S. J. Brodsky, Ref. 80.
[85]S. J. Brodsky and G. P. Lepage (to be published).
[86]See also, A. P. Kobushkin, Ref. 77; Y. M. Dobovik and A. P. Kobushkin, Ref. 78; Y. J. Kurant, Ref. 79; W. J. Romo and P.J.S. Watson, Ref. 79; S. Fredrikson and M. Järdel, Stockholm preprint TRITA-TFY-81-11 (1981).
[87]R. G. Arnold et al., Phys. Rev. Lett. 35, 776 (1979), 40, 1429 (1978). B. T. Chertok, in Progress in Particle and Nuclear Physics, Erice (1981); and Ref. 75. R. G. Arnold, SLAC-PUB-2334, published in the Proceedings of the Mainz Conference on Nuclear Physics with Electromagnetic Interactions (1979).
[88]For recent calculations which assume factorization of on-shell nucleon form factors see S. A. Gurvitz, Weizmann preprints WIS-81/47 PH (1981); Phys. Rev. Lett.
[89]P. V. Landshoff and J. C. Polkinghorne, Phys. Lett. 44B, 293 (1973).
[90]A. W. Hendry, Phys. Rev. D10, 2300 (1974); Indiana University preprint IUK-IT-60 (1980). There is, however, some question whether the oscillation is systematically observed when all experiments are combined (B. Chertok, private communication).
[91]S. J. Brodsky and G. P. Lepage, SLAC-PUB-2656, published in the Proceedings of the Lausanne International Symposium on High Energy Physics with Polarized Beams and Polarized Targets 1980: 169.
[92]A. H. Mueller, Ref. 1.
[93]J. F. Gunion, S. J. Brodsky, R. Blankenbecler, Phys. Rev. D8, 287 (1973).
[94]See G. H. Thomas, Proceedings of the Lausanne International Symposium 1980, and references therein.
[95]D. G. Crabb, et al., Phys. Rev. Lett. 41, 1257 (1978); E. A. Crosbie, et al., Univ. of Michigan preprint UM HE 80-2 (1980). J. R. O'Fallon, et al., ibid. 39, 733 (1977).
[96]A. Yokosawa, Proceedings of the Lausanne Symposium 1980.
[97]S. J. Brodsky, C. E. Carlson and H. Lipkin, Phys. Rev. D20, 2278 (1978).
[98]G. R. Farrar, S. Gottlieb, D. Sivers and G. H. Thomas, Phys. Rev. D20, 202 (1979).
[99]J. Szwed, Max Planck Inst. preprints MPI-PAE/PTH 33/80 and 34/80 (1980), and Phys. Lett. 93B, 485 (1980).
[100]For additional discussions of the theory of pp polarization effects see C. Avilez, G. Coche and M. Moreno, preprint IFUNAM 80-17 (1980); G. Preparata and J. Soffer, Phys. Lett. 86B, 304 (1979), G. A. Walters, Phys. Rev. Lett. 45, 776 (1980), M. C. Daniel, Barcelona preprint UAB-FT-65 (1980), and the contributions of M. Doncel, G. F. Walters, G. Preparata, J. Soffer, J. Szwed, and M. Moreno to the Lausanne Symposium 1980.
[101]See L. Heller, Proceedings of the KfK Summer School on Quarks and Nuclear Physics.
[102]See, e.g., D. P. Stanley and D. Robsen, Phys. Rev. Lett. 45, 235 (1980), Florida State University preprint (1981), and references therein.

[103]I. A. Schmidt and R. Blankenbecler, Phys. Rev. D15, 3321 (1977). I. A. Schmidt, SLAC Report 203 (1979), R. Blankenbecler, Ref. 83.
[104]L. L. Frankfurt and M. I. Strickman, Phys. Lett. 69B, 93 (1977); 94B, 216 (1980).
[105]S. J. Brodsky, Berkeley Workshop, Ref. 83.
[106]A. I. Vanishtein and V. I. Zakharov, Phys. Lett. 72B, 368 (1978). R. M. Woloshyn, TRIUMF preprint TRI-PP-81-12 (1981).
[107]For an interesting application, see H. J. Pirner and J. P. Vary, Heidelberg preprints (1980).
[108]For a recent measurement, see M. S. Goodman et al., Phys. Rev. Lett. 47, 203 (1981). For a general review, see T. H. Bauer, R. D. Spital, D. R. Yennie, and F. M. Pipkin, Rev. Mod. Phys. 50, 261 (1978).
[109]J. D. Bjorken, Acta. Phys. Pol. B2, 5 (1975), and lectures at the DESY Summer Institute (1975). H. Harari, Proc. of the 1971 International Symposium on Electron and Photon Interactions at High Energies, Cornell.
[110]V. I. Zakharov, N. N. Nikolaev, Sov. J. Nucl. Phys. 21, 227 (1975); V. I. Zakharov, Proc. of the 18th International Conference on High Energy Physics, Tbilisi (1976).
[111]See, e.g., W.-Y.P. Huang and E. M. Henley, Annals of Phys. 129, 47 (1980). Y. M. Dubovik and A. P. Kobushkin, Ref. 78.
[112]L. Landau and I. Pomeranchuk, Dok. Acad. Nauk USSR 92, 535 (1953).
[113]For a phenomenological discussion, see S. J. Brodsky, Ref. 83. See also A. Białas, Fermilab-Conf-79/35-THY; A. Białas, W. Czyż and W. Furmanksi, Acta. Phys. Pol. B8, 585 (1977); A. Białas, Fermilab-Pub-78/75-THY (1978); A. Białás and E. Białas, Fermilab-Pub-79/48 THY (1979); A. Białas, M. Blesyznski and W. Czy' Nucl. Phys. B111, 461 (1976).
[114]P. Damgaard, Cornell preprint CLNS 81/519 (1981).
[115]I wish to thank G. E. Brown for discussions of this point.
[116]See also M. Chemtob, Ref. 83. J. M. Nanyslowski and H. J. Weber, Zeit. fur Phys. B158, 497 (1979). V. P. Karnomonov, ITEP-8 (1980).